IGCP 572 Field Guide Book 2

GUtech Geoscience Workshop Publication 1

The Permian-Triassic transition in the Oman Mountains.

Transect of the Tethyan margin from shallow to deep-water deposits

IGCP 572 annual Meeting & Field Workshop in Oman

Editors, coordinators: Aymon Baud[1)] and Michaela Bernecker[6)]

Leaders and authors: Sylvain Richoz[2)], Leopold Krystyn[3)], Oliver Weidlich[4)], Aymon Baud[1)], Benoit Beauchamp[5)], Michaela Bernecker[6)], Fabrice Cordey[7)], Stephen Grasby[8)], Charles Henderson[9)], Jean Marcoux[†], Alda Nicora[10)] and Richard Twitchett[11)] (affiliation in next page)

Contents

Author's affiliation (page 1): 1) BGC, Rouvraie 28, CH-1018 Lausanne, Switzerland 2) Commission for the Palaeontological and Stratigraphical Research of Austria, Austrian Academy of Sciences c/o Institute of Earth Sciences, University of Graz, Heinrichstraße 26, 8010 Graz, Austria 3) Department of Palaeontology, Vienna University, Althanstrasse 14, 1090 Vienna, Austria 4) Wintershall Holding AG, Friedrich-Ebert-Straße 160, 34119 Kassel, Germany 5) The Arctic Institute of North America (AINA), University of Calgary, 2500 University Drive, N.W.Calgary, Alberta, Canada T2N 1N4 6)German University of Technology in Oman (GUtech), Athaibah, PC 130, Sultanate of Oman 7) Département Sciences de la Terre, CNRS UMR 5125 Paléoenvironnements Paléobiosphère, Université Lyon 1, 69622 Villeurbanne, France 8) Geological Survey of Canada-Calgary, 3303 33rd Street, N.W. Calgary, Alberta, Canada T2L 2A7 9) Department of Geoscience, University of Calgary, 2500 University Drive, N.W. Calgary, Alberta, Canada T2N 1N4 10) Dipartimento di Scienze della Terra Universita` degli Studi di Milano, Via Mangiagalli 34, Milano, 20133, Italy 11) School of Earth, Ocean and Environmental Sciences, University of Plymouth, Drake Circus, Plymouth, PL4 8AA, UK

Tribute to Jean Marcoux† (1940-2008)

By Aymon Baud

Jean examining the Smithian platy limestones of Wadi Shu'yab, Sumeini area, 2004

Jean Marcoux, in memory of whom this Guidebook is dedicated, spent at least 2-4 weeks each winter, from 1989 to 2007, studying the Tethyan margin in Oman. He participated actively in researches on the areas presented in this field guidebook.

He passed away on 17 June 2008 after a three-month battle against cancer in Orsay, France. His death interrupted a Professor's lifetime of passionate geological researches and fieldwork. Born on 8 October 1940 in Marseille, France, he started Geology at Paris VI University in 1966, got an assistant position in 1969 at Paris XI University (Orsay) and started in Brunn's laboratory a PhD thesis (French "Thèse d'Etat") on "The anatomy of the Antalya nappes in SW Turkey".

Very early in the 1970s Jean worked on the Permian and Triassic stratigraphy and took part in the IGCP project No 4 "Triassic of the Tethys realm" leaded by Prof. Zapfe from Vienna.
In 1980 he became full Member of the Subcommission on Triassic Stratigraphy (STS) and in 1982 a Member of the Working Group on the Permian-Triassic Boundary.

In 1989 he became full Professor in Geology at the Paris VII University. He was teaching on different student degrees, from general geology for beginners to geology of the Earth and paleogeography for Master students. In 1993, Jean was elevated *Professeur de 1ère classe* at Paris VII University. Jean was also very engaged in his country and became Chief Editor of the *Bulletin de la Société géologique de France* from 1997 to 1999 and his scientific contribution to Geosciences earned him the prestigious *Prix Fontannes* of the Geological Society of France in 1999.
An excellent teacher, Jean Marcoux first was a field geologist who could feel as comfortable in sedimentology as in tectonics, in magnetostratigraphy as in paleontology. He had an easy communication and got well with his colleagues and always wanted to share his enthusiasm and encyclopedic knowledge. He was always ready to do something for his friends, for his colleagues and helped many young geologists who wanted to start a scientific career.

For the Tethys research Program managed by J. Dercourt and starting in 1989, Jean was in charge of the Triassic palaeogeographical and palaeoenvironmental maps working group (Anisian and Norian maps) and participated in the Permian map (Murgabian) working group.
A team from Lausanne and Bern Universities, with our lamented colleague Tjerk Peters, invited him, in early 1989 to work on Oman exotics with the financial support of the Tethys program. From that time, Jean became very active on Permian and Triassic researches in Oman, participating with enthusiasm in three Congresses hold in Muscat (1990, 2001 and 2005) with talks and co-

organization of fieldtrips. He was adviser of PhD students from Lausanne: A. Pillevuit on Oman Exotics and S. Richoz on PT boundary.

Each winter, from 1995 to 2002 Jean and I organized 2-4 weeks of field studies on Permian and Triassic of Oman, working with PhD students V. Atudorei and S. Richoz, with French colleagues from BRGM, with colleagues from Milano, from Lyon and, sometimes, L. Krystyn joined us. Working with Jean in the Wadi Wasit area in 1998, we discovered some ammonoids from a block in the breccias we believed Permian in age. For determination we gave these ammonoids to L. Krystyn. Two years later Leo called us saying the ammonoids are basal Triassic in age and asking the coordinate of this finding and this was the start of the Wasit block story we will visit during our field workshop.

It is Jean also, informed by geologists of BRGM, who introduced us to the Buday'ah locality and asked F. Cordey, a specialist in Paleozoic radiolarians, to come with us.
With Jean also we started the study of the Permian-Triassic of the Sumeini area at the end of the 1990s. At that time, to go by car in the field area, we had to fly to Dubai and rent a car from there because the Oman border was not open to foreigners driving a car!

In January 2001, Jean helped me with L. Krystyn, S. Richoz and B. Beauchamp to organize a Pangea Symposium within the International Conference on the Geology of Oman. He participated actively in the Conference and to the two fieldtrips on Permian and Triassic, being co-author of the two field guidebooks of the Pangea excursions before and after the Conference.

When the Saiq Plateau opened to the foreigners in 2003, Jean went, with my PhD student Sylvain Richoz and me, to start the study of Late Permian and Early Triassic succession. He went again with me there from 2004 to 2007.

For High-school teachers and for University students from Paris, Lausanne and Zurich, he co-organized and guided excursions in Oman, conveying very impressively his knowledge.

In March 2007, Jean and I organized seven days of fieldworks to check some key part of his research program on "Gaps in the Mesozoic carbonate of the Oman Exotic". It was his last fieldworks in Oman and he has still a lot of researches that he wanted to continue. During all his studies in Oman, as his friends, he benefitted from the efficient help of the BRGM Residents in Ruwi and Qurm and, overall among them, from Jean Paul and Françoise Breton.

Jean, tu es parti trop tôt, nous avions tant de projets, tu laisses un grand vide
mais nous poursuivons ton œuvre et te dédions ce livret guide

Part of the Biography of Jean Marcoux and reference lists have been published in:

Baud, A., 2008, In Memoriam -Jean Philippe Marcoux (1940-2008). Permophiles, v. 52, p. 19-21.
Baud, A., 2008, Jean Marcoux, Géochronique, No 108, p. 17
Baud, A., 2009, In Memoriam -Jean Philippe Marcoux (1940-2008). Albertiana, v. 37, p. 6-14.
Sengör, A.M.C., 2008, In Memoriam -Jean Philippe Marcoux (8 October 1940-17 June 2008). Turkish J. Earth Sci., Vol. 17, p. 637–652

On the geology of Oman, Jean Marcoux collaborated in at least 15 articles or field guidebooks and 14 short notes or abstracts:

Articles

Angiolini, L., Bucher, H., Pillevuit, A., Platel, J. P., Roger, J., Broutin, J., Baud, A., **Marcoux, J.**, and Hashmi, H. A., 1997, Early Permian (Sakmarian) brachiopods from southeastern Oman: Geobios, v. 30, p. 378-405.

Angiolini, L., Carabelli, L., Nicora, A., Crasquin-Soleau, S., **Marcoux, J.**, and Rettori, R., 2007, Brachiopods and other fossils from the Permo-Triassic boundary beds of the Antalya Nappes (SW Taurus, Turkey): Geobios, v. 40, p. 715-729.

Angiolini, L., Nicora, A., Bucher, H., Baud, A., Vachard, D., Platel, J. P., Roger, J., Broutin, J., **Marcoux, J.**, Pillevuit, A., and Hasmi, H. A., 1996, Late Permian fauna from the Khuff Formation,south Oman: Permophiles, v. 29, p. 62-64.

Angiolini, L., Nicora, A., Bucher, H., Vachard, D., Pillevuit, A., Platel, J. P., Roger, J., Baud, A., Broutin, J., Al Hashmi, H., and **Marcoux, J.**, 1998, Evidence of a Guadalupian age for the Khuff formation of southeastern Oman: Preliminary report (with paleontological appendix by A. Nicora): Rivista Italiana di Paleontologia e Stratigrafia, v. 104, p. 329-340.

Baud, A., Atudorei, V. N., and **Marcoux, J.**, 1999, The Permian-Triassic boundary interval (PTBI) in Oman : Carbon isotope and facies changes, *in* Yin, H., and Ton, J., editors, International Conference on Pangea and the Paleozoic-Mesozoic Transition: Wuhan (China), China University of Geosciences Press, p. 88-89.

Baud , A., Beauchamp, B., **Marcoux, J.,** and Twitchett, R., ed., 2003, Pangea Special Issue: Selected papers from the Pangea Symposium, Muscat, January 2001: Palaeogeography, Palaeoclimatology, Palaeoecology, v. 191, p. iii (265-404)

Baud, A., Béchennec, F., Cordey, F., Krystyn, L., Le Métour, J., **Marcoux, J.**, Maury, R., and Richoz, S., 2001a, Permo-Triassic Deposits: from the Platform to the Basin and Seamounts, Conference on the Geology of Oman, Field guidebook: Muscat, Oman, 54p..

Baud, A., Béchennec, F., Cordey, F., Le Métour, J., **Marcoux, J.**, Maury, R., and Richoz, S., 2001c, Permo-Triassic Deposits: from shallow water to base of slope, Conference on the Geology of Oman, Field guidebook: Muscat, Oman, 40p..

Broutin, J., Roger, J., Platel, J. P., Angiolini, L., Baud, A., Bucher, H., **Marcoux, J.**, and AlHasmi, H., 1995b, The Permian Pangea. Phytogeographic implications of new paleontological discoveries in Oman (Arabian peninsula): Comptes Rendus De L Academie Des Sciences Serie Ii Fascicule a-Sciences De La Terre Et Des Planetes, v. 321, p. 1069-1086.

Lapierre, H., Samper, A., Bosch, D., Maury, R. C., Bechennec, F., Cotten, J., Demant, A., Brunet, P., Keller, F., and **Marcoux, J.**, 2004, The Tethyan plume: geochemical diversity of Middle Permian basalts from the Oman rifted margin: Lithos, v. 74, p. 167-198.

Maury, R. C., Bechennec, F., Cotten, J., Caroff, M., Cordey, F., and **Marcoux, J.**, 2003, Middle Permian plume-related magmatism of the Hawasina Nappes and the Arabian Platform: Implications on the evolution of the Neotethyan margin in Oman: Tectonics, v. 22, p. art. no.-1073.

Pillevuit, A., **Marcoux, J.**, Stampli, G., and Baud, A., 1997, The Oman exotics : a key to the understanding of the Neotethyan geodynamic evolution: Geodinamica Acta (Paris), v. 10, p. 209-238.

Richoz, S., Baud, A., of, w. c., Krystyn, L., Twitchett, R., and **Marcoux, J.**, 2005, Permo-Triassic Deposits of the Oman Mountains: from Basin and Slope to the shallow Platform, *in* (IAS), I. A. o. S., editor, 24th IAS regional Meeting, Field guidebook: Muscat, Oman, 57 p.

Stampfli, G., **Marcoux, J**., and Baud, A., 1991, Tethyan margins in space and time: Palaeogeography, Palaeoclimatology, Palaeoecology, v. 87, p. 373-409.

Abstract, short notes

Angiolini, L., Baud, A., Broutin, J., Hasmi, H. A., **Marcoux, J.**, Platel, J. P., Pillevuit, A., and Roger, J., 1995, Sakmarian brachiopods from southern Oman, *in* Coper, P., and Jin, J., editors, Third international brachiopod congress: Sudbury (Canada), Laurentian University, p. 4.

Baud, A., Cordey, F., Krystyn, L., **Marcoux, J.**, and Richoz, S., 2001, The Permian-Triassic boundary in Oman, a review., Geology of Oman, Pangea Symposium: Muscat, Oman.

Baud, A., **Marcoux, J.**, and Stampfli, G., 1989, L'enregistrement sédimentaire fourni par les exotiques d'Oman du Permien au Jurassique, *in* Soc. geol. de France, editor, Tethys, 12-13 décembre 1989: Paris, p. 32.

Baud, A., **Marcoux, J.**, and Stampfli, G., 1990, Evolution of the Oman margin, from rifting to passive margin stage (Permian to Early Mesozoic). Symposium on ophiolite genesis and evolution of oceanic lithosphere.: Muscat, Ministry of petroleum and minerals, Muscat, Oman., v. Abstract 3.1.

Baud, A., Septfontaine, M., Stampfli, G., and **Marcoux, J.**, 1989, observation de niveaux stratifiés de calcaires hallstatt et d'Ammonitico-Rosso sur l'exotique de Ba'id. *in* Soc. geol. de France, editor, Colloque Tethys, 12-13 décembre 1989 Abstract.

Cordey, F., Baud, A., Béchennec, F., Gorican, S., Krystyn, L., **Marcoux, J.**, Robin, C., and Richoz, S., 2001, Permian-Triassic deep water sediments of the Wadi Wasit revisited, Geology of Oman, Pangea Symposium: Muscat, Oman. Abstract

Marcoux, J., 1990, A peculiar piece of the Neotethyan passive margin: the Exotics from Turkey, Oman and Himalayas., Symposium on ophiolite genesis and evolution of oceanic lithosphere.: Muscat, Ministry of petroleum and minerals, Muscat, Oman., p. OM 3.1.

Marcoux, J., Barrier, L., Gorican, S., Moix, P., Durlet, C., Bartolini, A., and Bechennec, F., 2005, Enregistrement du temps dans les environnements carbonatés. Exemple des exotiques d'Oman. Résultats préliminaires et problématique., Réunion annuelle de l'ASF, Abstract volume.

Marcoux, J., Baud, A., and Richoz, S., 2006, The oceanic base of slope record of the Permian-Triassic crisis: view from Tethys (Oman) InterRad 11 & Triassis Stratigraphy Symposium: Wellington, N.Z., p. 87**.**

Maury, R. C., Cotten, J., Bechennec, F., Caroff, M., and **Marcoux, J.**, 2001, Magmatic Evolution of the Tethyan Permo-Triassic Oman margin, Geology of Oman, Pangea Symposium: Muscat, Oman Abstract book.

Pillevuit, A., Stampfli, G., Baud, A., and **Marcoux, J.**, 1990, Initiation de l'ouverture Tethysienne en Oman, Paleomap & G.S. Tethys: 11, 12 et 13 décembre à Paris. Abstract

Pillevuit, A., Stampfli, G. M., Baud, A., and **Marcoux, J.**, 1992, Late Permian opening of the Neotethys in Oman: Géochronique, v. 42, p. 85.

Richoz, S., Atudorei, V., Baud, A., and **Marcoux, J.**, 2001a, Lower Triassic isotope stratigraphy of the Sumeini slope deposits (Maqam C, NW Oman), Geology of Oman, Pangea Symposium: Muscat, Oman, Abstract.

-, 2001b, Upper Permian to Lower Triassic carbon isotope record : review and new data in the Oman Mountains, from the shallow platform to the basin., Geology of Oman, Pangea Symposium: Muscat, Oman Abstract.

Roger, J., Angiolini, L., Aubry, M. P., Baud, A., Bourdillon, C., Broutin, J., Bucher, H., Le Callonec, L., Galbrun, B., Al Hashmi, H., **Marcoux, J.**, Philip, J., Platel, J. P., Razin, P., Renard, M., and Al Suleimani, Z., 1995, New data from the Oman expeditions, Peri-Tethys Scientific Meeting: Milano Italy, p. 18-19.

Part A –Introduction to the Permian –Triassic of the Oman Mountains

1- Prelude.

Geological studies carried out in Oman by many projects have provided a profound insight into its geological history, as summarized by the 1/500000-scale map of the northern chain (Glennie et al., 1974) and by the 1/1000000-scale map of the whole Oman (Le Métour et al., 1993a; Béchennec et al., 1993a). The alpine northern Oman Mountains, extending for 700 km from the Musandam Peninsula in the north to the Batain coast in the southeast, was uplifted at the end of the Miocene along the northeastern edge of the Arabian Peninsula. Six major structural units are identified from the base up (Fig. 1):

1- The Crystalline Basement of Late Proterozoic age.
2- The Sedimentary Basement of latest Proterozoic to Ordovician age.
3- The Middle Permian-Late Cretaceous carbonate Arabian Platform (Hajar Unit).
4- The Sumeini and Hawasina nappes mainly made up of continental slope and basin. deposits thrusted onto the Arabian Platform during the Late Cretaceous.
5- The Samail Ophiolite, a fragment of Neotethys oceanic lithosphere obducted onto the Oman continental margin in the Late Cretaceous.
6- The post-nappes sedimentary cover of end-Cretaceous-Tertiary age.

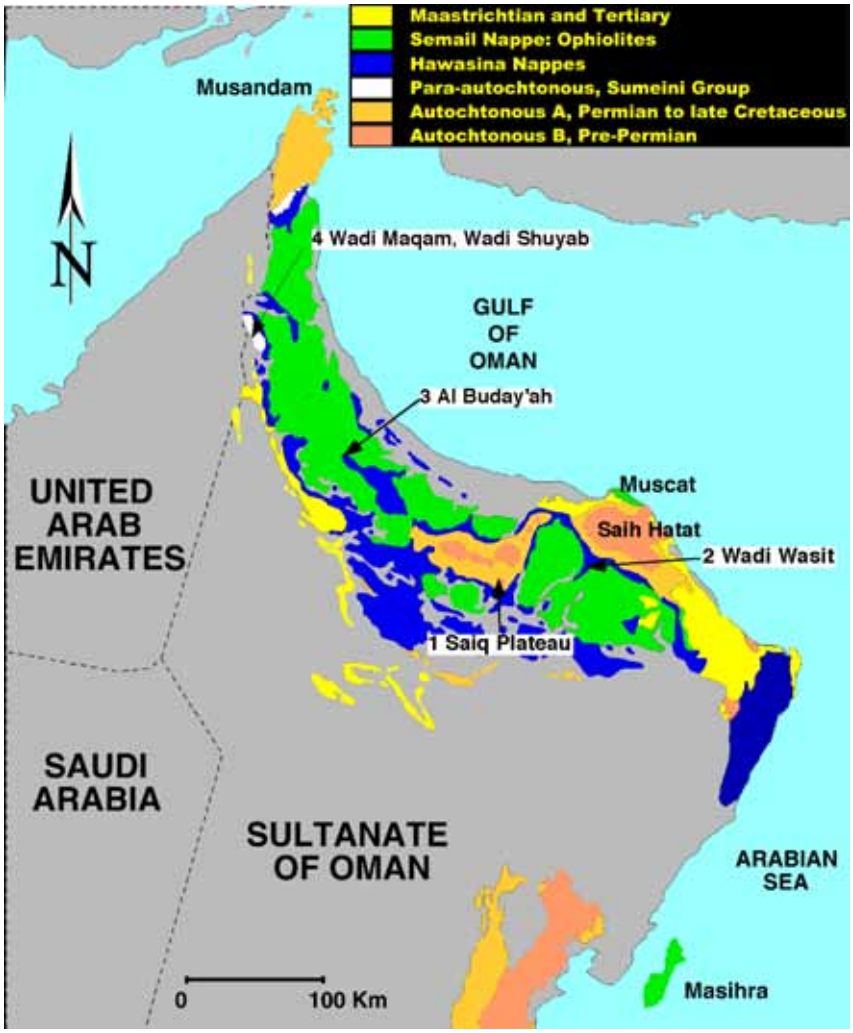

Fig. 1: Geological sketch of the Oman Mountains.

2- Permian birth and evolution of the Arabian passive margin

Our analysis is based on our own data (Baud et al., 2001a, b, Richoz et al., 2005, Richoz, 2006,) on Béchennec (in Baud et al., 2001a), on Pillevuit 1993, Pillevuit et al. (1997), on Weidlich (2007), Weidlich and Benecker (2003) and new data from field works with B. Beauchamp in 2007 and 2009, with S. Grasby in 2007, with C. Henderson and A. Nicora in 2007 and their new conodont determinations.

2.1 Summary.

At the end of the Palaeozoic the continents were gathered together to form the Pangean supercontinent and in its southern half, Oman and the Arabian Peninsula formed part of the Gondwana continent (fig. 2) as well as Africa, Iran, India, etc. (Scotese and McKerrow, 1990). During the Late Carboniferous-Earliest Permian period, the Gondwana continent was subjected to glaciation (Al Khlata tillite in Oman).

The Neotethyan opened with the northward drifting of the Iran/Mega Lhasa microcontinent (Baud et al., 1993, 2001) followed a rifting – extensional phase in the Sakmarian (hypothesis developed by Saidi, 1997, Besse et al., 1998, Angiolini et al., 2003a et b, and by Maury et al., 2003) or in the Roadian-Wordian (hypothesis presented here in fig. 3, and developed by Baud et al., 1993, Pillevuit, 1993, Pillevuit et al., 1997, Baud et al., 2001a, b). Thermal subsidence, with the development of the continental margin, is well recorded in the Wordian-Capitanian carbonate succession and continued during the Lopingian. Tectonic instability of the margin, with bock tilting, platform drowning and (fault) breccia deposits start at the dawn of the Triassic with the main climax during the Dienerian and the Smithian. A renewed tectonic instability with plume related volcanism started offshore in the Carnian with the creation of atoll like isolated carbonate platforms (Kawr) and the opening of a new basin (Umar). At the end of the Triassic, all the known parts of the continental margin and adjacent ocean and atoll areas were finalized.

2.2 The precursors of Neotethyan tectonism.

The end of the glacial period in the Early Permian resulted in a global rise in sea level, which subsequently submerged part of the continent. This is reflected in the marine siliciclastic and carbonate deposits laid down during the Early Permian (Sakmarian-Artinskian) identified in the Haushi-Huqf area and Interior Oman (Saiwan Fm., Dubreuilh et al. 1992; Miller and Furnish, 1957; Hudson and Sudbury, 1959; Angiolini et al., 1997) and in the Djebel Qamar, north of Oman Mountains (Asfar Fm., Pillevuit, 1993, Pillevuit et al., 1997). Furthermore, reworked blocks of Early Permian (Artinskian) shallow-marine carbonate are also identified in Hawasina units of the Batain plain (Pillevuit, 1993, Pillevuit et al., 1997) documenting the northeasternward extension of a rim basin. However, such marine deposits are unknown in the central and southeastern part of the Oman mountains (Djebel Akhdar and Saih Hatat) indicating that, at this time, this region constituted a positive zone; this is probably in relation with a flexural doming precursor of the Neotethyan tectonism, initiating a shoulder and concomitant rim basins where the marine deposits laid down.

2.3 The first stage of the Neotethyan extension (Fig. 2).

The first stage of the Neotethyan extension begins in the Late-Early/Early-Middle Permian and is documented by:

1. An angular unconformity between the Early Permian Saiwan Fm. and the Middle Permian Gharif Fm., in the Haushi-Huqf area;

2. An angular unconformity between the Early Permian Asfar Fm. and the Late-Early/ Middle Permian Qamar Fm., in the Djebel Qamar area (Northwestern part of the Oman Mountains);
3. Horst and graben tectonics clearly identified in the Oman Mountains (Djebel Akhdar and Saih Hatat) by the differential erosion between blocks (Le Métour, 1988; Rabu, 1988) and by the syn-rift-type deposits of the lower part of the Saiq Formation.

Global sea level rose to a maximum during the Late-Early Permian (Kungurian, Haq et al., 1987); however, only rare shallow-marine carbonate of this age is found in Oman, as reworked blocks in proximal turbiditic facies of the Hawasina units on the Batain Coast (Béchennec et al., 1992a) where probably the former "rim basin" persisted: then most of Oman remained emergent (Fig. 2). Subsequently, resulting of rapid erosion of the shoulder initiated in Late-Early Permian, the terrigenous siliciclastics deposits of the Gharif Fm. (Kubergandian-Murghabian of Broutin et al., 1995) and of the base of the Qamar and Saiq Fms. were laid down in a continental environment.

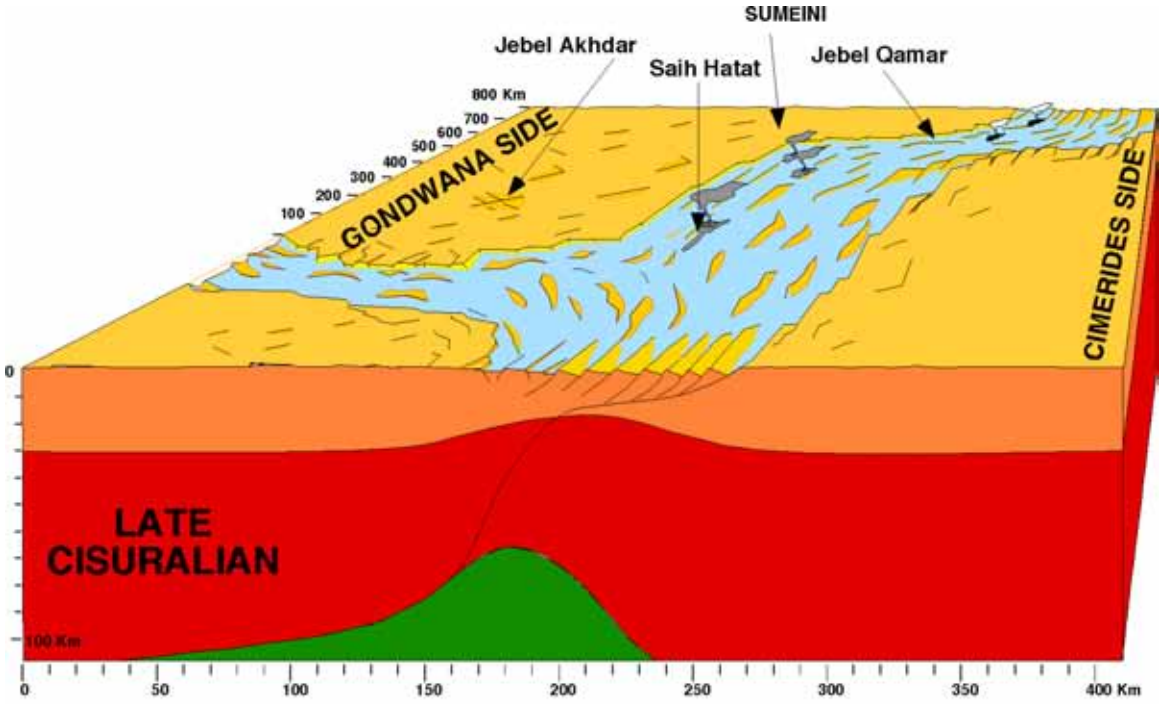

Figure 2: Geological sketch 3D from mantle (green) to upper crust (orange) of the rifting of the Cimmerides from Gondwana margin in Late Cisuralian time (modified from Pillevuit 1993).

2.4 From rifting to break-up, the Neotethyan opening

2.4.1 Rifting (horst and graben tectonics) on the margin of the Arabian Peninsula (fig. 2).
When the Djebel Akhdar became a stable platform in Guadalupian time, the horst and graben tectonics initiated in Late-Early/Early-Middle Permian developed a climax in the Saih Hatat. This gave rise to considerable thickness variations between the relatively condensed carbonate successions on the horsts and very thick successions in the grabens where the deposits in places, are made of conglomerates and olistoliths of shallow-marine carbonate. Furthermore, two intervals of volcanic and volcaniclastic rocks are related to this tectonism (Le Métour, 1988). This is particularly well developed in the Hulw graben (Saih Hatat) where the earliest interval located at the base of the carbonate succession is about 500m thick and is mainly made of tuffite and tuff with accessory andesite-rhyodacite. The later interval, 20 to 150m thick, is located in the middle part of the Saiq carbonate succession; it essentially comprises basalt, trachyandesite and rhyodacite with

accessory tuff and dolerite and rhyodacite plugs. The intermediate to acid rocks of the earlier episode correspond to sub-alkaline rhyodacite, whilst those of the later one are transitionnal in character, probably corresponding to a magmatic suite that was differentiated from an alkaline to transitional magma (Le Métour, 1988; Béchennec et al., 1991; Pillevuit, 1993; Pillevuit et al., 1997, Lapierre et al. 2004, Chauvet et al. 2008).

2.4.2 Thermal subsidence of the northeastern margin of the Arabian Peninsula

At the dawn of the Wordian (Middle Permian), the "Fusulinid Sea" transgressed over most of Oman with the exception of the Djebel Ja'alan and the Huqf-Dhofar axis; this transgression enabled the establishment of a vast carbonate platform in Djebel Akhdar, a 700m-thick succession of cyclic shallow marine carbonate, the Saiq Fm (Middle-Late Permian, basal Triassic, this vol., see also Baud et al. 2001, 2005, Richoz et al. 2005, Richoz, 2006); a similar succession occurs in Saih Hatat (Chauvet, 2007, Weidlich and Bernecker, 2003 and this vol.) in the Musandam (Bih Formation, Maurer et al. 2009) as well as in the Interior Oman and in the Haushi area (Khuff Fm., Dubreuil et al., 1992; Angiolini et al. 1998, 2003). Clearly, for us, this transgression was the result of the break-up of the Neotethyan rift (Fig. 3) and the associated thermal subsidence.

2.4.3 The breakdown of the Gondwana: formation of the Arabian passive margin (fig. 3).

In Middle Permian (Wordian), breakdown of this part of the Gondwanaland became established with northward drifting of the Iran/Mega Lhasa microcontinent (Baud et al., 1993); subsequently the most striking effect of the climax of the Neotethyan extension was the formation of a continental slope (Sumeini) and a basin (Hawasina) that constituted with the adjacent Arabian Platform, the southern continental passive margin of the Neo-Tethys. Furthermore early-rifted blocks detached from the edge Arabian shield edge formed isolated proximal platforms along the continental slope (later they were incorporated in the Hawasina Nappes).

The continental margin slope deposits are clearly identified (with slumps and intraformational breccia) in the northwestern part of the Oman Mountains (Djebel Sumeini), where they form the basal part of the Maqam Fm. dated as Middle Permian (Wordian, Pillevuit, 1993; Pillevuit et al., 1997; or Roadian, Krystyn, this vol.). Different type of deep water black limestones are also identified in the basinal units of the Batain Plain (southeastern part of the Oman Mountains), the "Qarari Limestone" (Shackleton et al., 1990; Béchennec et al., 1992a; Wyns et al., 1992) with a base dated as Roadian (Middle Permian, Immenhauser et al., 1998) and the top as Wuchiapingian.

The distal isolated platform identified as nappes in Baid and Djebel Qamar areas by Béchennec, 1988; Béchennec et al., 1992b; Pillevuit, 1993, Pillevuit et al., 1997, are mainly made of Middle-Late Permian open shelf carbonates. The Djebel Qamar unit includes a fragment of the pre-Middle Permian Basement (Rann, Ayim and Asfar Fms., Pillevuit, 1993) overlain in unconformity by the Late Early-Early Middle Permian shallow-marine carbonate Qamar Fm. with his quartz-sandstone basal member. The Baid unit is truncated at the base and is made of about 100 m of the Middle-Late Permian (Capitanian-Wuchiapingian) shallow-marine carbonate (Baid Fm., Béchennec, 1988; Pillevuit, 1993, Pillevuit et al., 1997, Baud et al., 2001). The distal paleogeographic position of these Permian tilted blocks in regard with the Arabian Platform is documented by:

(1) The differences in terms of facies (open marine with ammonoids) with those restricted to the others parts of the Oman Mountains (Djebel Akhdar, Saih Hatat, Musandam);

(2) The presence of reworked boulders originating from these isolated platforms in the calcirudites of the proximal units of the basinal Hawasina Nappes.

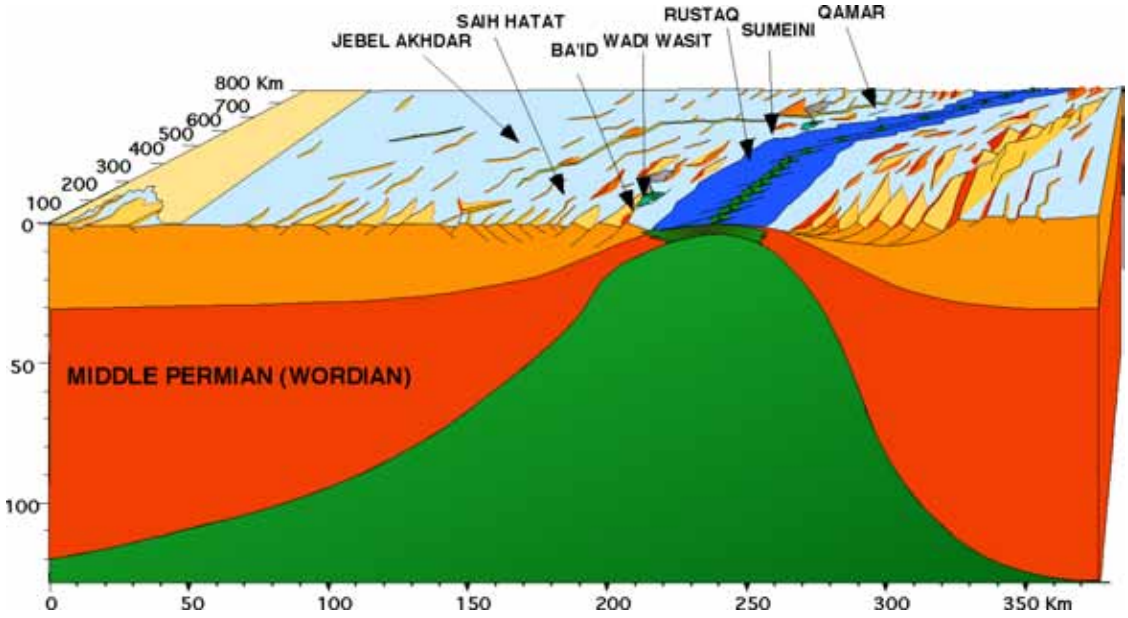

Figure 3: Geological sketch 3D of the Neotethys break-up and the onset of the Arabian passive margin in Middle Guadalupian time (modified from Pillevuit 1993).

Basinal facies of the Middle Permian are present in the Hawasina Nappes at the base of numerous tectonics units, made up of Formations from the Hamrat Duru Group. These successions starts generally with thick volcanic sequences (Al Jil Fm. and Buday'ah Fm.); they are particularly well exposed to the north of the Hawasina Window (Buday'ah area) and of the Djebel Akhdar (Al Ajal region) and in the southern flank of the Saih Hatat (Wadi Wasit area); they have been also identified locally, near Nahkl and Rustaq and in the Batain plain near Al Ashkharah. Predominantly these volcanic rocks comprise tubular pillow basalt and subordinated andesitic and trachytic lava, hyaloclastite transitional and tuff (Béchennec, 1988; Béchennec et al., 1991; Béchennec et al., 1992a-b-c, Pillevuit, 1993, Pillevuit et al., 1997). These volcanic rocks are either of MORB type or alkali basalt-related; however N-MORB (depleted) have not been found as most of the studied samples range from MORB to enriched MORB (Maury et al., 2003, Lapierre et al. 2004, Chauvet et al. 2008). The volcanic succession is filled and overlain by red ammonoid limestones dated as Middle Permian (Capitanian) followed by radiolarian chert and shales newly dated as Lopingian in Buday'ah (this volume) and occurring in Rustaq and also Al Ashkharah areas (De Wever et al., 1988; Béchennec et al., 1992a-c). In the Wadi Wasit area, the volcanic series is capped by red cephalopods-bearing carbonate, dated Middle Permian (Wordian, Blendinger et al., 1992; Pillevuit et al. 1997, Baud et al. 2001b), by shales and breccia with reworked blocks of Middle Permian to basal Triassic platform carbonate (Béchennec et al., 1992b; Pillevuit, 1993, Pillevuit et al., 1997, Weidlich and Bernecker, 2007, Krystyn et al., 2003, Twitchett et al., 2004).

Near Nahkl the volcanic series includes blocks of Middle Permian shallow-marine carbonate and is overlain by pelagic limestone (Weidlich, 2007). In the Rustaq area the volcanic succession is also capped by a condensed carbonate sequence (Hallstatt facies type) dated as Middle Permian (Wordian, Blendinger et al., 1992, Pillevuit et al. 1997, Baud et al. 2001b, Richoz et al., 2005). Following the peak of the thermal subsidence in the Wordian-Capitanian, a stable carbonate platform became established on the Arabian Peninsula. The Saiq, Khuff and Hagil Fms, show a strong regressive tendency at the end of the Guadalupian, with restricted environment facies and a reduced biophase, mainly associated with a global fall in sea level at this time (Haq et al., 1987), and climate changes (Isozaki, 2009). During the Lopingian, the subsidence as recorded in the Saiq mega-cycle B (up to 300m of shallowing upward cycles) is still well active.

3- The Permian-Triassic transition and the Triassic deposits on the Arabian passive margin.

3.1 From the Permian-Triassic transition to the basal Triassic (Fig. 4).
At the end of the Permian, regressive conditions up locally to emersion (?) are recorded as well on the Arabian carbonate platform (Djebel Akhdar, Saih Hatat, Musandam). On the slope of the continental margin, we observe a shallowing in the Sumeini unit deposits.
Shallow tidal influenced carbonate platform are the main component of the Induan dolomitized deposit in the Djebel Akhdar (Unit C1-C4 of the Saiq Formation) that is now dated by conodonts (description this vol.). During the Dienerian, part of the margin is affected by renewed extensional regime, tilting and drowning resulting in erosive deposition and accumulation of carbonate breccia (Unit C2 of the Saiq Formation) followed in the Djebel Akhdar by high energy, partly oolitic dolomitized shallow water deposits, Smithian in age (Unit C3) and renewed breccias (Unit C4). The Saiq-Mahil transition is probably still in Dienerian (Chemiostratigraphical correlations, Richoz 2006).

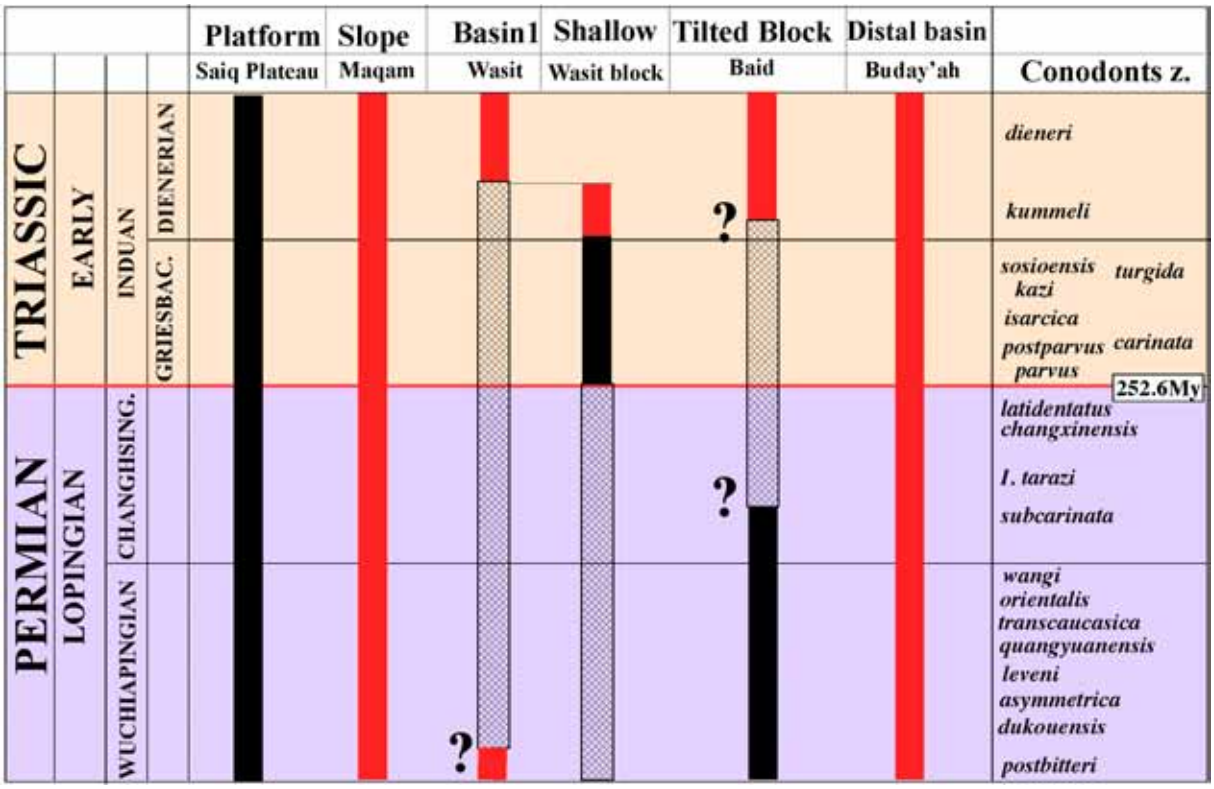

Figure 4: Recorded sedimentation and gaps of the visited localities (+Baid tilted block). Shallow water deposits in black and open to deep marine deposits in red.

On the slope of the continental margin, a continuous carbonate deposition and shale has been recently precisely dated from Changsingian to Spathian. Overlying the Wuchiapingian-Changhsingian deep-water chert and dolostone (upper Member B of the Maqam Fm), we note the deposition of upper Changsingian shallowing siliceous strongly bioturbated lime mudstones. A huge facies change occurs with the Griesbachian papery, laminated calcimicrobial mudstone overlying the boundary clay (base of C1c Member of the Maqam Fm). The calcarenite, calcirudite turbidites and avalanches with shallow water upper Permian lime clasts start in the Dienerian (instability period). The incredibly thickness of the Smithian deposits (platy limestones, shales and megabreccia up to 900m of thickness, middle and upper Member C of the Maqam Fm) indicate

high carbonate productivity on the platform and a very active subsidence at the base of slope (Watts, 1985; Baud et al. 2001; Richoz et al. 2005, Richoz, 2006).

On the Baid Exotic block, after karstification of part of the tilted Permian carbonate platform and the Dienerian drowning event, the Dienerian-Smithian deep-water red ammonoid limestone is filling fissures and cavities (Hallstatt breccia) and is deposited over the Permian limestones (Tozer and Calon, 1990; Pillevuit, 1993; Pillevuit et al., 1997, Baud et al. 2001, Richoz, 2006).

In the proximal deep-water basin (Wadi Wasit units) the Lopingian allodapic limestones are partly eroded by a submarine avalanche breccia (Dienerian) containing Permian to basal Triassic mega-blocks. One of these blocks with a unique Permian-basal Triassic record has been analyzed in Krystyn et al. (2003) and Twittchett et al. (2004). Upper Dienerian-Smithian deep-water platy limestone overlay the Lower Dienerian mega-block breccia.

In the distal Hawasina basin (Buday'ah), the Upper Permian radiolarian chert deposits are overlain by Changhsingian siliceous shales and calcareous shales followed by Griebachian laminated platy limestones and shales and Dienerian-Smithian papery limestones (see this vol.).

3.2 The Olenekian to Rhaetian evolution of the margin (Fig. 5a).
On the Arabian platform we note dolostone successions (350m for the Sudair Fm.; 500-800m for the Mahil Fm.; 850m for the Ghail, Milaha and basal Ghalilah Fms., in Musandam, Spathian to Rhaetian). A low subsidence is indicated by shallowing upward sequences with frequent sub-aerial exposures. Emersion and laterite deposits at the end of the Triassic follow a first order sea level fall.

Due to climate change at the dawn of the Spathian (Galfetti et al., 2007) terrigenous deposits start on the Arabian platform with yellow to green clay recorded in the Mahil and the Sudair Fms., respectively in the Saih Hatat/Djebel Akhdar and in the Interior Oman and are the main component of the Maqam D unit (Spathian-Anisian yellow to green shales) on the slope of the continental margin. It is followed by Ladinian radiolarites pointing to stable deep-sea condition. During the Carnian-Norian time, a pervasive instability is documented by coarse calcirudites interbedded in the chert and calcarenite succession of Maqam D and E units (Watts, 1987, Watts & Garrison, 1986, Bechenec et al, 1993b, Baud et al, 2001b, Richoz et al. 2005, Richoz, 2006).

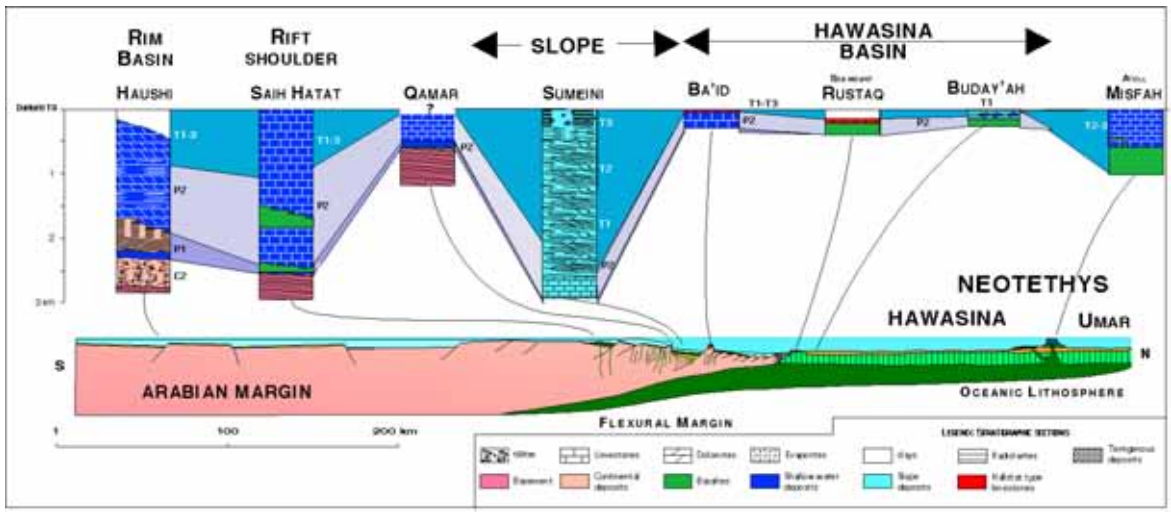

Figure 5a: 2D sketch of the Oman margin during Late Triassic (modified from Pillevuit et al., 1997).

On the Baid tilted block, the tectonic instability is also documented by angular unconformities and by clast-supported breccia with Late Permian remains, in the Hallstatt type succession from Olenekian up to Lower Jurassic (Tozer and Calon, 1990; Pillevuit, 1993; Pillevuit et al., 1997, Krystyn in Baud et al. 2001). The Smithian calcimicrobial mounds have been described by Baud et al., 2005 and recently by Woods & Baud, 2008.

In some area of the distal deep-water basin (Hawasina basin in Diba zone and the Central Oman Mountains), volcanic rocks are interbedded in the Ladinian-Norian basal cherty member of the Matbat Fm. (Béchennec et al., 1992c; Le Métour et al., 1992b), giving clear evidence of a renewed extensional regime.

The Late Triassic evolution of the distal part of the Hawasina Basin is documented by the creation of the Misfah distal Platform and by the Umar Basin. A strong subsidence is reflected by the huge thickness of the Late Triassic shallow-marine carbonate deposited on the distal platform. The Kawr and Umar Groups which crop out as several tectonic units at the summit of the stacked Hawasina Nappes, comprise a thick basal volcanic unit that display the characteristic of intraplate magmatic series and range from intraplate tholeiites to alkali basalt (Béchennec, 1988; Béchennec et al., 1991; Pillevuit, 1993; Pillevuit et al., 1997; Maury et al., 2003). In the Misfah setting this volcanic unit is overlain by a Norian marly nodular limestone (Subayb Formation,) and by a thick (600m) shallow-marine carbonate Formation (Misfah, Pillevuit, 1993), Norian-Rhaetian in age (Krystyn in Baud et al. 2001b). The presence of hardgrounds and, in places, microkarsts on top of the platform sequence reflect the end-Triassic sea level fall.

In the adjacent Umar Basin, the Late Triassic sedimentary succession consists of pelagic limestone and radiolarian chert without any terrigenous influx; the only clastic sediments are calcirudite and megabreccia made of reworked boulders of shallow-marine carbonate originating from the Misfah Platform.

4- Carbon isotope stratigraphy (S. Richoz, Fig. 5b)

Many studies have concentrated on the Permian-Triassic boundary interval for a long time (see a review in Corsetti et al. 2005, Yin et al., 2007, Richoz et al., in press), but recently the Lower Triassic received more attention (Atudorei, 1999; Tong et al., 2002, 2007; Payne et al., 2004; Zuo et al., et al 2006; Richoz 2006, Horacek et al., 2007a,b,c, 2009, in press, Galfetti et al., 2007a,b).

In order to obtain a better image of the carbon isotopic variations in the Upper Permian and Lower Triassic, high-resolution carbon isotope values were measured on 16 sections in Iran, Turkey and Oman (Richoz 2006). A reliable synthetic curve (fig. 5b) for the Tethyan realm was obtained. In Oman, 9 sections, from the platform to the basin, were measured. 4 sections (Sal and Wadi Wasit and Wadi Maqam in Richoz et al., 2005, Richoz 2006, Richoz et al., in press; Wasit Block in Krystyn et al., 2003) with a good biostratigraphic control help us to better constrain the synthetic curve. In the other hand, the synthetic curve allows to improve the correlation potential of other sections as the Wadi Sahtan one (Richoz et al., 2005, Richoz 2006,) or Saiq Plateau (presented here).

In Oman, Permian $\delta^{13}C_{carb}$ values from various sections fluctuate between +3‰ and 6.6‰. The Permian-Triassic boundary is present only in autochtonous (Wadi Sahtan, Saiq Plateau, Wadi Aday), in slope deposits (Wadi Maqam) and in basinal distal position (Buday'ah). Wadi Sahtan and Saiq Plateau gave very similar results. Buday'ah reveals a strong alteration of the $\delta^{13}C_{carb}$ signal but the $\delta^{13}C_{org}$ presents still reliable curve (Grasby and Beauchamp, this volume). In autochtonous

sections and Wadi Maqam, the decrease of the isotopic curve shows different steps, beginning in the upper Changhsingian and finishing above the first appearance of *H. parvus*.

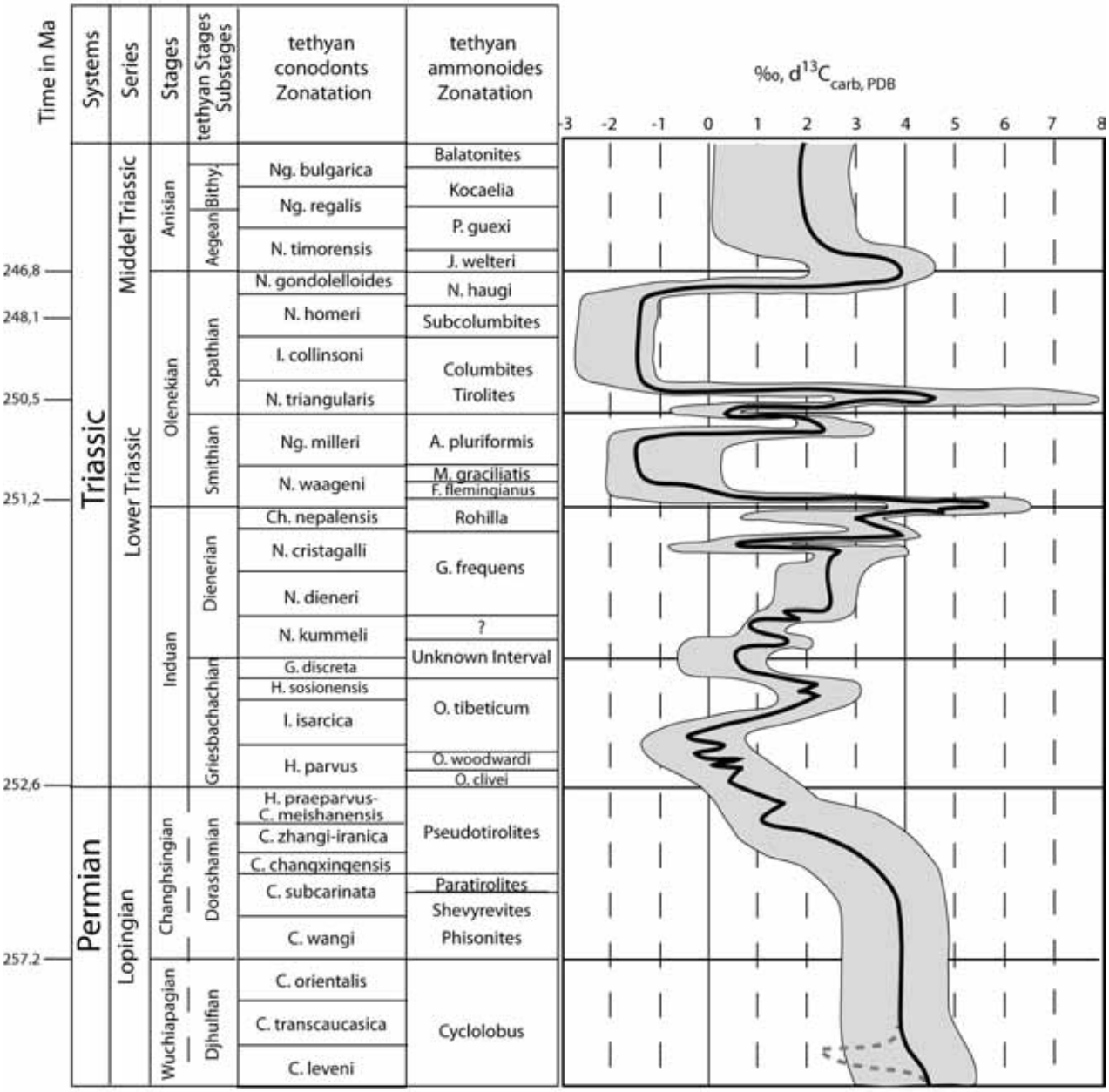

Figure 5b: Tethyan synthetic carbon isotopic curve for Upper Permian to Lower Triassic. Gray band is the observed variations in between sections (Modified after Richoz 2006)

The negative excursion is of 1.6‰ in Wadi Sahtan and 1.1‰ in Wadi Maqam before the event boundary and 1.1‰ respectively 3.7‰ after the event. Values increase in the second Griesbachian conodont zone (*I. isarcica*) from 1.5‰ in Wadi Maqam and Sahtan. The Upper Griesbachian decrease and homogenous values around +2‰ in the Dienerian are poorly constrained in Oman. The main reason is that the Dienerian sediments are condensed. The Wadi Sahtan section records a rapid negative shift in the uppermost Dienerian. This shift is well biostratigraphically well constrained in another Oman section (Wadi Wasit south, Richoz, 2004).

A double peak is then characteristic and occurs around the Dienerian/Smithian Boundary. The amplitude of the two peaks is from 1.1‰ to 5.5‰. They are among the more important positive excursion in all the Phanerozoic. The Middle and Late Smithian is the longest period of isotopic stability in the Early Triassic. Values are between +0.5‰ in Wadi Sahtan –1.4‰ in Wadi Maqam. Around the Smithian/Spathian boundary, these values have a short-term positive excursion of 2‰ in Wadi Sahtan, 3‰ in Wadi Maqam and up to 10‰! in the basinal sediments of the Batain plain, north-east Oman (Richoz, 2006). Isotopic values return then to negative values during the Sapthian. A last positive shift occurs at the Olenekian/Anisian boundary (Baud et al., 1996; Atudorei, 1999), but it is not well recorded in Oman. Isotopic values are then homogenous around +2‰ during all the Middle Triassic.

It appears clear that great disturbance in the isotopic record occurs during Lower Triassic time. The only such other large variations are recorded in Proterozoic time (Brazier et al., 1996). The classical image of a unique, large extinction with a very long recovery time has to be reviewed. The well-known Permian-Triassic boundary negative excursion is probably more the precursor of a long time of chemical change in the ocean.

Part B – Description of the visited outcrops

The Permian - Triassic stratigraphic nomenclature we make use of (Fig. 6)

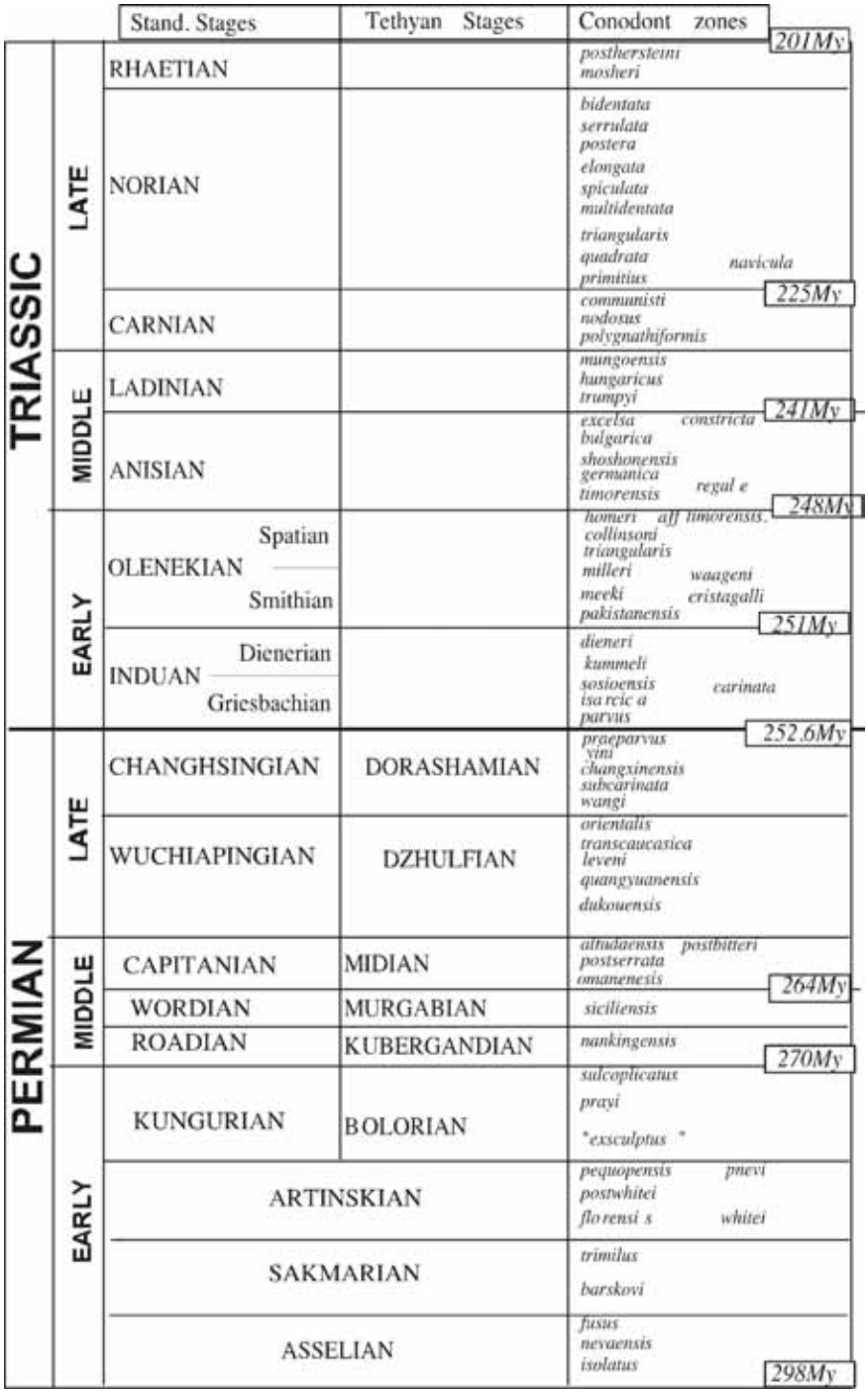

Figure 6: Permian-Triassic Time scale with standard and Tethyan stages names (modified from Richoz (2006).

In the last ten years, many changes occurred in the Permian-Triassic time scale and zonations as documented in a recent time-table (Fig. 6). The Tethyan stage names used in some part of this guidebook are shown according to their correlative standard stages.

<u>February 22, 2010</u> – The Permian-Triassic transition at Wadi Aday, Saih Hatat, Capital area

(O. Weidlich, M. Bernecker)

Routing (Figs 7-9): Starting at 9 a.m., February 22, from Hotel Ibis (Muscat), we will follow the Sultan Qaboos highway towards Muscat. At Wadi Aday roundabout, we will turn right and follow the road to Quriyat. We will pass Wadi Aday which crosscuts Permian-Jurassic rocks of the Autochthonous B in approximate north-south direction. After about 3 km we will stop to investigate Permian-Triassic strata of the Saiq and Mahil formations in small wadis (Fig. 8-9).

Figure 7: Google Map showing starting point of excursion at GUtech (red dot) and study area at Wadi Aday (red rectangle).

Figure 8: Google satellite map of the study area at Wadi Aday, Saih Hatat.

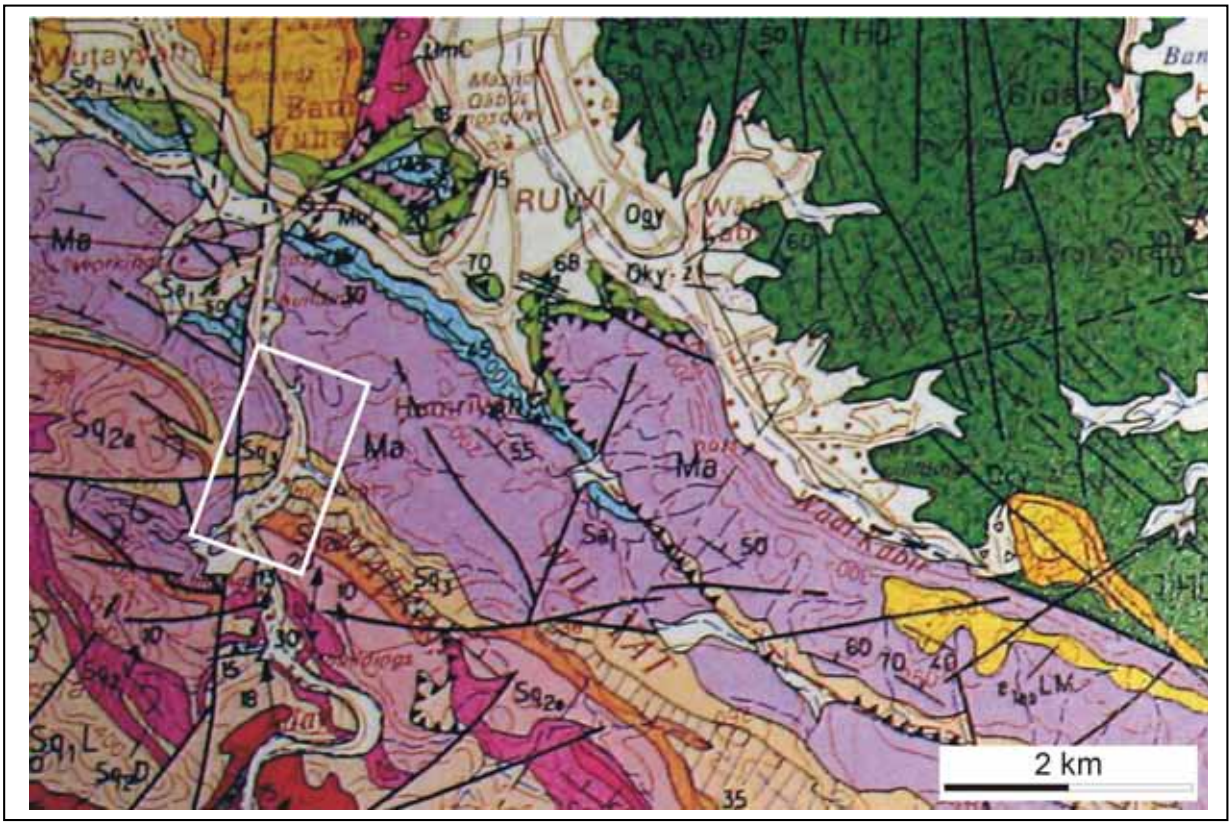

Figure 9: Geological map of the study area (Le Metour et al., 1986). The excursion will cover members of the Saiq Formation (Sq2a: light pink, Sq2b: orange, Sq3: light brown) and the basal Mahil formation (Ma). See text for details.

Introduction: With emphasis on the end-Permian mass extinction and the Early Triassic recovery phase, we examine during this excursion sedimentary rocks of the Late Permian - Early Triassic Saiq Formation from the eastern rim of the Arabian Plate at Wadi Aday. The thick sequence of carbonate and siliciclastic deposits offers the opportunity (1) to study the impact of the end-Permian mass extinction on carbonate production and (2) to discuss how perturbations of Early Triassic ocean chemistry influenced the recovery patterns of biota of epeiric carbonate platforms.
Stable carbon isotope data and biota of the mostly dolomitized carbonates indicate repetetive perturbations of the biogenic carbonate factory as evidenced by a negative carbon isotope shift at the PTB, followed by positive and negative excursions during the Early Triassic recovery. The described sequence at the rim of the Arabian plate differs from inner platform settings, where a shorter recovery phase has been observed for shallow-water benthos. Our findings support the idea of differences in the kinematics of the end-Permian mass extinction. In the vicinity of the epeiric Arabian platform, recovery of calcified bentic metazoans was rapid in inner platform areas and prolonged at the rim due to oceanic perturbations of the Tethys.

Geology of the Saih Hatat: The tectonic window in the vicinity of the Saih Hatat provides excellent exposures of the

- Sedimentary Basement of latest Proterozoic to Ordovician age.
- Middle Permian-Late Cretaceous carbonate Arabian Platform (Hajar Unit).

During Middle Permian – Early Triassic times a long-lived epeiric carbonate platform developed in the vicinity of the Arabian Plate. These carbonate-dominated deposits, which are commonly called Khuff formation in most regions of the Middle East, contain the most prolific gas reservoir in the Middle East and are therefore of extraordinary importance. In the central and eastern Oman Mountains time-equivalent platform carbonates of the Khuff formation have been traditionally described as Saiq Formation (Glennie et al. 1974). The currently favoured facies model for the Middle Permian – Early Triassic carbonates of the Khuff and Saiq formations is a homoclinal ramp system with gentle facies transitions towards east. In an ideal transect from west (land) to east (Tethys), facies associations pass from marginal marine siliciclastics into inner platform lagoonal carbonate-anhydrite cycles and finally into open marine platform carbonates and slope deposits of the rim of the Arabian plate. According to Le Metour et al. (1986) the Saiq Formation covers the following members at Wadi Aday (Fig. 9):

Top

Ma Bedded dolostone, grey or pink

SQ3 Black sparitic limestone and yellow shale
Dolomitic limestone,stromatolitic
Clayey dolostone and siltstone, quartz sandstone

SQ2b Silicified limestone and dolomitic limestone, yellow patina
Sandstone and platy, yellow-weathering dolomitic limestone, silicified black limestone

SQ2a Massive dolostone, yellow patina
Grey and white banded dolostone
Grey-black dolomitic limestone
Beige micriyic limestone

Sq2v Mafic to intermediate volcanic rocks

Sq1l Limestone and dolostone
Massive dolostone

Sqv1 tuffite, white tuff, schist and conglomerate

Base

Having the aforementioned ramp model in mind, carbonates of the Saiq Formation in the Saih Hatat (Fig. 10) differ from the carbonates of the Saiq Plateau (see excursion Feb. 23) in terms of facies associations and carbonate secreting metazoans to some extent. The carbonates of the Saiq formation in the Saih Hatat display a vertical succession from Guadalupian photozoan carbonate to Lopingian heterozoan carbonate and to Early Triassic predominantly heterozoan carbonate producing associations with photozoan intervals at the base (Fig. 11). Dolomitized carbonates of the Middle to Late Triassic Mahil Formation are dominated by photozoan carbonates (terminology used in the sense of Beauchamp and Desrochers, 1997). The Middle Permian to Early Triassic depositional history of the eastern rim of the Arabian plate was addressed for the Saih Hatat by Weidlich and Bernecker (2003, 2007) and Weidlich (2007, 2010). The excursion is based on results submitted for publication by Weidlich and Bernecker. Close to the rim of the Arabian Plate, the Lopingian – Early Triassic was a time of intense tectonic activity during rifting of the Neo-Tethys. In the study area, volcanic rocks, breccias with a high fitting of the clasts and slumping structures documented rift pulses. Synsedimentary faults locally dissected the carbonate platform and caused drastic lateral facies changes.

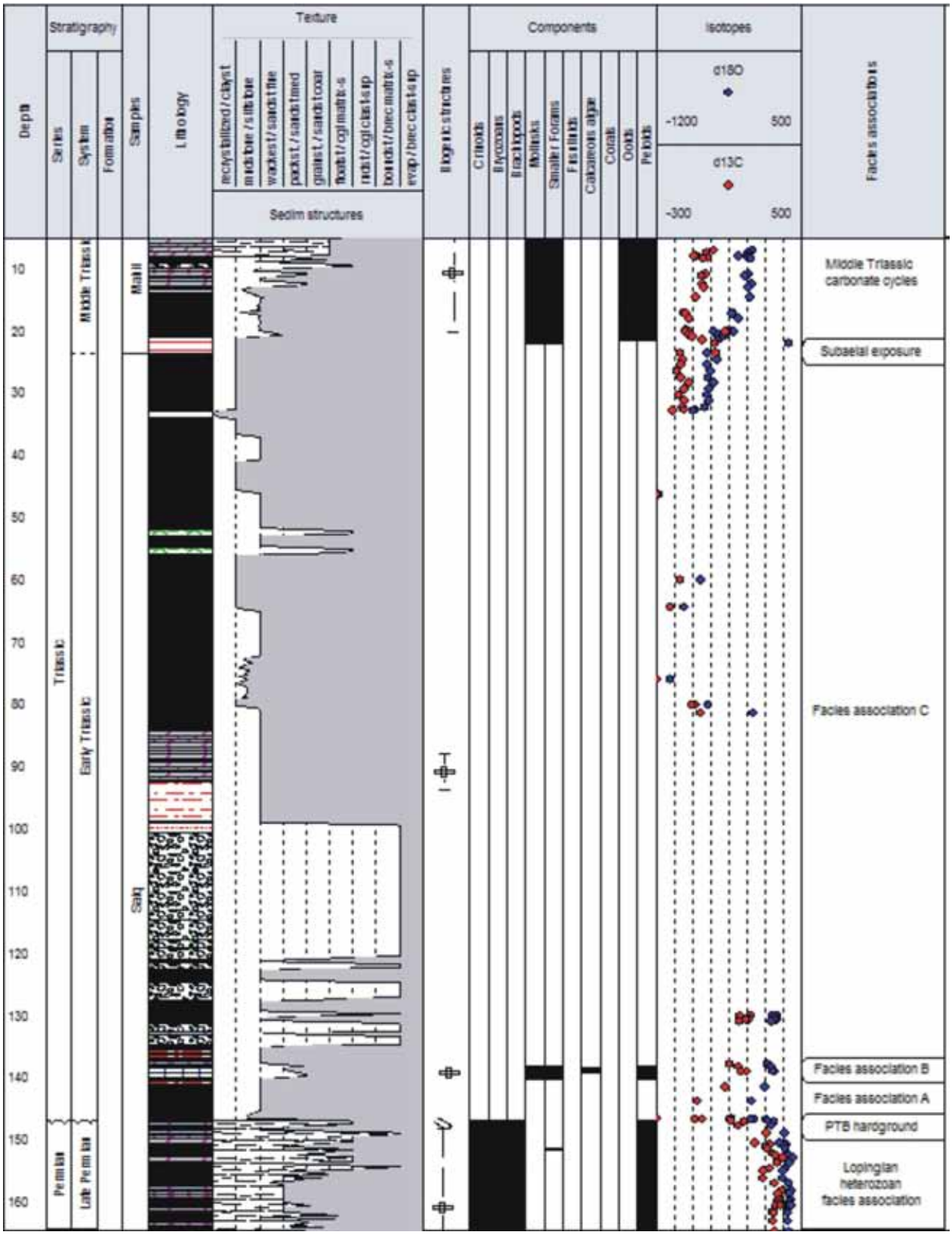

Figure 10: Composite section of the study area (from Weidlich & Bernecker submitted).

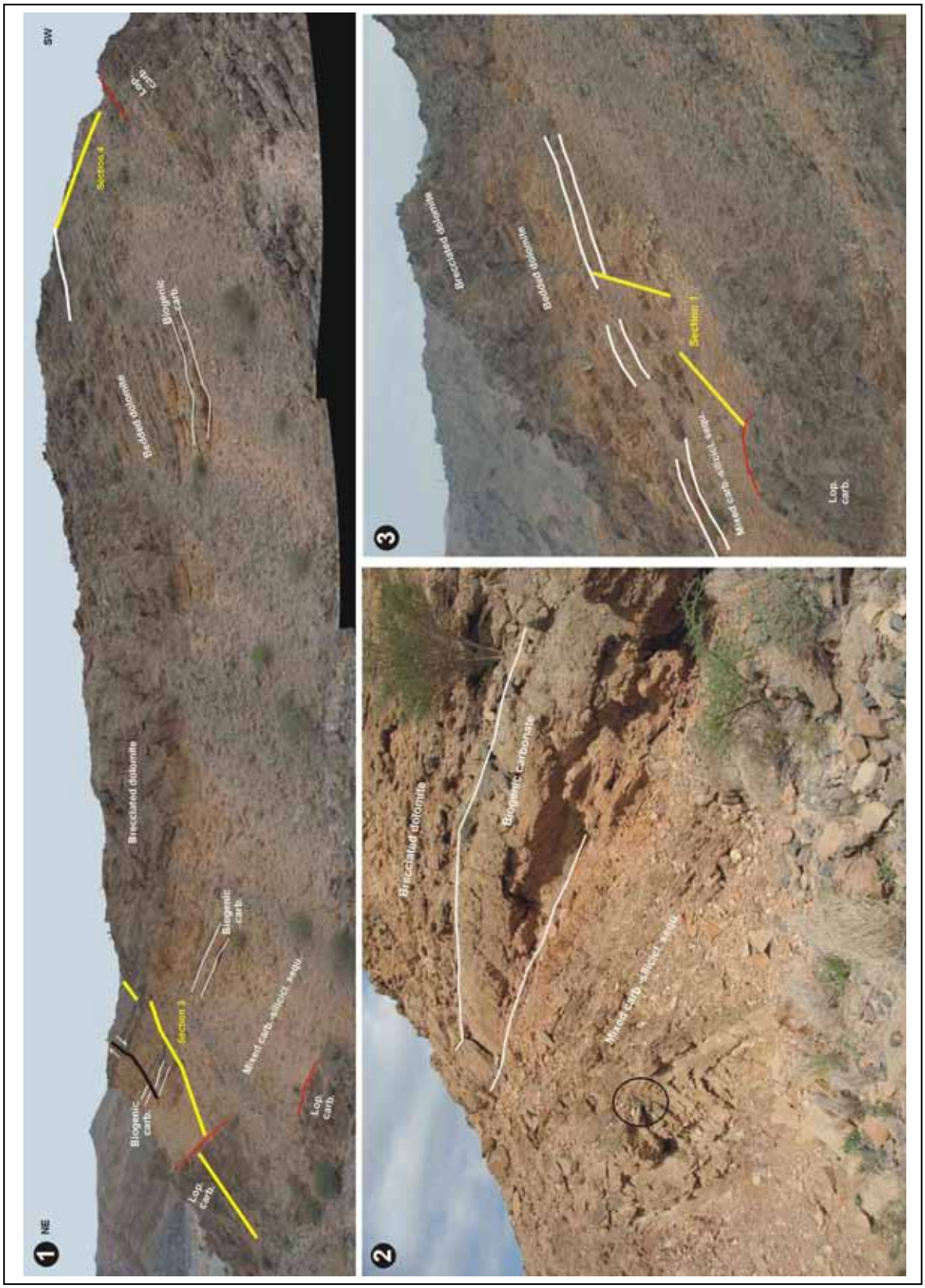

Figure 11: Outcrop appearance of Permian-Triassic sections near Wadi Aday. (1) Photomosaic covering sections 3 and 4. Dip of bedding planes of Lopingian carbonates varies from block to block; red line highlights the PTB. (2) Early Triassic sequence exposed at section 3 above the (3) Field photograph of section 1.

Changhsingian carbonates and PTB: In the visited transects, textures and microfabrics of the sedimentary rocks have been mostly well preserved despite pervasive dolomitization (mimetic non-planar equidimensional replacement dolostone) and metamorphism (obduction of the Semail ophiolite). Post-obduction tectonism is responsible for northward tilt of strata.

The focus of this excursion is on the uppermost 20 m of the Changhsingian Saiq Formation (Figs. 12-13), where the age-diagnostic foraminifer *Colaniella nana* has been found. The almost completely dolomitized carbonates are well exposed in a wadi southeast of Wadi Aday. There, Lopingian carbonates, with bed thicknesses between 5 to 80 cm, form resistant cliffs with weathered surfaces in dark greyish, brownish or blackish colours. Synsedimentary rift pulses, a consequence of the renewed opening of the Neo-Tethys, affected the Lopingian platform carbonates at the eastern rim of the Arabian plate in several dimensions. Evidence for tectonic instability during or soon after the deposition of the carbonates comprises, on the metre scale, bedded platform carbonates intercalated with breccias and on the cm-scale mineralized and sediment-filled fissures and microbreccias.

Biota of the Lopingian Saiq Formation include brozoans, crinoids and brachiopods, all typical of a fully marine environment and contrast to the Guadalupian members of the Saiq Formation where calcareous algae, fusulinids, calcisponges, cerioid corals, alantoconchid bivalves prevail. The Lopingian facies association consists in decreasing abundance of the following facies types:

- Bryozoan crinoid floatstone
- Brachiopod floatstone
- Mudstone to skeletal wackestone
- Monomict lithoclastic float-/rudstone

The above described facies types exhibit a random distribution within the Lopingian section because no trend or pattern has been observed. The last bed of the Lopingian facies association is bryozoan crinoid floatstone with patches of brachiopod floatstone. This bed is capped by a prominent **discontinuity surface** with the following features:

- The surface has an irregular wavy habit in the field with smooth depressions and dissolution-enlarged fissures. The relief, with a maximum height of 15 cm, is a combination of syndepositional normal faults and discontinuity-related processes that will be mentioned below. Polished slabs and thin sections provide on the sub-centimetre scale evidence for corrosive sharp edges of the discontinuity.
- A characteristic phenomenon of the discontinuity is a variety of mineralization products ontop the surface and within the underlying strata. (i) Most conspicuous are brownish-blackish goethite and limonite crusts with a thickness between 0 and 2 cm. (ii) Open fractures, clast of microbreccias and burrow structures are lined by reddish-brownish and black crusts. (iii) Obvious is also the diffuse reddish-brownish penetrative staining of dark grey dolomitized limestone with a maximum depth of 5 - 10 cm. (iv) Down to a depth of 1 m, intraparticle pores of skeletal grains and moulds of grains can be filled with brownish iron oxids. (v) Finely dispersed pyrite occurs with varying abundance in the sediment and pyrite in intraparticle pores and fractures.
- *Thalassinoides*-like burrow structures developed beneath the surface prior to mineralization. The biogenic structures are filled either with wacke-/packstone resembling the surrounding sediment or crinoid packestone with iron-rich brownish matrix.
- Aside from the above mentioned criteria, a sharp negative excursion in the $\delta^{13}C_{carb}$ composition of about 4‰ was detected (Figure 10).

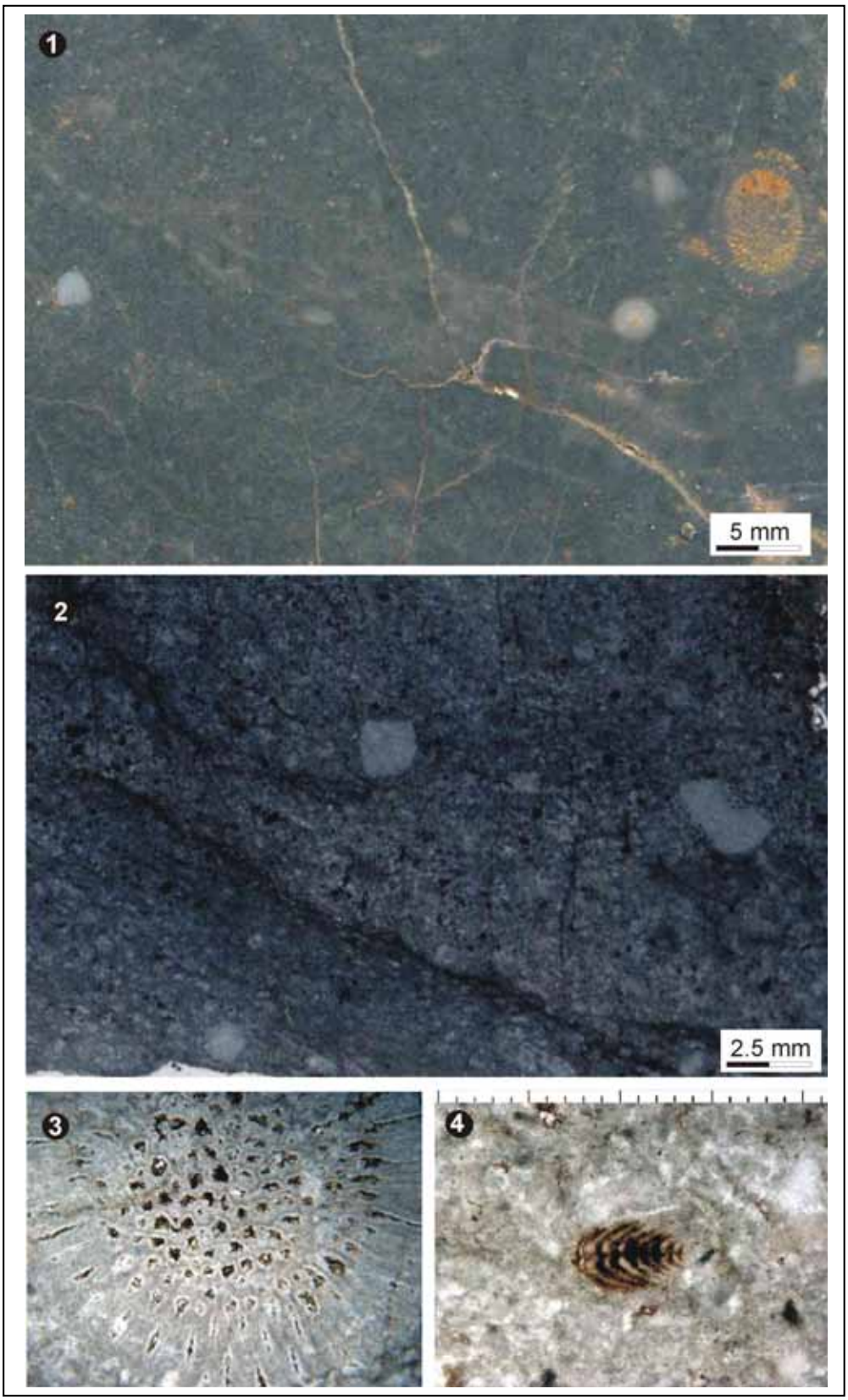

Figure 12: Changhsingian heterozoan facies below the Permian-Triassic boundary. (1) Polished slab of bryozoan-crinoid floatstone. Note Fe-oxid stain. (2) – (3) Photomicrograph of packstone matrix of bryozoan-crinoid floatstone with framboidal pyrite. (4) Sagital axial section of smaller foraminifera Colaniella nana, indicative of a Changhsingian age.

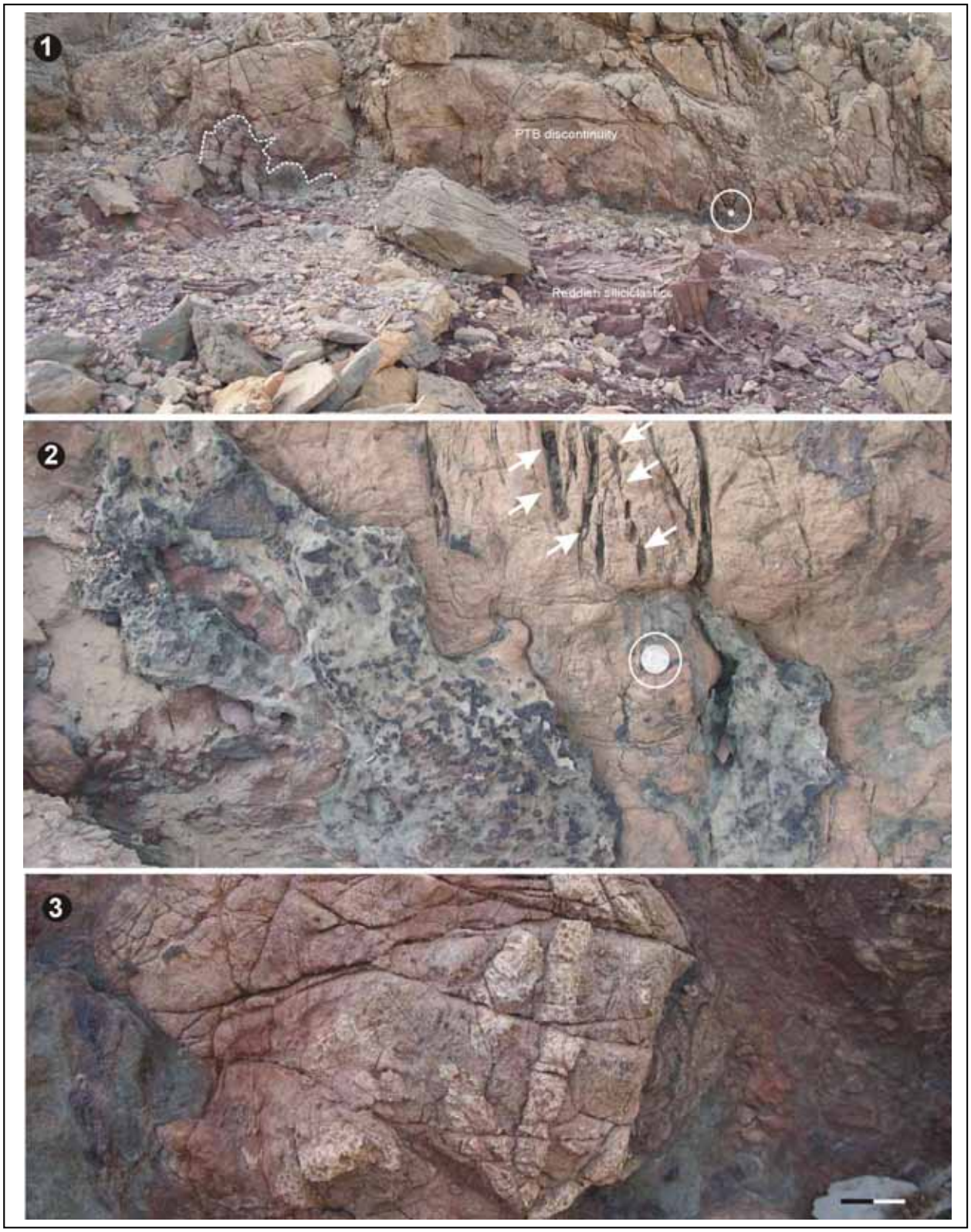

Figure 13: Changhsingian heterozoan facies, PTB and basal Early Triassic clastic facies association, section 1. (1) Permian-Triassic discontinuity surface and unfossiliferous siliciclastic mudstone with nodules of Fe and Mn oxids (stippled white line) overlain by fine-grained red siliciclastics. (2) Unfossiliferous siliciclastic mudstone with nodules of Fe and Mn oxids fills the depressions and fissures of the unconformity. Arrows highlight sediment-filled fractures. (3) The Lopingian dolomitized carbonate below PTB contains bryozoans (centre of photograph).

Early Triassic Saiq Formation: Synsedimentary block faulting, a result of rift events in the Neo-Tethys, created during and after the PTB the accommodation space for the following sequence:

- **Facies association A – Mixed carbonate-silicilastic sediments with upward increasing carbonate content:** The graben structure was filled in the deepest part with reddish or brownish siliciclastic silt- and fine-grained sandstone. The thickness of the mixed carbonate-siliciclastic facies association varies between 0 to 16 m depending on the position along the transect. Bank thicknesses are in the dimension between few milimetres to few centimetres. The lack of macrofossils and ichnofossils as well as the presence of nodules of iron and manganese oxids remain the most striking features of this facies and contrast with underlying bioclastic carbonates of Lopingian age. The reddish fine-grained siliciclastics pass into yellowish friable siltstone and fine-grained calcareous sandstone and are overlain by alternations of thin-bedded yellowish carbonaceous siltstone and dolomitized mudstone. The upper part of the sediment fill of the small graben structures reflects the change from siliciclastic-rich, friable deposits to carbonate-rich thin-bedded rocks. The sequence is terminated by reddish mudstone and siltstone. Synsedimentary slumps and folds indicate the sporadic occurrence of tectonic pulses during the deposition of this unit. Petrography of the carbonaceous siltstones and dolomitized mudstone reveals that indistinctly bioturbated mudstones alternate with occasionally deposited thin packstone intervals. The deposits contain nodules of iron and manganese oxids. Low-relief thin stromatolites were observed which consist of well cemented laminae. Measured stable carbon isotopes show a drastic negative excursion as $\delta^{13}C_{carb}$ values exhibit a negative shift.
- **Facies assocciation B – Bioclastic carbonate with grain- and mud-support fabrics**: Obvious is from the distance in the field an approximately 1.0 to 1.5 m thick carbonate bank with massive appearance. Upon closer examination, the following sequence becomes evident from base to top: The lowermost unit, probably 20 cm thick, is dolomitized mudstone with burrow structures filled with bioclastic packstone. The geopetal fill comprises notably recrystallized bioclasts, the debris of crinoids and small mollusks. The main unit, about 1 m thick, is characterized by a drastic facies change, as the dolomitized unit is dominated by strongly bioturbated wacke-/packstone with recrystallized mollusks (microgastropods and thin bivalves) and grainstone with peloids, mud clasts, cortoids, echinoderm debris, smaller foraminifera and rare dasycladacean algae. Peloids also comprise fecal pellets without internal structure. Smaller foraminifera, such as *Pilamminella* sp. and *Earlandia* sp., indicate an Early Triassic age. Disarticulated crinoid ossicles have iron-stained rims and are intensely bored. Microborings resemble clionid sponges, which are known from Permian Rugosa (Weidlich, 1996) and have not been reported from Early Triassic strata so far. Interparticle pore space was cemented by bladed to fibrous isopachous calcite and blocky calcite. The massively bioturbated carbonate contains small unconformities which are already visible in the field. Petrographic evidence for the corrosive nature is the steep to overhanging microrelief. Some of these are overlain by microsparitic mud- to wackestone which pass into strongly bioturbated wacke- to packestone and grainstone as below. In addition, simple and straight borings are visible in the field and in thin section. The uppermost 30 cm are dominated by indistinctly bioturbated mudstone with bivalve floatstone lenses. The thin-shelled bivalves resemble *Halobia* sp. The facies is capped by a low-relief, erosional unconformity and is overlain by mudstone with scattered bioclastic debris at the bottom. $\delta^{13}C$ values display positive excursion. A second horizon of bioclastic carbonate was observed locally (Fig. 10).
- **Facies association C – Bedded dolomitized mud- to wackestone with microbialites and trace fossil horizons**: The bioclastic carbonate is overlain by an about 40 m thick alteration of thin-bedded dolomitized mudstone and silty mudstone with variable colour. XRD data point to dolostone, ankerite, calcite, quartz and muscovite as dominant minerals. An about 20 cm thick bank of **laminated microbial bindstone,** consisting of laterally linked low-relief hemispheroids, occurs at the base of this facies asociation. The lateral continuity is unknown since the unit is

surrounded by tectonic breccias. The typical facies comprises thinly bedded yellowish, dark grey and light grey intercalations of dolomitized mudstone with bed thicknesses varying between 5 to 15 cm. Characteristic sediment structures are horizontal bedding, erosional small channels (diametre 20 to 30 cm) and liquefication of unconsolidated sediment. Locally, the sediment is intensely brecciated. Angularity and high fitting of clasts indicate a tectono-sedimentary origin of the deposits without significant lateral transport of the clasts. The uppermost 8m of this unit are increasingly dominated by beds of bioturbated mudstone or microbial bindstone. **Bioturbated dolomitized mudstone** beds, with a thickness of 10 to 20 cm, are dark and light-coloured sediment containing the ichnotaxon *Planolites*. The thrombolites exhibit a laminated internal structure with a very low relief. The prevailing textural types are mudstone as well as peloidal wackestone and fine-grained packstone with a typical clotted fabric. Obvious are stromatactis-like cavities that are partly cemented and partly filled with geopetal sediment. From the ceiling of the cavity dolostone with brown bands indicative of multiple precipitation events and/or changing pore water chemistry has been found. The unit is capped by a brecciated bed. This facies association displays an increase in stable carbon isotope values (Fig.10).

- **Facies association D – Thinly bedded yellowish silty dolostone and black calcite**: Above the brecciated bed the texture changes towards alterations of extremly thin-bedded (1.5 to 2.5 cm) yellowish dolostone and silty dolostone and black calcite. This unit attains a total thickness of about 60 m. The sequence starts with yellowish dolostone mudstone followed by black calcite. Most of the yellow mudstone is finely laminated dolostone and ankerite with varying perecentages of quartz and muscovite; it contains dark grey layers which are heavily faulted from time to time. The basal black calcite is heavily bioturbated; the dominant biogenic structures, which resemble *Planolites* and *Thalassinoides*, are mostly parallel to bedding. Higher up in the section, beds yield individual burrow structures that exhibit a spreitenbauten-like fabric. The black calcite is strongly recrystallized; petrographic analysis of representative samples confirmed that sea floor cements might have played a significant role in the formation of the black calcite. It consists of centimetre-scale calcite crystals with pronounced twin lamellae. These precipitates resemble Olenekian seafloor cements of the Union Wash Formation of the southwestern U.S. (Woods et al., 1999). This facies association displays a negative and positive shift of $\delta^{13}C_{carb}$ (Fig.10). The sequence is interrupted by two conglomeratic beds. Slumps and debris flow deposits are associated with the dark calcite. The black calcite is capped by a pronounced subaerial exposure horizon (Weidlich, 2010) followed by Middle Triassic ooid bioclast grain- and packstone.

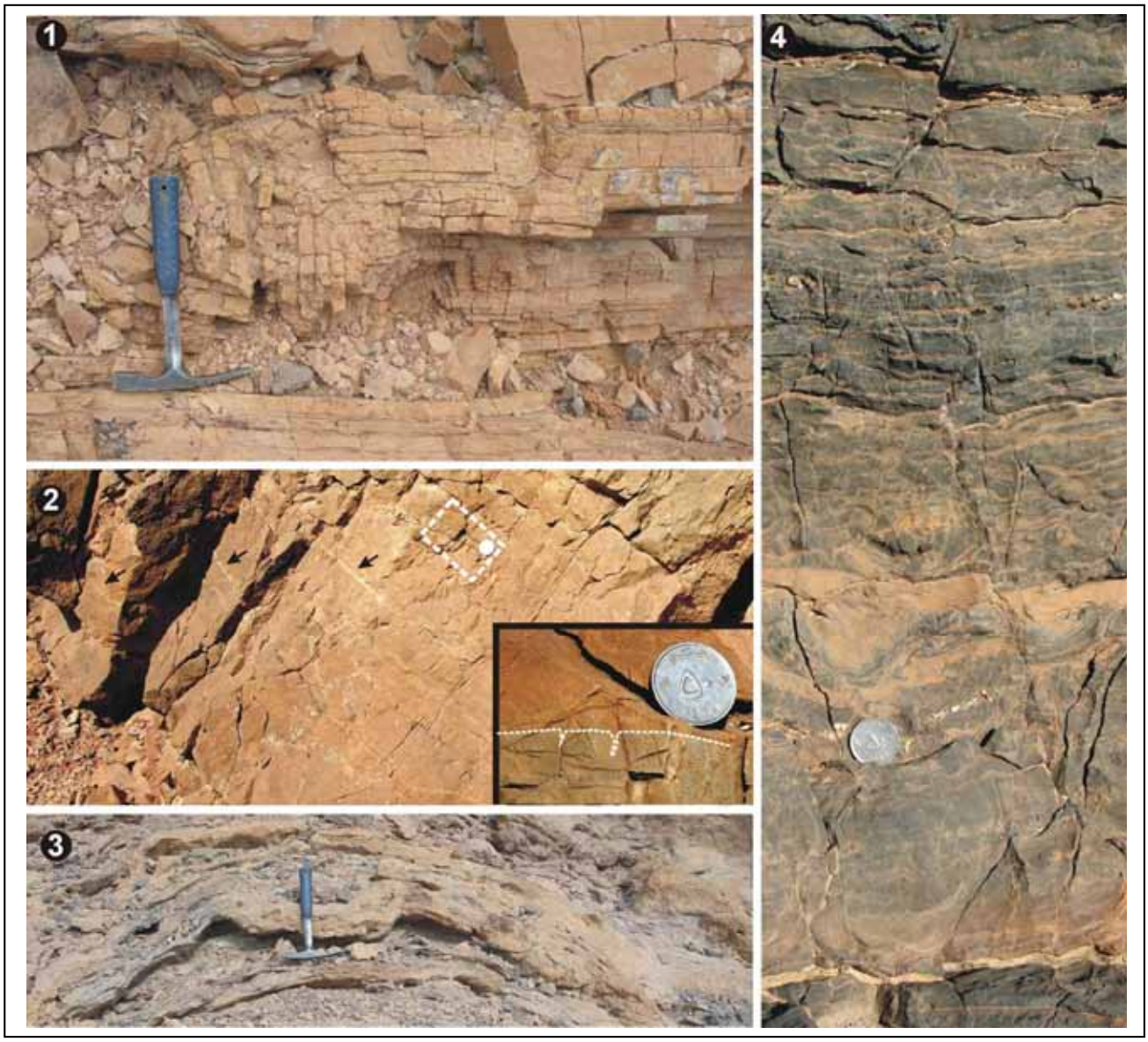

Figure 14: Close-up field photographs illustrating from base to top the reestablishment of Early Triassic carbonate platform facies, section 3. (1) Field photograph of mixed carbonate-silicilastic facies association with upward increasing carbonate content. Slumped package of sediments indicates synsedimentary tectonic activity. This unit contains thin stromatolites. Size of hammer is 32 cm. (2) Field impression of the bioclastic carbonate facies association with grain- and mud-support fabrics. Note light grey discontinuity surfaces (black arrows) separating amalgamated bioclastic pack- and grainstones. Inserted close-up illustrates a discontinuity. Diametre of coin is 2.5 cm. (3) Field photograph of bedded dolomitized muddy facies association with microbialite. (4) Upper part of the bedded dolomitized muddy facies association with microbialite. Note slumping structure. Coin is 2.5 cm in diametre.

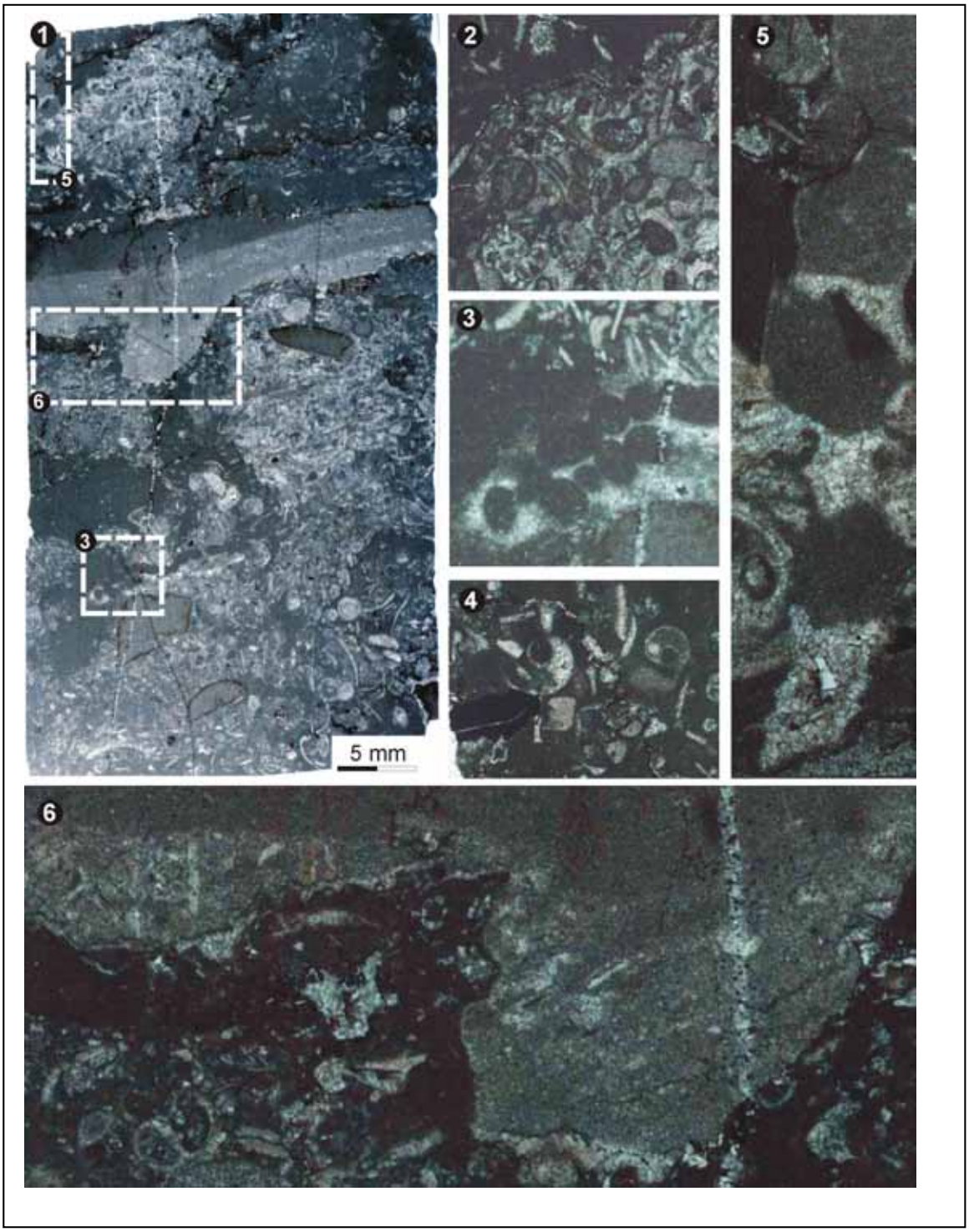

Figure 15: Representative thin sections of Early Triassic bioturbated bioclastic carbonate platform facies. (1) Overview of thin section illustrating the bioturbation of mircogastropod wackestone and bioclastic pack-/grainstone with Fe-stained crinoid ossicles of grainstone. The two sediment types represent different hydrodynamic regimes and depositional environments. (2) Close-up view of bioturbated sediment. Bioclastic pack- to grainstone contains dasycladacean algae, shell debris and cortoids (recrystallized bioclasts with thin micrite envelope). Boundary between the two types of sediments is sharp but not erosive. (3) Close-up view of internally structureless fecal pellets. (4) Photomicrograph of wackestone with microgastropods. (5) Photomicrograph view of microboring affecting the lithified biogenic sediment. (6) Close-up view of corrosive discontinuity surface. See text for details.

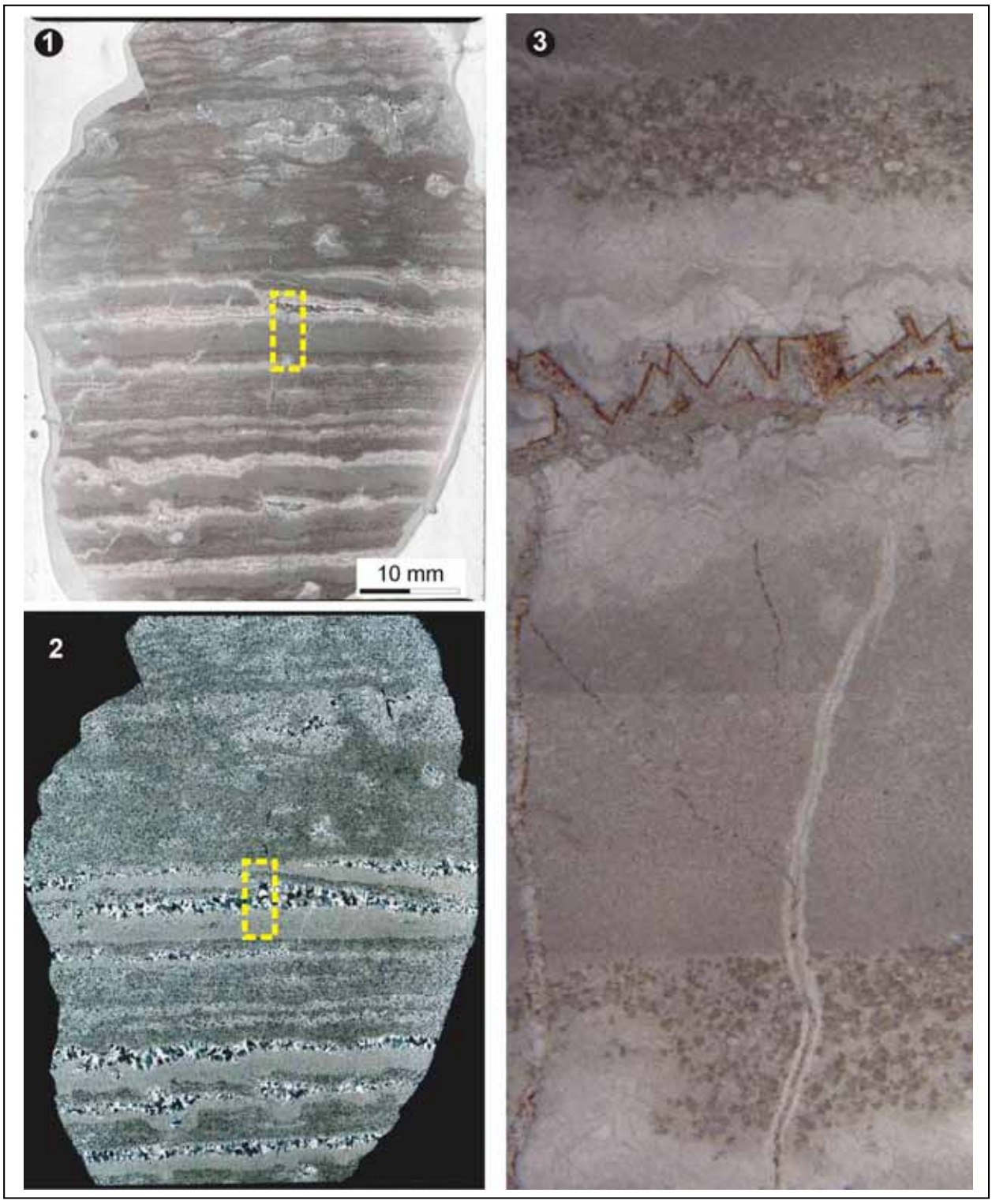

Figure 16: Representative thin section of Early Triassic microbialite, sample 292x. See Fig. 14 for field impression. (1) - (2) Overview of thin section under PPL and XPL. See text for details. 3 Close-up-view of Stromatactis cavity. Note sediment infill of cavity and pendant zoned planar-e dolostone rhombohedra.

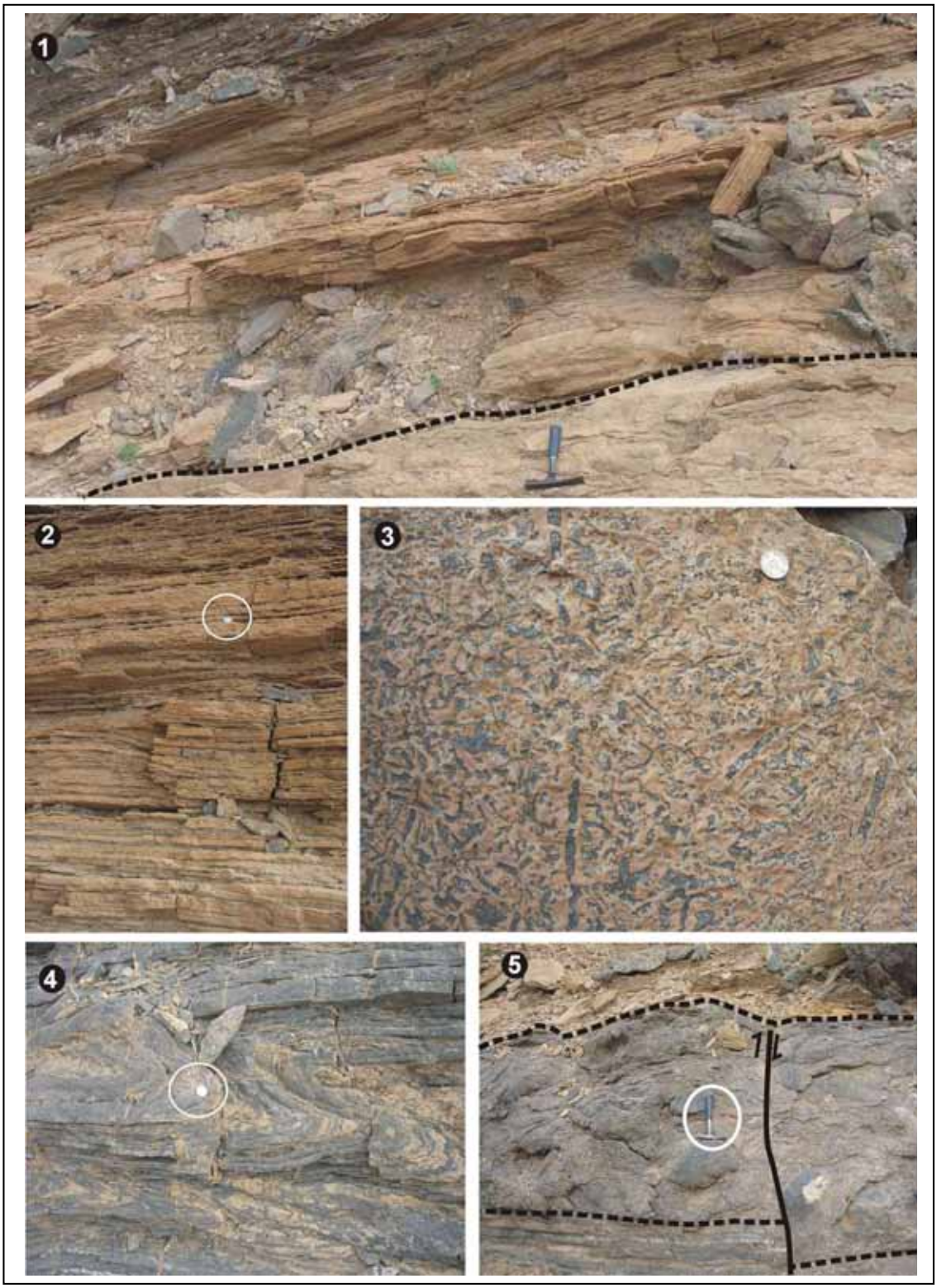

Figure 17: Close-up field photographs of Early Triassic transect. (1) Top of bedded dolomitized muddy facies association. (2) Yellowish dolomitized mudstone. (3) View on bedding plane with Thalassinoides and Planolites-like trace fossils, top of bedded dolomitized mudstone. (4) Slumping structure of black calcite, thinly bedded facies association with yellowish silty dolostone and black calcite. (5) Conglomerate, thinly bedded facies association with yellowish silty dolostone and black calcite.

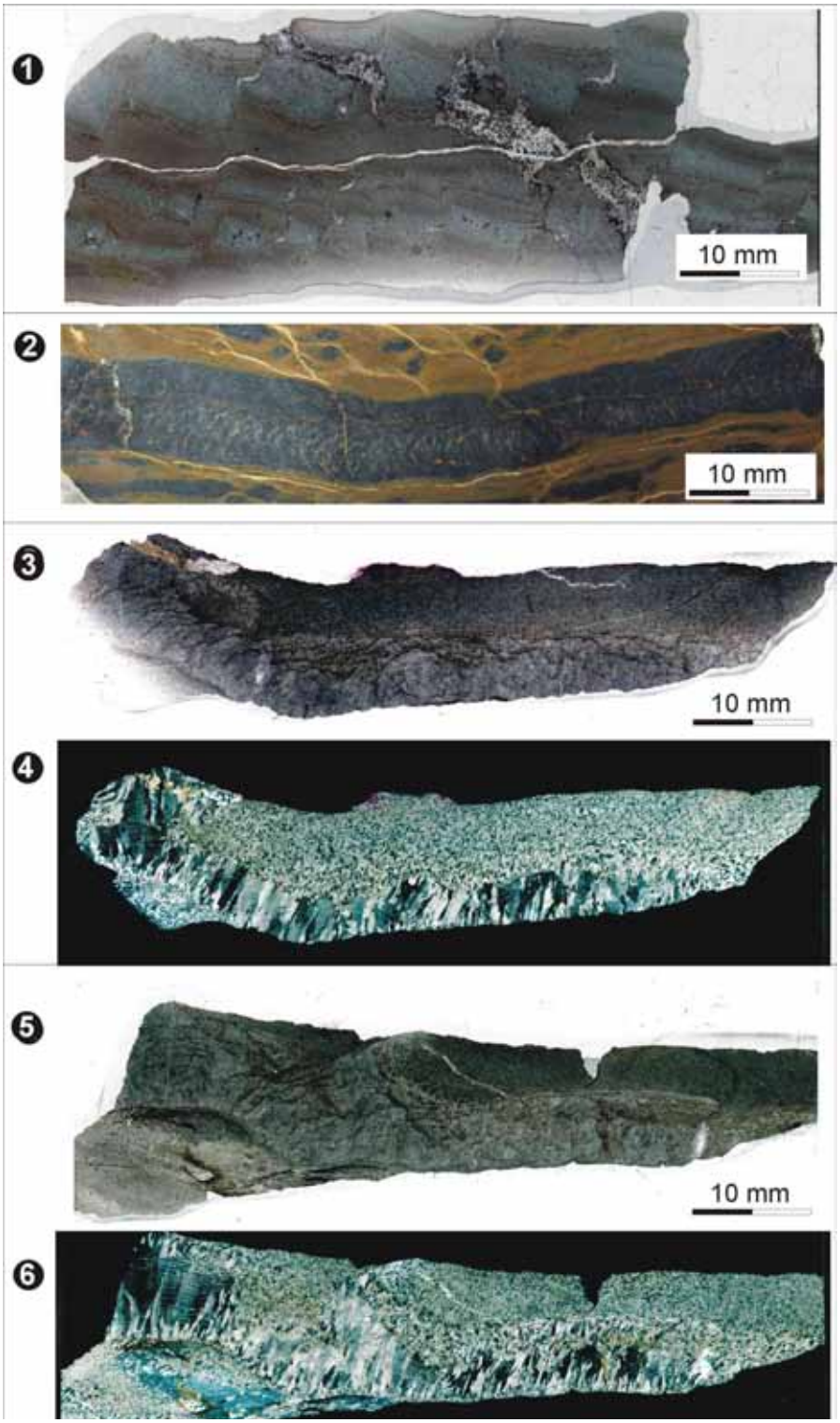

Figure 18: Close-up views of bedded dolomitized mudstone with trace fossils and microbialites (facies association C) and thinly bedded yellowish silty dolostone and black calcite (facies association D). (1) Photomicrograph (plane-polarized light) of intercalations of dolostone with silty dolostone, facies association C. Abundant micro-faults of dolomitized mudstone indicate rapid synsedimentary lithification of mudstone prior to tectonic brecciation. (2) Polished slab of spreitenbau (trace fossil). (3) – (4) Paired photomicrographs (plane-polarized and cross-polarized light) synsedimentary seafloor cement. (5) – (6) Paired photomicrographs (plane-polarized and cross-polarized light) synsedimentary seafloor cement.

Conclusions: The results of this excursion shed new light on the complexity of the Early Triassic post-extinction recovery. A sequence of about 130 m of Late Permian-Early Triassic sediments accumulated at the rim of the Arabian platform. Based on our data, we propose the following sequence of events for the end-Permian mass extinction and the Early Triassic recovery:

(1) Biogenic carbonate production dominated by members of the heterozoan carbonate factory; collapse of carbonate sedimentation at the end of Permian.

(2) During the early aftermath of the mass extinction, siliciclastic sediment accumulation dominated while carbonates were corroded.

(3) Re-start of carbonate production in a "marine abiotic default mode".

(4) Rapid but short-lived recovery pulse of benthic heterozoan carbonate production.

(5) Switch to abiotic and microbial carbonate production, trace fossils indicate presence of uncalcified benthos, limited carbonate production by microbes.

(6) Return to abiotic default mode of carbonate production during 2nd negative carbon isotope excursion, absence of trace fossils indicates deterioration of environmental conditions.

(7) Recovery of photozoan carbonate production after subaerial exposure and reflooding of the Arabian plate.

Unfavourable Early Triassic oceanographic conditions were suggested for the Neo-Tethys, including oceanic anoxia and variations of calcium carbonate saturation (e.g., Baud et al., 2007; Woods and Baud, 2008) under postulation of rapid recovery (Twitchett et al., 2004). Permian-Triassic sections of the inner platform described from Saudi Arabia (e.g., Vaslet et al., 2005) and Iran (e.g., Insalaco et al.., 2006) support this interpretation and have in common with our data that the end-Permian mass extinction seriously hit calcified benthic metazoans in all environments. By contrast, Early Triassic facies developments at the eastern rim of the Arabian plate (our data set) parallels only to some extent the epeiric inner platform development. Special feature of the platform rim setting, as described before, are 1) Fe- and Mn mineral crusts on the PTB discontinuity surface followed by condensed sediments with Fe- and Mn-nodules, 2) limited importance of microbialites which are a common and repetitive phenomenon elsewhere (Baud et al., 2007) and 3) pulsed, short-lived recovery of the heterozoan carbonate production which was followed by a thick sequence of abiotically precipitated carbonate.

We conclude that inner platform environments of the Arabian plate recovered faster than platform rim settings. This discrepancy was already described as differential severity of the end-Permian massextinction and the Early Triassic recovery period (Weidlich and Bernecker, 2007). Our observation coincides with the statement of Miller and Foote (2009) who recognized differences in the kinematics of mass extinctions. Their statistical data set suggests higher extinction rates for end-Permian taxa of 'open-ocean–facing settings' and higher origination rates for Early Triassic 'epicontinental' taxa.

February 23, 2010 -The Permian-Triassic transition on the Saiq Plateau

(A. Baud, B. Beauchamp, C. Henderson, S. Richoz).

Routing (Fig. 19): Starting at 8 p.m., February 23, from Hotel Ibis (Muscat) we will move to Birkat al Mawz following the Muscat-Nizwa highway. From Birkat we will take the scenic road climbing to the village of Saiq on the Saiq plateau at about 2000m in elevation. North of the village we will take a side road in direction of the village of Hajirate and stop in a quarry on the left (Fig. 6 left).

Figure 19: right, Google Map with road itinerary in red; left, Google Earth picture of the outcrops area, with in red, the road itinerary; –red bar, place of the 3 visited sections, below the abandoned quarry (Quarry coordinates: N23°10' 00'' E 57° 39' 50'').

Introduction: One of the best exposure of the Permian-Triassic transition of the Oman Autochthonous is situated on the southern flank of the Djebel Akdhar antiform, around the mountain village of Saiq (Fig.) at the altitude of 2000m about 100km SW of Muscat. It is the type area of the Permian Saiq Formation defined by Glennie et al. (1974).
Due to gentle regional diP, the high quality and easy access of the outcrops, each strata of the Saiq and Mahil Formations can be followed over hundreds of metres (Fig. 20).

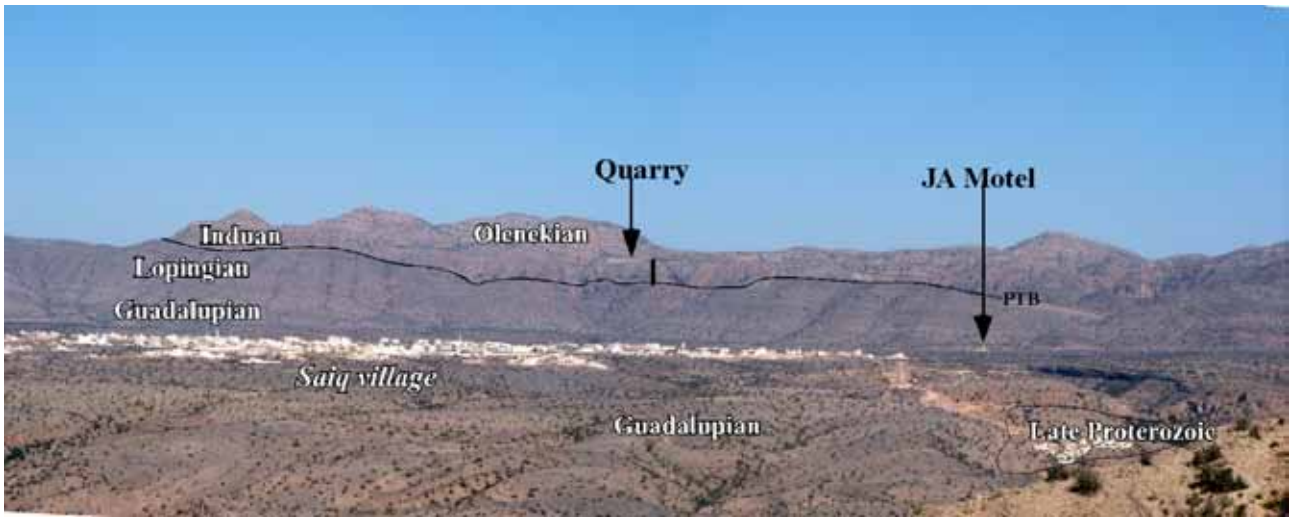

Figure 20: Panorama of the Saiq plateau, corresponding to the map (Fig. 6 left) with age of the Permian-Triassic units. Vertical bar near the Quarry =PTB examined section with the 3 stops of the day (car parking in the basal Mahil Formation, coordinates: N23°10' 00'' E 57° 39' 50'').

According to the geological map of Nakhl, contact faults are concentrated in the northern and western part of the Saiq Formation outcrops (Fig. 21).

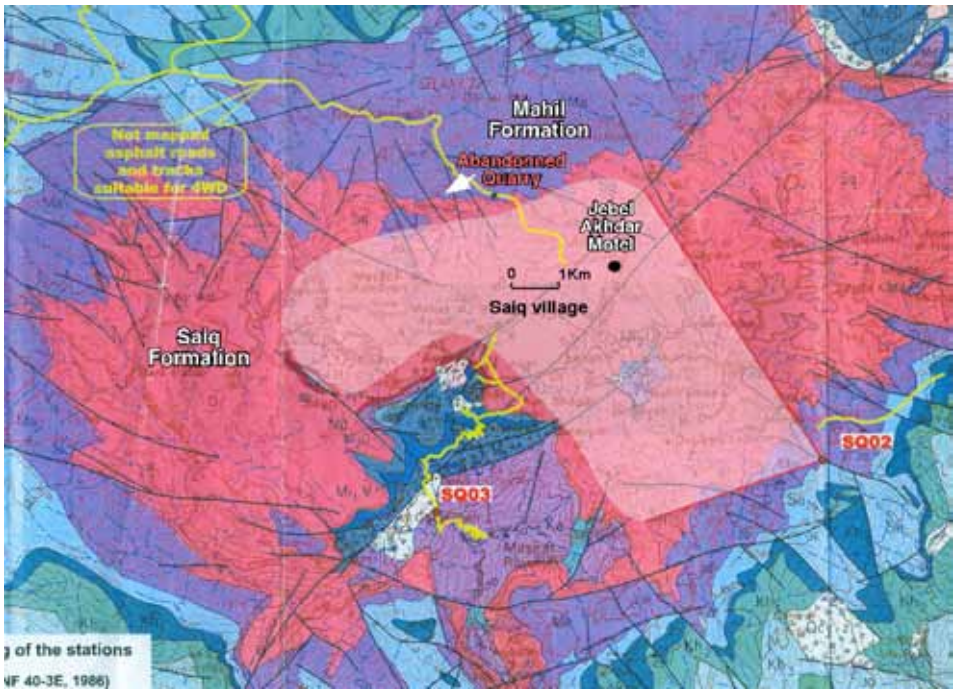

Figure 21: Geological map of the Saiq Plateau (Extract from the geological map of Nakhl, from Rabu et al., 1986). Saiq Formation in pink and Mahil Formation in violet.

The Permian-Triassic section is more than 1000m thick and consists of dolomitized shallow water carbonate (Middle-Upper Permian to upper Triassic) except the basal part (Middle Permian) that escapes to dolomitization processes and consists of shallow water fossiliferous limestones (Units A2 to A4, Fig. 23). The three stops of the day will be close to and below the abandoned quarry (Figs. 19-21).

The Saiq Formation (Fig. 22).
The Saiq Formation on the Saiq Plateau has been studied first by Montenat et al. (1976). The basal part of the Saiq Formation, not shown on the figure, has been described by Rabu (1988) and consists of 20 to 30m thick transgressive sediments with basal conglomerate, siltstone followed by marls and bioclastic limestone lenses dated of Lower Guadalupian (Roadian? -Wordian) by foraminifers. Coy (1997) studied the dolomitization of the Akhdar Group on the Saiq Plateau with an extensive description of the lithology and the diagenetic processes. In 2004, he leaded an excursion of the Geological Society of Oman with a description of the upper Saiq depositional model (Coy, 2004).
The top part of the Saiq Formation is defined by following base of the Mahil Formation. The BRGM team (Rabu, 1988, Le Metour, 1990) who studied extensively the Geology of Oman autochthonous for the official Geological map proposed to fix the base of the Mahil Formation at the first terrigenous level (sandstones or clay mudstone) red, orange or yellow in colour, appearing with a change of colour from dark to light of the stratified dolostone succession. Biostratigraphically not well constrained, the Saiq-Mahil boundary has been associated with the Permian-Triassic Boundary (PTB). Using the chemostratigraphy with the carbon isotope curve tool, we have been able to show that the expected PTB was situated about 100m below the Saiq –Mahil boundary in the Wadi Sathan section (Atudorei, 1999, Baud et al., 1999, Richoz et al., 2005, Richoz, 2006). On the Saiq Plateau, the Saiq –Mahil boundary outcrops well in an abandoned

quarry North and above the village of Saiq (Figs. 19-21), along a mountain road to the village of Hajirate.

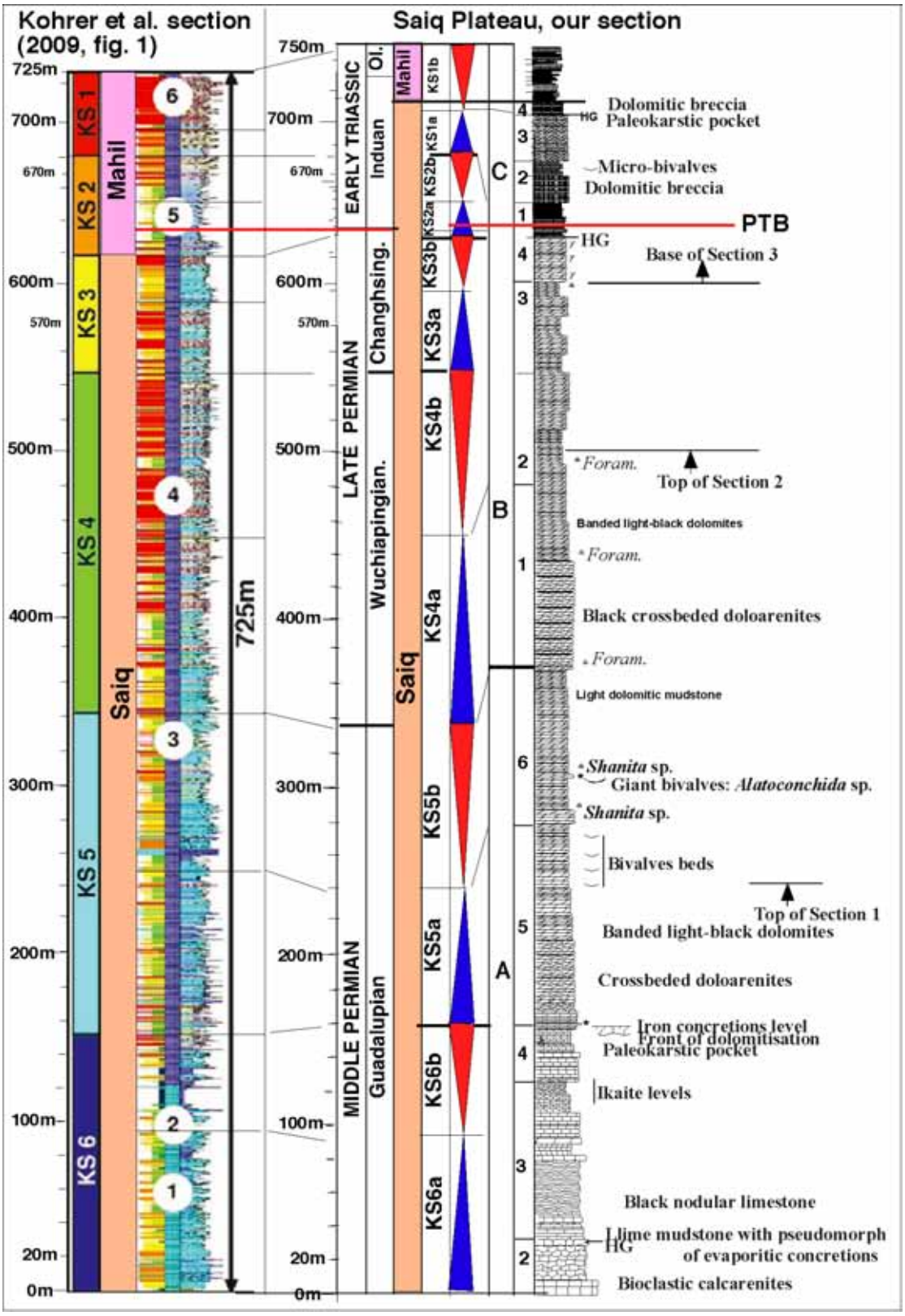

Figure 22: Saiq –lower Mahil composite section on the Saiq Plateau. On the left is the statigraphic column published by Kohrer et al., 2009; on the right is our composite section with our stratigraphic units and the proposed sequences (red and blue triangles) of Kohrer at al., 2009.

correlated boundary does not correspond to the boundary chosen by Kohrer et al., 1999 that is situated about 100m below and their Mahil Sequences KS2-KS1 correspond to our Saiq Member C (Fig. 22).
This Saiq Plateau composite section (Middle Permian-Lower Triassic) consists of a 800m thick succession of limestone and dolostone arranged in shallowing upward cycles (Fig. 9). The Saiq This Formation, about 725m thick, has been subdivided in three Members (A, B and C) and contains four main Transgressive-Regressive cycles (T-R 2nd order cycle). These three Members have been correlated and are more or less corresponding to the Weidlich (2003) supersequences P2 to P4 and are corresponding with the following Kohrer et al. (2009) sequences: Member A with KS6-KS5, Member B with KS4-KS3, Member C and the lower part of the Mahil Formation with KS2-KS1.

Discussion (Fig. 23).
The main recent progress in the study of the Saiq and Mahil Formations have been presented by Baud et al., 2001, Richoz, 2006, Richoz et al, 2005, Richoz et al. in press from the Wadi Sathan. (North-West of the Djebel Akhdar). Weidlich and Bernecker (2003, 2007) described the Saiq and Mahil Formations in the metamorphic Saih Hatat and subdivided the Saiq in 4 Supersequences P1 to P4 and the Mahil in 3 Supersequences Tr1 to Tr 3. The P2 to P4 Supersequences are more or less corresponding our transgressive – regressive cycles A to C.

According to Al-Husseini (2006), the lower Member of the subsurface Khuff Formation in Oman (P 17 to P 19 of Osterloff et al., 2004) is correlated with our Unit A2 and A3. The middle Khuff Member (P 20 to P 40 of Osterloff et al., 2004) corresponds to our A4 and B1-4 Units. The upper Khuff Member (Tr 10 to Tr 20 of Osterloff et al., 2004) correlates with our cycle C (upper Saiq), and must be basal Triassic in age. The base of the Sudair Formation is correlated with the base of the Mahil Formation (Fig. 23).
Taking into consideration the data of Insalaco et al., (2006) in the Zagros, Al-Husseini (2006) suggested the following correlations: the Lower Dalan Member corresponds to our Unit A2 and A3, the Nar Member to Saiq A4, the upper Dalan Member to Saiq B and the Kagan Formation to SaiqC (see Fig. 23).

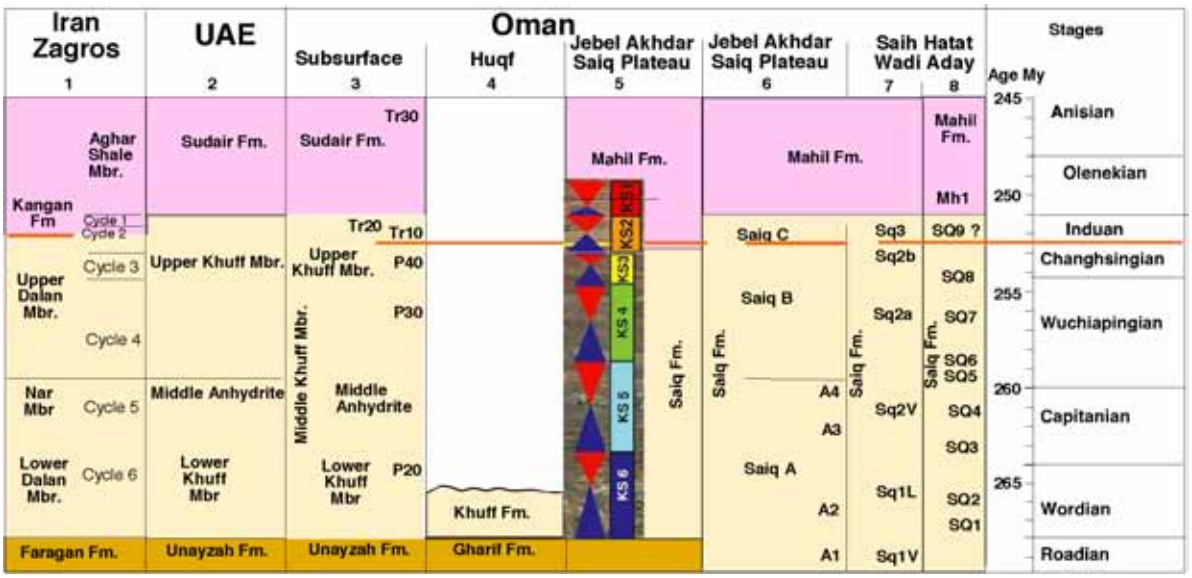

Figure 23: Correlation chart modified and completed from Al Husseini 2006. Data from: 1- Insalaco et al, 2006, 2-4 Al Husseini 2006, 5- Kohrer et al., 2009, 6- our data, 7- Le Metour, 1988, 8- Weidlich & Bernecker, 2003 and this vol.

Description
The lower part of the Saiq Formation with the Member A (corresponding to P2 in (Weldlich and Bernecker, 2003), 400m thick, has been subdivided in 4 units from the base up:
- The A1 unit, partly terrigenous (the lower Saiq of Rabu, (1988) is not examined here.
- The A2 to A4 units (=Kohrer's KS6 sequence), are an about 150m thick pile of limestones that escape to late dolomisation processes and consists of shallowing upward transgressive sequences (Fig. 9). Concentration of iron oxides and paleokarstic pockets at the top record a local emersion of the shallow shelf.

The paleontological content is given in Montenat et al. (1976), with description of the Middle Permian foraminifera, calcareous algae, incertae sedis and marcofauna as bivalves, brachiopods, crinoids and bryozoans. Concerning the age, these units were dated by these authors as *Neoschwagerina schuberti* zone of Middle Murgabian corresponding to a Wordian age, that is supported by the recent finding of the conodonts *Hindeodus excavatus* and *Hindeodus wordensis* by C. Henderson and A. Nicora (Nicora et al., 2009) that ranges from mid-Roadian to Lower Capitanian in the type Middle Permian of West Texas (Wardlaw, 2000).

- The A5 and A6 units (=Kohrer's KS5 sequence), 230 m thick, made of banded light to dark grey dolostone that are partly fossiliferous with large fusulinids beds, bivalve beds and in the upper part by a spectacular giant bivalve *Alatoconchida* sp. level (Fig. 24).

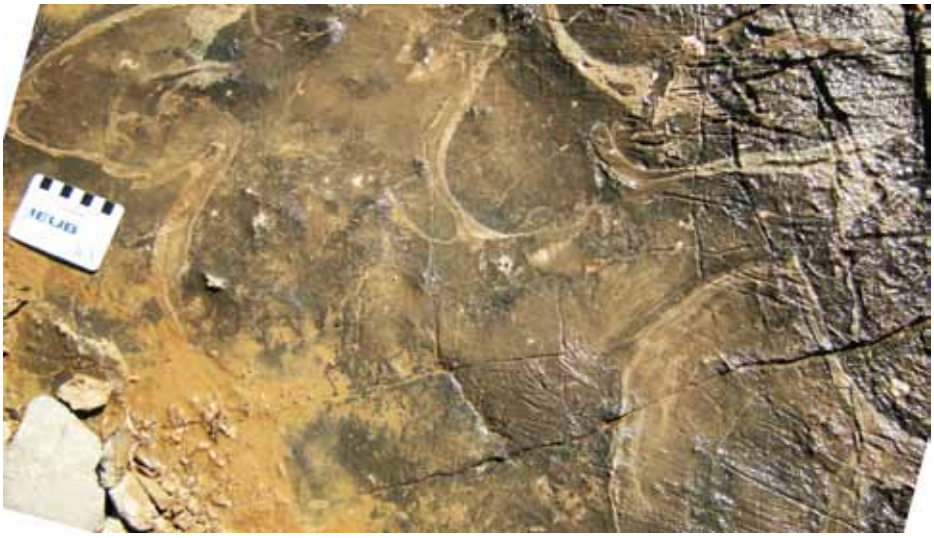

Figure 24: bed surface with shells of Alatoconchida sp.

For the middle part of the Saiq Formation, a previous Lopingian age was based on Staffella cf. *sisonghensis* according to Rabu et al. (1990), but these *Stafella* have been redetermined as *Shanita* by Zaninetti et al. (1979) and now it is giving a Capitanian age according to Insalaco et al. (2006) and to Gaillot and Vachard (2007).
The upper part of the Saiq Formation (300 m) consist of two Member noted B and C (Fig. 22). Both Members are mainly made up of dolomitized high-energy calcareous sands.

The Member B is about 190m thick. Its lower part with B1 and B2 units (=Kohrer's KS4 sequence) is characterized by a thick sequence of high-energy dolopackstone to dolograinstone documenting major flooding of the shelf.
The upper part with B3 and B4 units (=Kohrer's KS3 sequence) is made of well-bedded dolostone.

The B4a unit is the regressive part of the Member B. The base consists of metric-bedded dark bioclastic dolostone with rugose corals colony of *Wentzelella*-type. Within the upper 5 m, there are many levels with solitary rugose corals of *Wentzelella*-type, bryozoan and crinoid concentrations, which probably represent the last skeletal carbonate just below the extinction event surface (E1, Fig. 11).
A possible Late Wuchiapingian - Changhsingian age (Gaillot and Vachard 2007) of the B4a unit is based on the discovery of *Paradagmarita monodi* in another correlative Saiq section by Lys (1988) and by the presence of *Hemigordiopsis* sp. in correlative unit of Wadi Sathan section (Richoz, 2006).

Stop 1 (Fig. 25).
This stop concerns the unit B4b (Fig. 25) that crop out about 100m below the abandoned quarry. This unit contains the Permian-Triassic transition (PTT) and start with a 30cm thick dolorudstone with some pebbly layers of mudclasts overlain by 1m of laminated micropeloid dolo boundstone (microbialite?). Above the colour change from dark brown to light grey as shown by the Fig. 25, there are 6m of thin-bedded (5 to 30cm thick) dolo-wackestones and mudstones with occasional laminations.

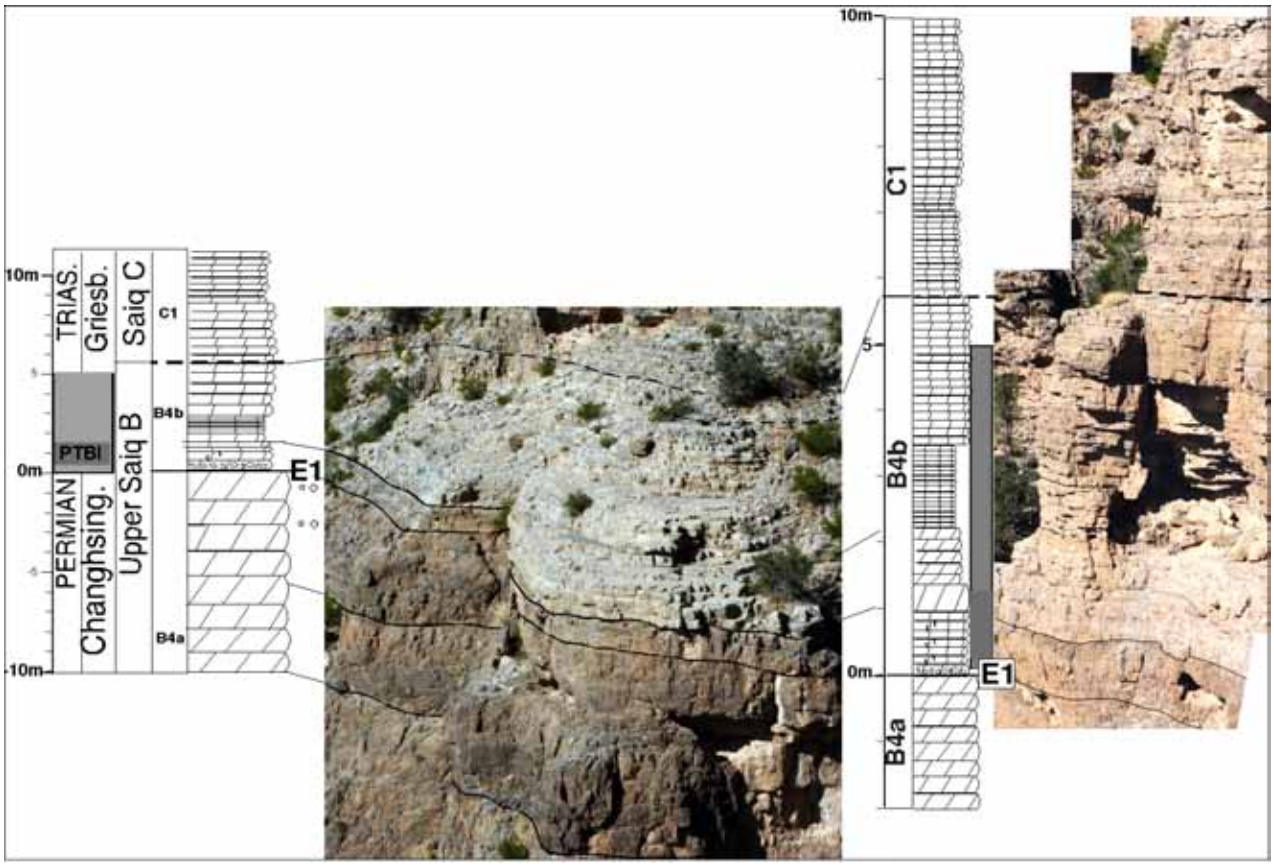

Figure 25: Close up view of the unit B4b with the Permian-Triassic Transition (coordinates: N 23°06' 00'' E 57° 39' 57'').

Isotope stratigraphy (S. Richoz, Figs 26a and b).
The Saiq and Mahil Formations are composed mainly of dolostone. As shown by (Atudorei, 1999) in the Wadi Sathan, within the basal Unit A2 of the Saiq Formation where a front of dolomitization occurs, the dolomitization processes do not affect significantly the carbon isotopic composition of the primary carbonate sediments and the dolostone have generally a typical marine carbon isotope

signature. The $\delta^{18}O$ values of dolostone are however significantly affected and about 3‰ lower than their counterparts from limestones.

As in other part of the Neotethys, δ13C display in Saiq Plateau very high positive values up to 5.6‰ in Upper Permian. In Wadi Sahtan, a first negative shift occurs there between Units B3 and B4 with a drop from 4.6‰ to 3.4‰ (Richoz et al., 2005; Richoz 2006) and a rapid negative shift of 2.8‰ appears within an 8 m thick interval of the transition between B and C Members. We have not enough samples here in Saiq Plateau to characterize this first part of the decrease. Looking on chemostratigraphy provided by Richoz, 2006 and Richoz et al., 2005 and in press (Fig. 26a and b), the very similar lithological and isotopic evolution between the Wadi Sathan section and the Saiq Plateau section help us for very precise correlations.

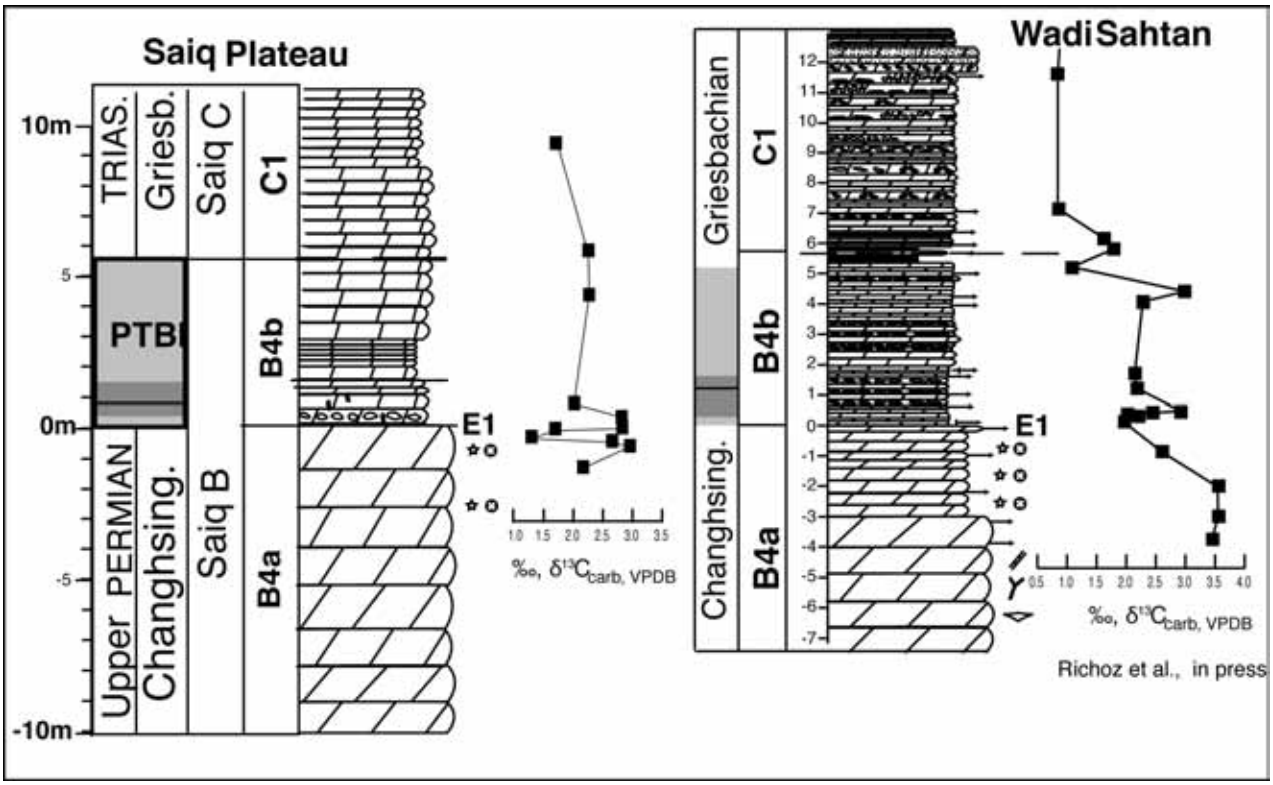

Figure 26a: Correlation of the Permian-Triassic Transition between Saiq Plateau section and Wadi Sathan section with the Carbon isotope curve record (cf. Richoz, 2006, Richoz et al., in press).

We can observe than a minimum is reached 15cm below the extinction level (Figs 25 and 26). As in many other Tethyan sections a rebound of 1,1‰ is observed just above the Extinction level (Richoz et al., in press). In Tethyan realm, H. parvus is known to appear just after the minimum following this rebound (Richoz et al., in press). With this well known and adopted criteria of the C isotope shift, we assume to set the Permian Triassic Boundary (PTB) in the topmost B4 unit, between the dolo-boundstone and the dolo-wackestone between 2 and 6 m above the extinction event (E1, Figs. 25, 26a and b).

The unit B4b from the upper part of the Saiq Formation can be well correlated with the Wadi Sathan section. The Permian-Triassic transition (PTT) is placed at the base of this unit as shown on the Figs. 25 and 26. The FAD of H. parvus is know to appear just after a first small positive peak within the decreasing isotopic values (Richoz et al., in press). According this, we place the Permian-Triassic boundary interval (PTBI).

The Member C is characterized by lower positive values (Fig. 26b) around 1,7‰, progressively higher until 2,8‰ at the base of C3 before decreasing to 2,2‰ at the top of the Saiq Formation. This curve corresponds to the Griesbachian-Dienerian trend (Fig 5, Richoz 2006).

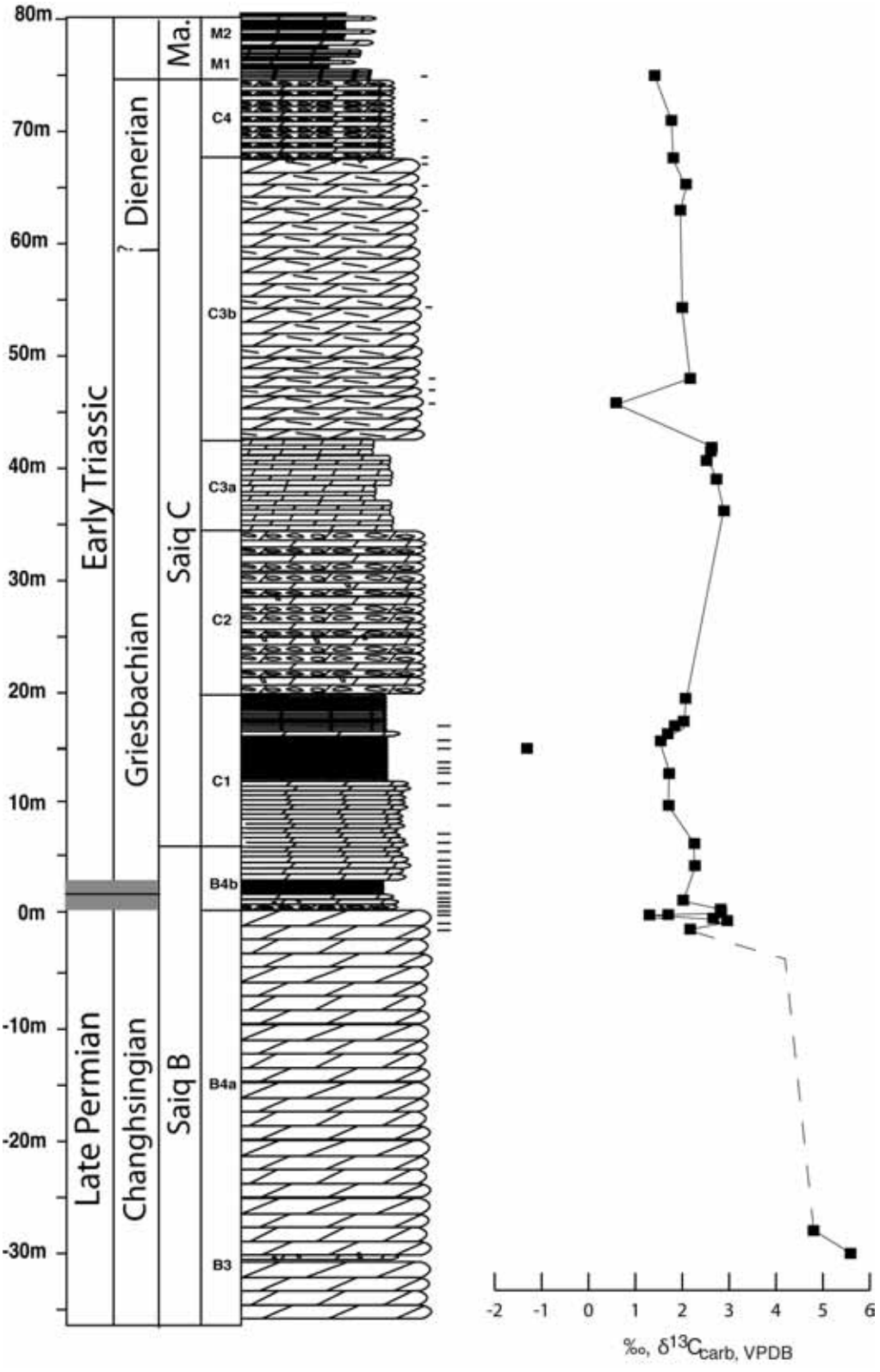

Figure 26b: The Carbon isotope profile of the upper Saiq Formation on the Saiq Plateau section (S. Richoz).

The Triassic Member C (Figs. 26b and 28) comprising the Kohrer's KS2 and part of KS1sequences is 70m thick and has been subdivided in four units C1 to C4.
As this Triassic Member C was biostratigraphically not well constrained due to poor biodiversity following the Permian mass extinction and poor record in dolomitic strata, we organized field studies for conodontss with C. Henderson and A. Nicora. They recovered conodonts at one level: *C. kazi, Neoclarkina* cf. *krystyni* and *C. carinata* in the upper part of C1 that give a Late Griesbachian age.
We found thin levels of microbivalves and microgastropods typical for oxygen-deficient dwarfed faunas in the upper part of the C3a unit.

Stop 2 (Figs. 27-29)
We will look at the first unit C1 (Figs. 26a and 29) of the Member C, that starts with the first dark grey dolostone and consists of 13m of beige to black thin-bedded (5 to 30cm thick) dolomudstone with some soft pebbles alternating with thin-bedded doloarenite with lamination and cross bedding. Four main microfacies are illustrated at the Figure 29.

The unit C2, 14m thick, consists of a lithoclast dolorudstone. Its erosive base (E2, Fig. 27) record a cartographic low angle unconformity and the lithoclasts accumulation is due to rapid lithification and tectonic instability with bloc tilting. In the Musandam Bih Formation, dolomitic breccia occurs in the same stratigraphic position, above the Permian-Triassic transition beds according Maurer et al., 2009.

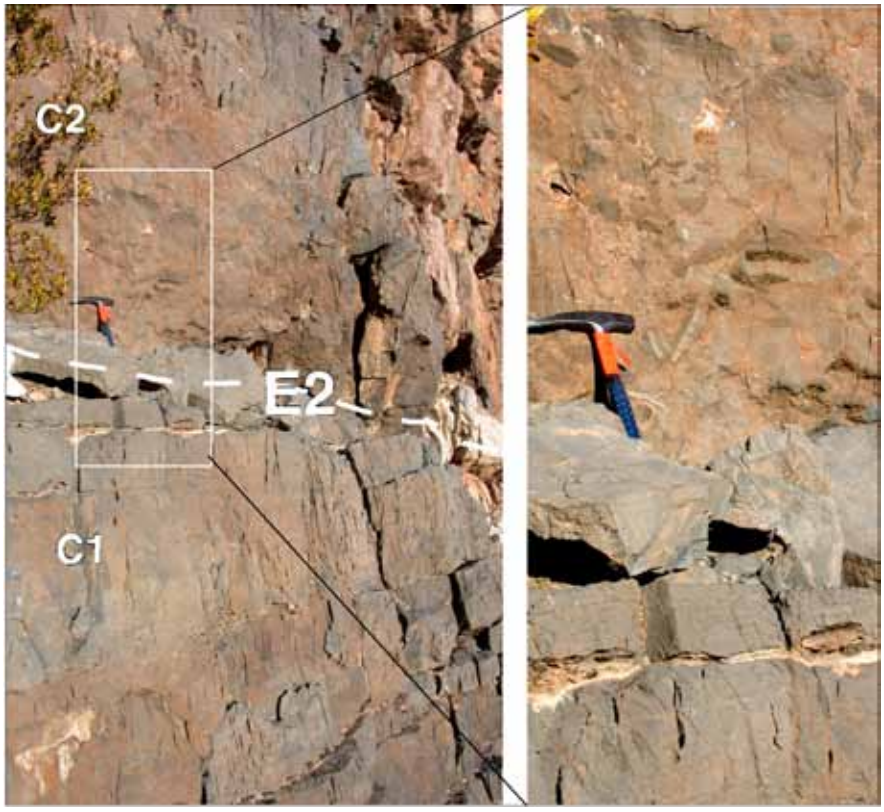

Figure 27: Close view of the erosional surface E2 with (right up) the composite, heteromorph breccia of the base of the C2 unit

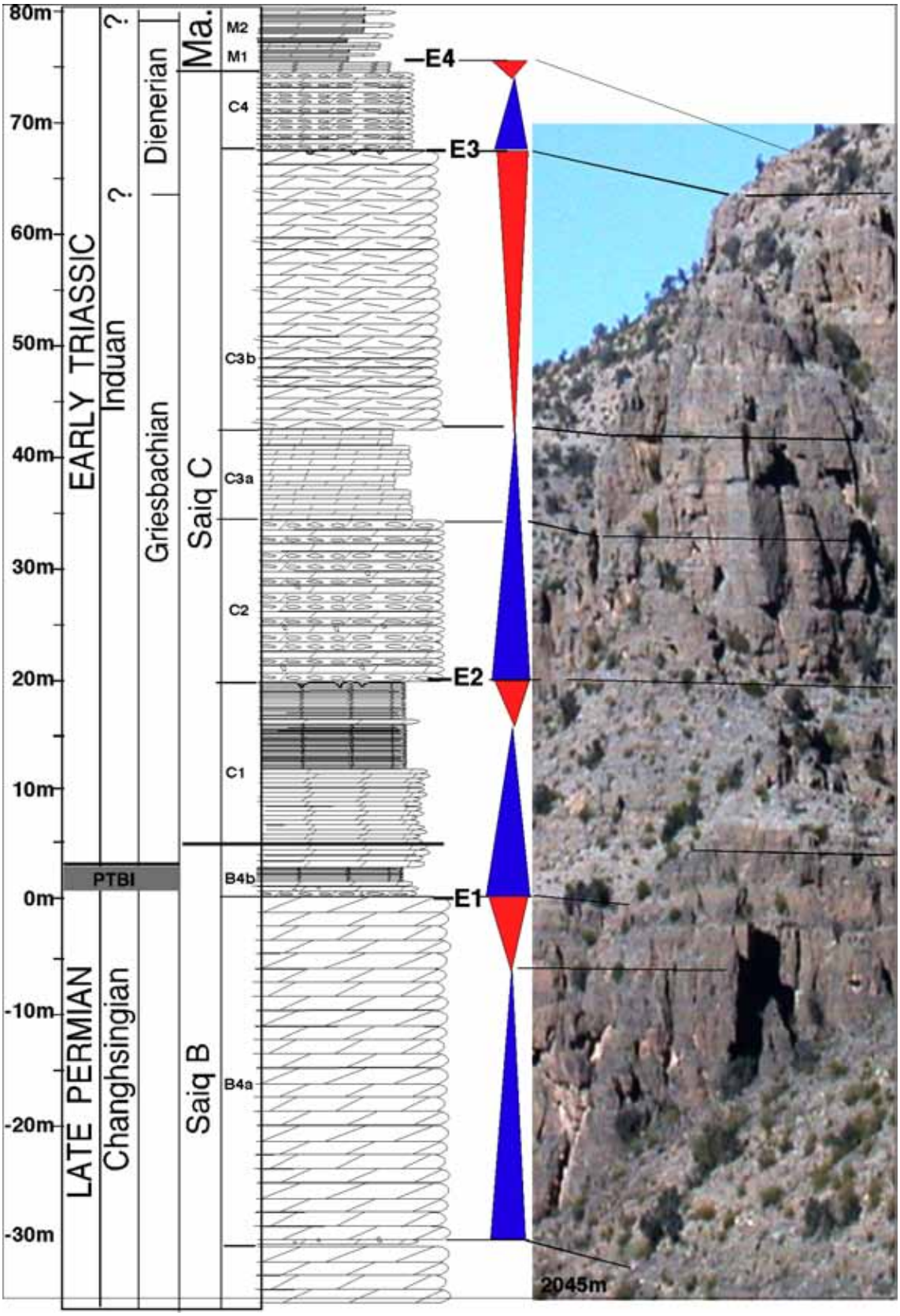

Figure 28: Top of Member B and member C of the Saiq Formation with the corresponding outcrop picture and the observed 3rd order sequences (red and blue triangles). It is not correlated with KS2 and KS1 of Kohrer et al., 2009. E1= Extinction Event, E2= Erosional surface, E3= Early lithified surface, E4=exposure surface.

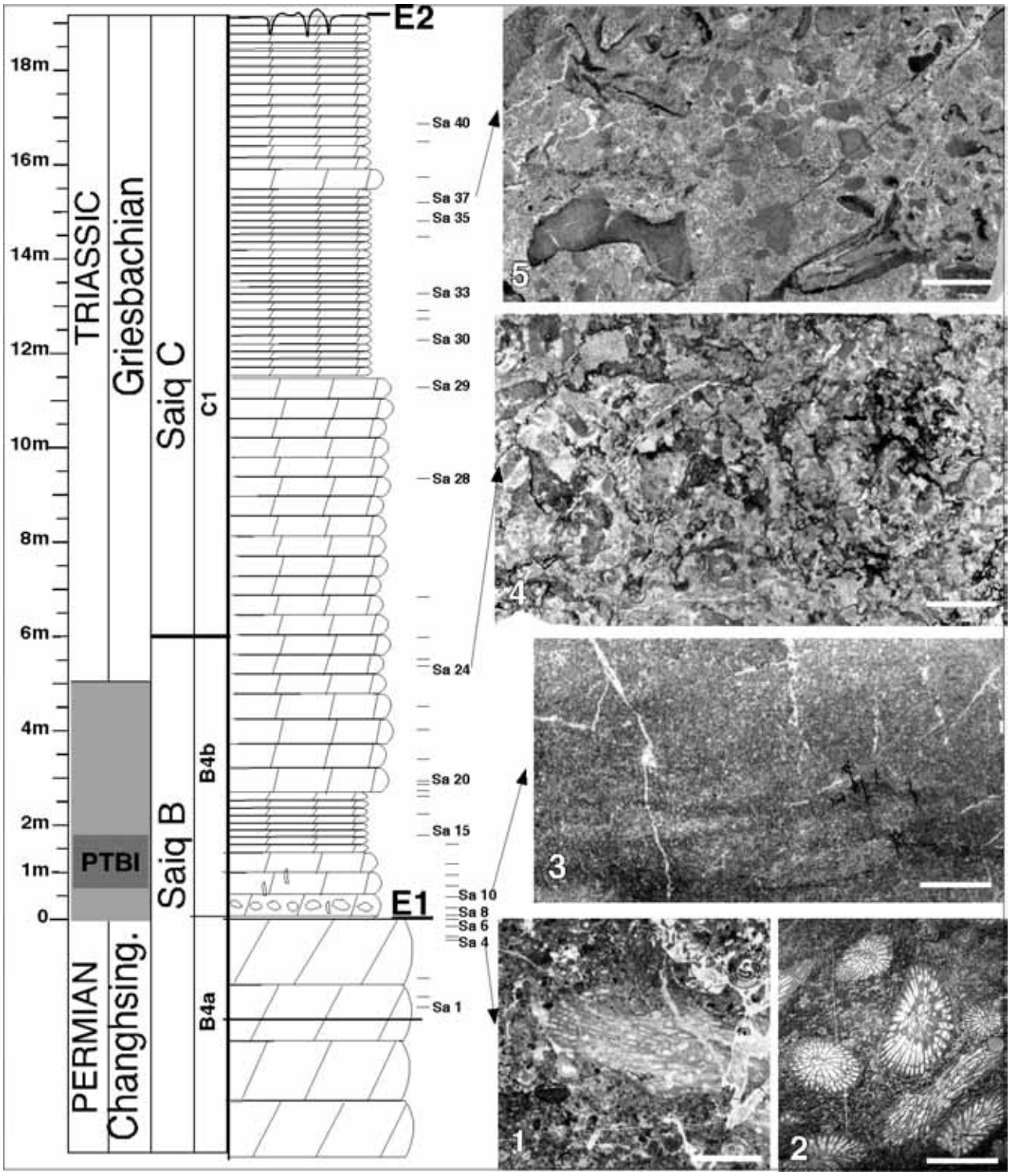

Figure 29: Microfacies at the Permian-Triassic transition. White bar scale is 0.5mm.
1- dolo- bioclastic packstone with bryozoan (in the middle); 2- Dolo-packstone with Rugosa corals of Wentzelella-type, top of correlative unit B4a of Wadi Sathan; 3- dolo- peloid wackestone-packstone; 4- dolo- intraclastic packstone; 5- heteromorph dolo- intraclastic packstone.
E1= Extinction Event, E2= Erosional surface

Stop 3 (Fig. 30 to 33).
We will look at the top of the Saiq Formation with the units C3 and C4 and the base of the Mahil Formation. The unit C3, 34m thick (Fig. 28) is subdivided in C3a and C3b. The C3a unit (8m) contains dolomudstone, dm thick beds of bioclastic dolopackstone with micro-bivalves and rare microgastropods and peloid-intraclast dolomitic grainstone (Fig. 30a). Oolitic dolograinstone (Fig. 30b) dominates the C3b interval (26m), forming dm thick crossbedded dolostone beds. Intensive dolomitization largely obliterated the microfacies. Where the original texture is preserved, ooids are recognized as round grains with relics of internal layering.

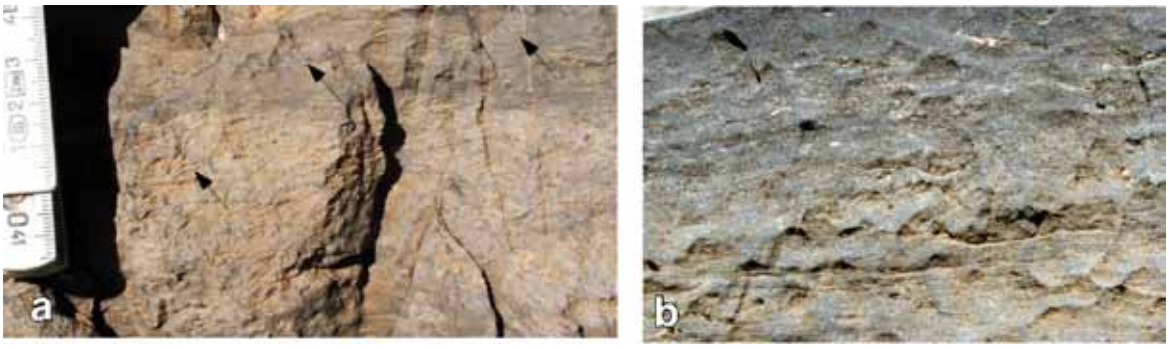

Figure 30: Facies of Unit C3; a-bioclastic dolopackstone with micro-bivalves (arrows) and intraclasts, b- Dolomitized oolitic grainstone with intraclasts. Scale in mm on the left.

The top of C3b Unit is marked by an irregular, early-lithified surface of hardground type (E3, Figs 28 and 32) with pockets filled by clasts from the overlying dolobreccia, indicating an interruption in sedimentation, possibly with subaerial exposure.
The unit C4 is only 7 m thick and consists of angular lithoclasts dolorudstone overlain by 50cm of thin bedded black dolomudstone. Large mud cracks characterize the upper surface (E4 in Figs. 28 and 32).
It is interesting to note that rapid early-marine cementation appears widespread in the unit C1, C2 and C4 of the Saiq Formation (unit C, Lower Triassic). It is partly responsible for the abundance of lithoclasts breccia and flat pebbles in this stratigraphic interval and also in the lower part of the Mahil Formation (Richoz, 2006) and the record of hard grounds or cemented exposure surfaces as shown on the Figs. 31, right and 32 (E4).

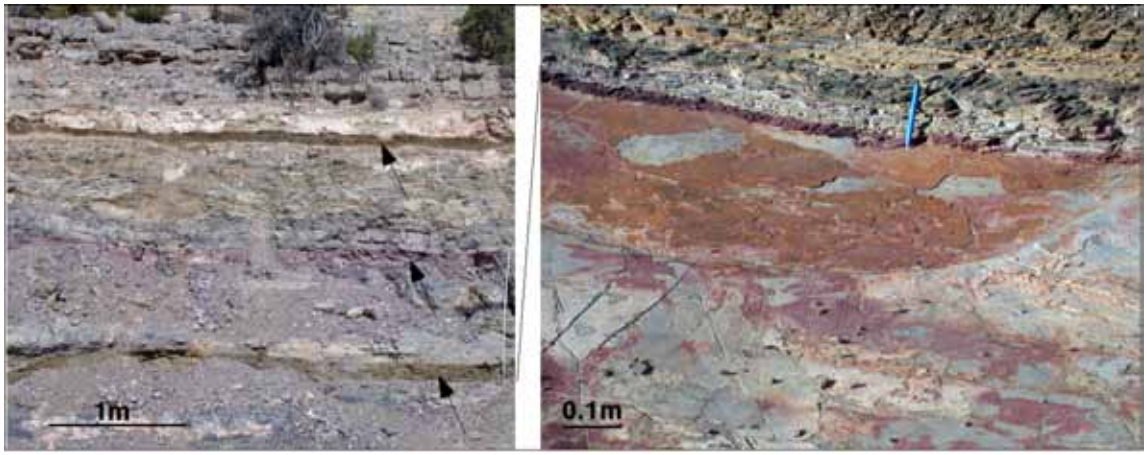

Figure 31 left: The multicoloured clay mudstones in the basal Mahil Formation. Right: Hardground surface

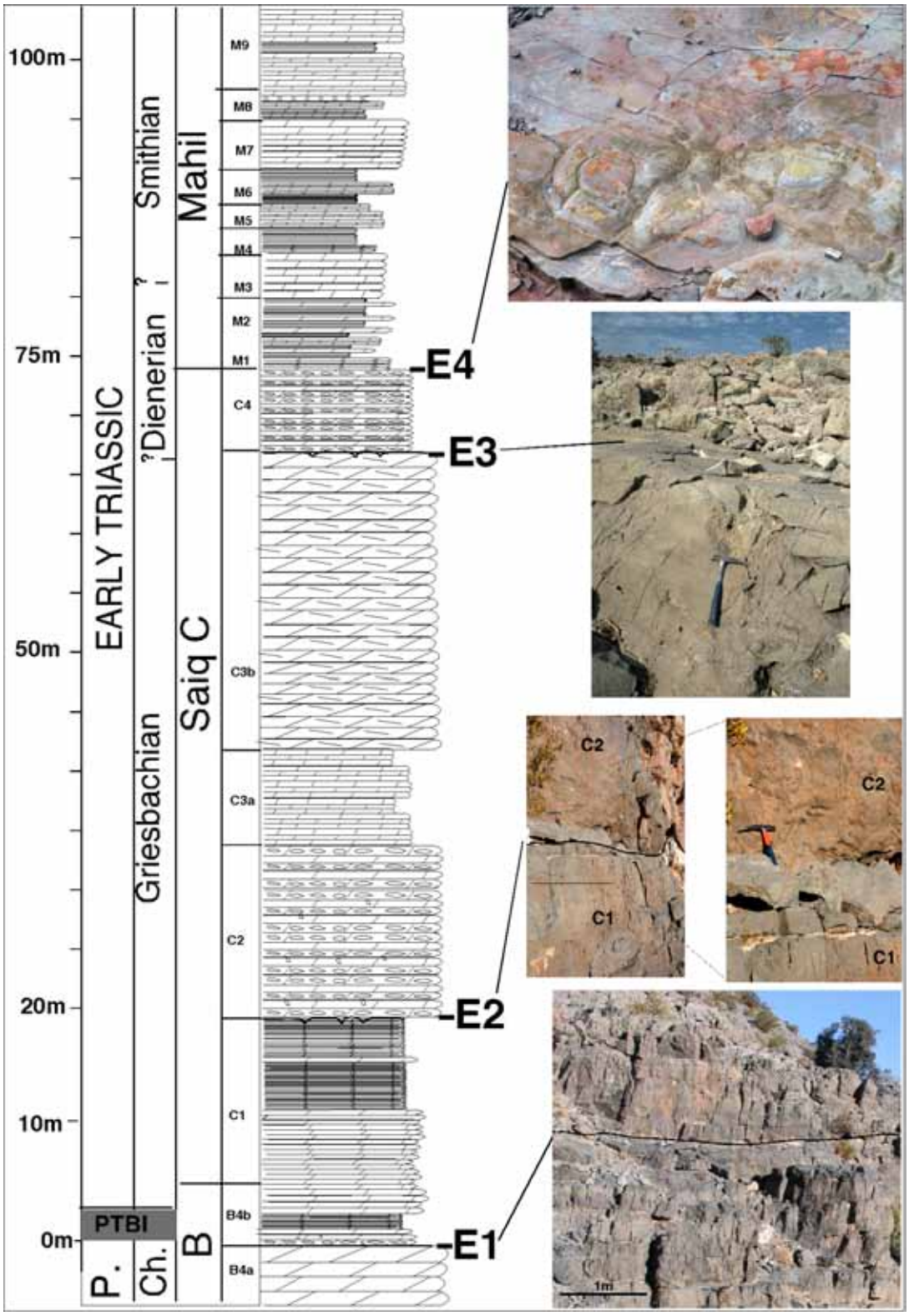

Figure 32: Exposure or erosional surfaces in the upper Saiq Formation.E1- Hardground near the top of the dark dolostone. E2- Erosional contact at the base of the C2 dolostone breccia unit. E3- Hardground at the top of the C3b grainstone unit. E4- Hardground with cracks near the base of the Mahil Formation.

The base of the Mahil Formation outcrops well in the abandoned quarry and is characterized by a sudden fine terrigenous input with green, brown and red clay mudstone (Fig. 31).

The Mahil Formation overlies a subaerial and exposed surface that forms the top of the Saiq Formation (E4, Fig. 32).
The lower part of this Formation, examined herein (Fig. 33), is divided in two main lithologic units, M1 and M2, further separated in subunits. Very small foraminifera and bivalves (Claraia) are present in the unit M2 of the Formation.

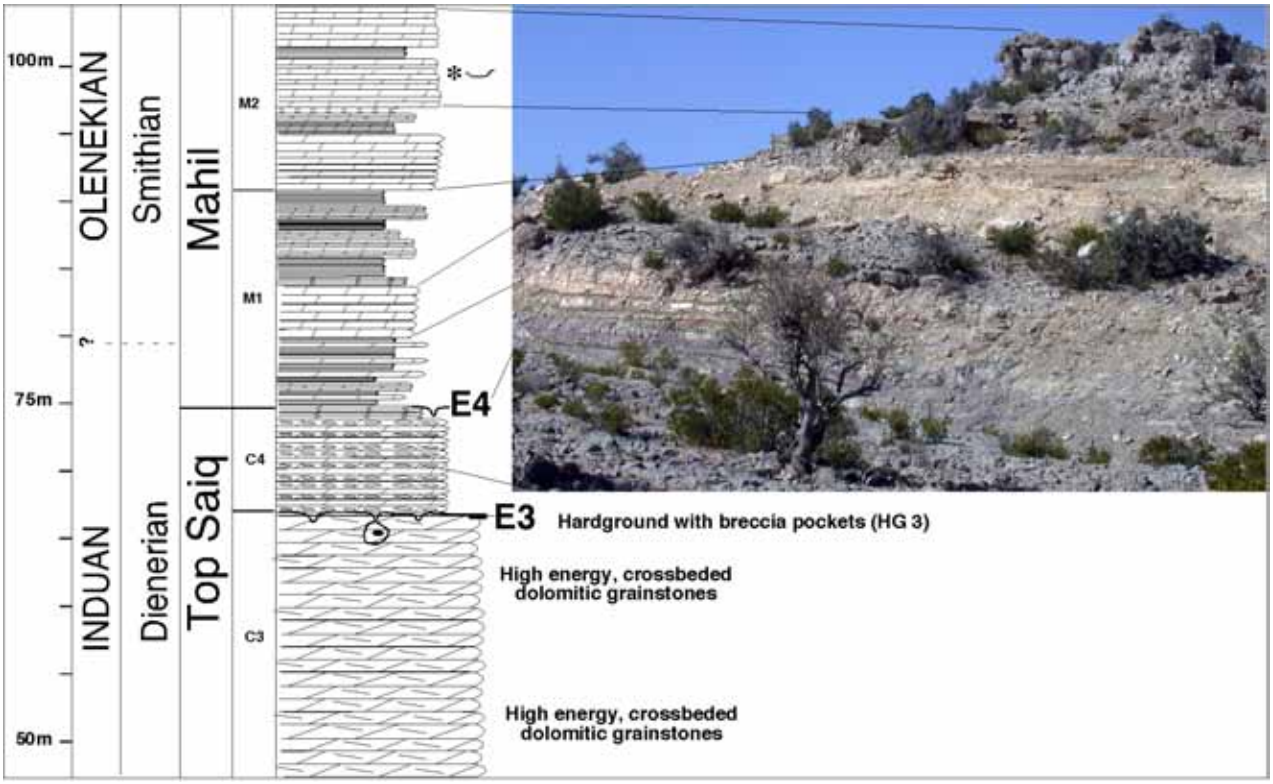

Figure 33:The basal Mahil Formation outcrops well in an abandoned quarry above the Saiq village (situation in Figs. 19, 20 and 21).

<u>February 24, 2010</u> -The Permian-Triassic transition in the Wadi Wasit area.

(Stop 1: A. Baud, C. Henderson, L. Krystyn, S. Richoz and B. Beauchamp . Stop 2: L. Krystyn, S. Richoz, R. Twitchett and A. Baud).

Routing (Fig. 34): Starting at 8 a.m., February 24, from Hotel Ibis (Muscat) we will move to Ba'id village following first the Muscat-Nizwa highway up to Bidbid and then the road in direction of Sur to Wadi Tayn –Wadi Adam crossing and follow the Wadi Tayn road to Ba'id and turn at the Wadi Wasit entrance to Naqsi village for stop 1 (Fig. 35). Coord.: N 23°06'49'' E 58°20'55''.

Figure 34: Google Map with road itinerary in red and alternative scenic road crossing the Saih Hatat Range in green.

Figure 35: Google Earth picture of the outcrops area, with in red, the road itinerary

Introduction

The Bai'd tectonic window is located in the Central Oman Mountains, to the south of the autochthonous units of the Arabian platform in the Saih Hatat (Fig. 20) and below the Samail ophiolite (Figure 36). It forms an anticline with a roughly N-S trending axis that exposes imbricate slices of the Hawasina sedimentary and volcanic units. The Wadi Wasit area provides one of the best and the most extensive exposures of Permian and Triassic deep-water sediments (Baud et al. 2001) in the Hawasina allochthon (Figure 36).

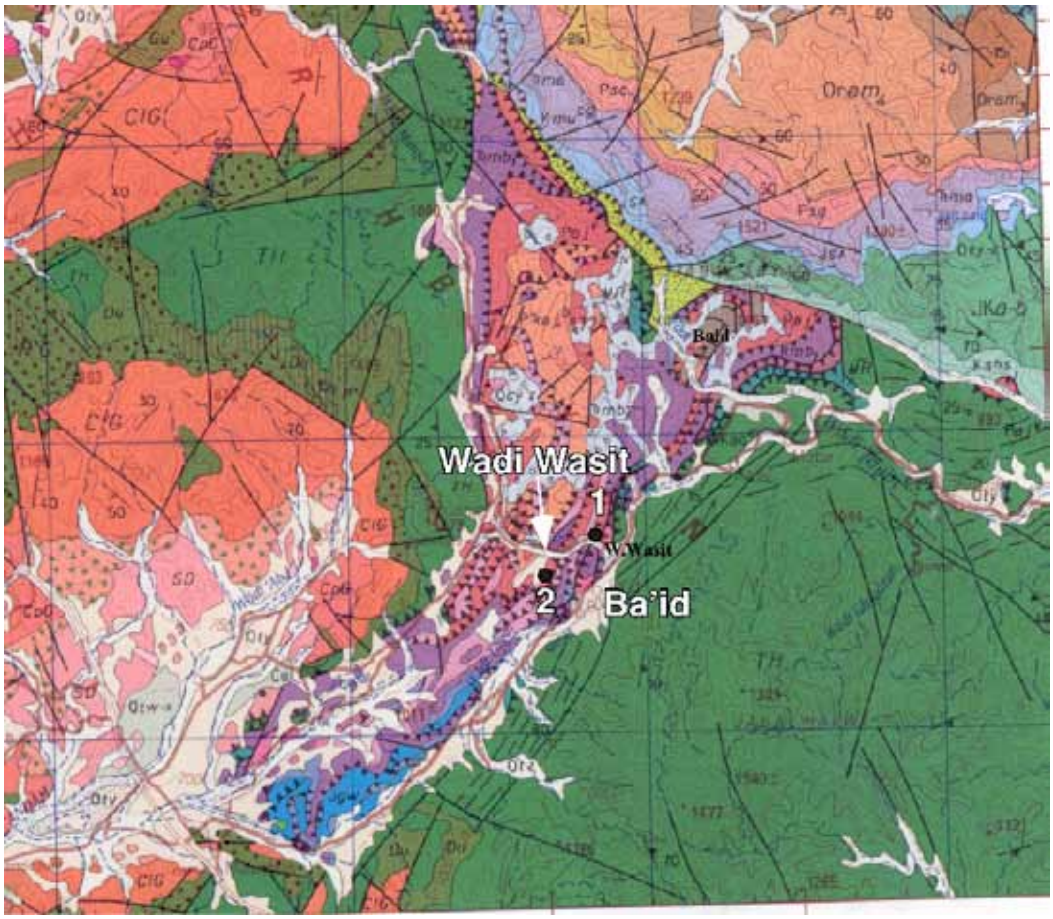

Figure 36: Geological map of the Wadi Wasit area (from Béchenec et al., 1992b). 1- Wadi Wasit section (stop1); 2- Wasit block (stop 2).

The general stratigraphy of the Bai'd window (Permian and Triassic Al Jil Formation, sensu Béchennec, 1988; 1992a) consists of a 250m thick Middle Permian volcano-sedimentary sequence (Pillevuit et al., 1997) of pillow basalt with 4 main intercalations, 10 to 30m thick, of cherts, of volcanic breccias, of calcareous gravity flow deposits with Lower and Middle Permian shallow shelf or reef boulders and of cephalopod red lime wackestones (Fig. 37).

Recently C. Henderson and A. Nicora recovered *Mesogondolella idahoensis lamberti* near base of section (Fig. 37) giving a latest Kungurian-earliest Roadian age. At 45m is *Mesogondolella pingxiangensis* (Roadian), at 80m *Jinogondolella cf. nankingensis* and *Jinogondolella aserrata* (latest Roadian - Early Wordian). Higher up, at 230m (Fig. 37 enlargment) are *Mesogondolella n. sp. A*. and *Jinogondolella cf. shannoni* (Capitanian), at 235.5m *Mesogondolella n. sp. A*. and at 237.5m *Jinogondolella altudaensis* of Late Capitanian age (conodonts illustration in Plate 1, below).

Plate 1. All conodonts from Wadi Wasit section. All same magnification (scale bar = 0.5 mm). 1-4, Jinogondolella altudaensis (237.3 m). 5-8, Mesogondolella n. sp. A (235.5 m). 9-14, Mesogondolella n. sp. A. (230 m). 19-22, Jinogondolella cf. shannoni (230 m). 15-16, Jinogondolella cf. nankingensis (80 m). 17-18, Jinogondolella aserrata (80 m). 23-28, 31-36, Mesogondolella pingxiangensis (45 m). 29-30, 37-38, Mesogondolella idahoensis lamberti (near base of section). Age relationships indicate latest Kungurian-earliest Roadian at the base, Roadian at 45 m, latest Roadian-early Wordian at 80 m, Capitanian at 230 m and late Capitanian at 237.3 m).

Overlying are nodular, cherty and turbiditic (allodapic) limestones. After a stratigraphic gap of nearly 10 My, the Lower Triassic record begins with breccias of Dienerian age. These are followed by platy limestones of Late Dienerian to Smithian age, dated at different places by conodonts such as *N. waageni, Platyvillosus costatus, Neospathodus cristagalli* (det. L. Krystyn in Baud et al., 2001).

The breccias sandwiched between Permian turbiditic and Lower Triassic platy limestones, are of variable thickness and are very widespread. They are channelized, clast-supported debris flows deposits (Figure 24), which cut deeply into the underlying calcareous or volcanic rocks of Middle Permian age (Blendinger 1988, 1995; Pillevuit, 1993; Pillevuit et al., 1997). These, often dolomitized breccias consist mostly of Guadalupian reefal blocks, which originally formed the margin of the Permian carbonate platform. The reef biota of the Permian reef boulders deposited in these deep-water sediments has been compared with the El Capitan reference section of West Texas (Weidlich et al., 1993; Weidlich, 1996; Weidlich and Senowbari Daryan, 1996). Calcareous and dolomitic parts of the breccia tend also to be silicified, making palaeontological studies difficult, as fossils are difficult to extract.

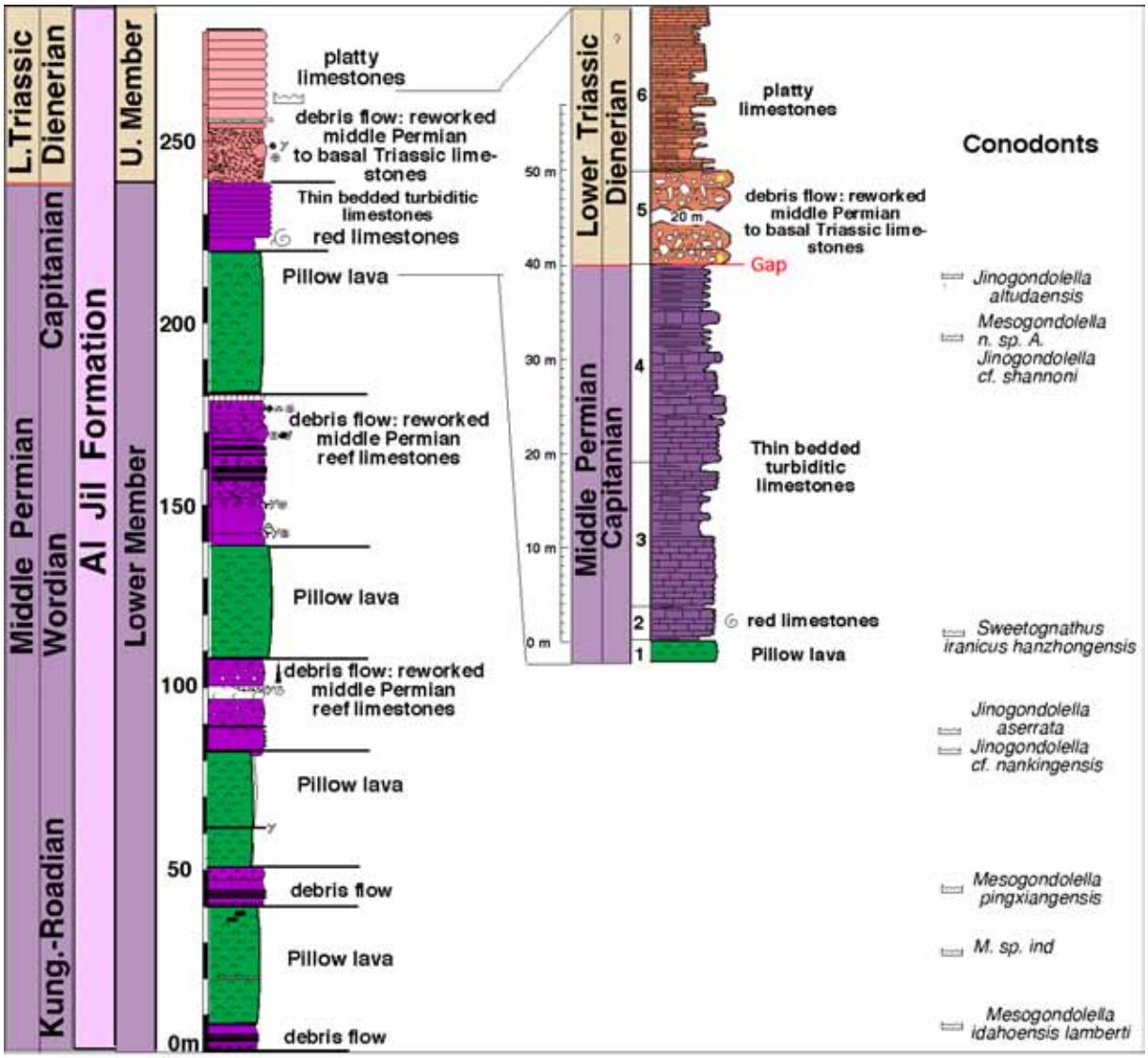

Figure 37: Wadi Wasit composite section (modified from Pillevuit et al. 1997); section A modified from Atudorei (1999); Conodonts (see Plate 1, p. 50) recovered and determined by C. Henderson and A. Nicora (Henderson et al., 2009).

A unique, entirely calcareous breccia, which occurs 1 km south of the middle part of Wadi Wasit, includes several small-sized blocks of lowermost Triassic bivalve-bearing limestones. The largest one, with a size of about 200 m^3, the Wasit block, will be examined in detail at our stop 2 (cc. Fig. 38).

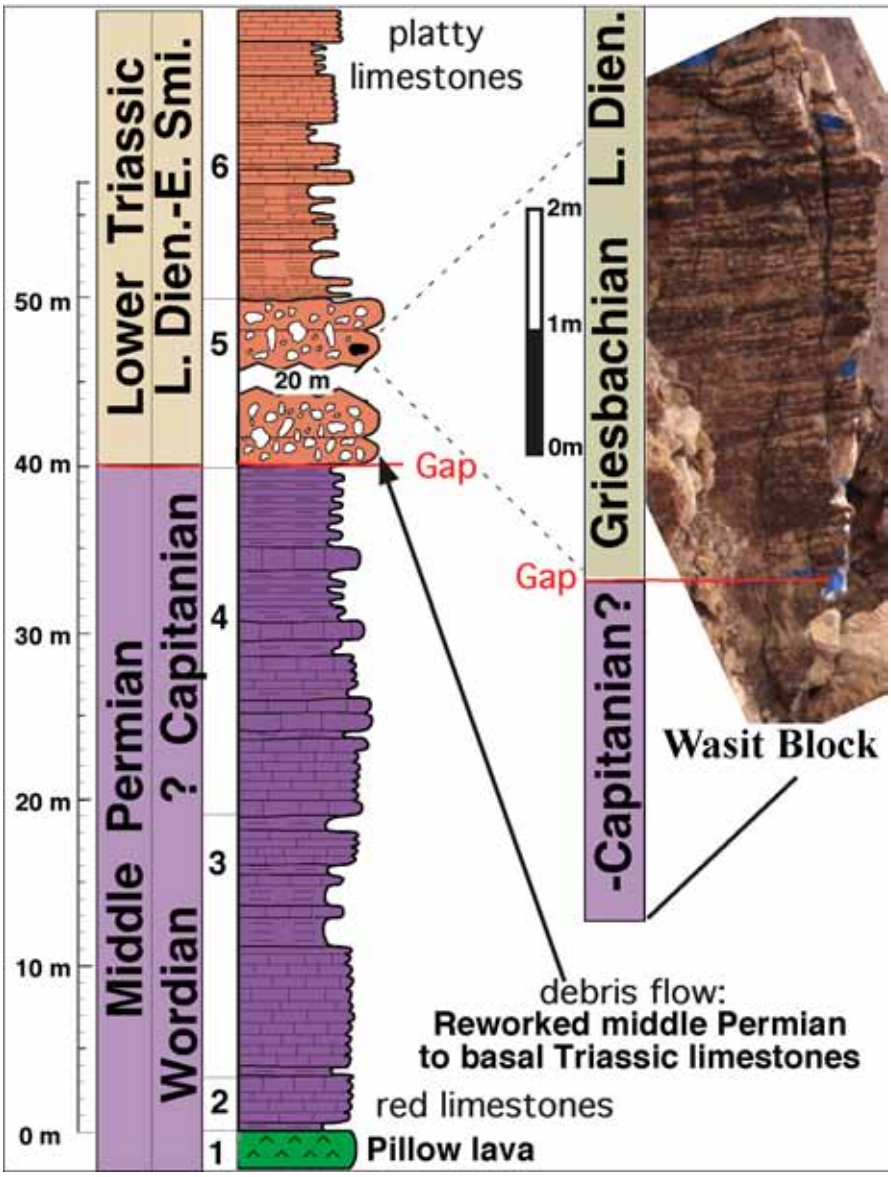

Figure 38: Stratigraphic sketch of the upper Al Jil Formation in the Wadi Wasit area (modified from Atudorei, 1999) with stratigraphic view of the Wadi Wasit block.

Stop 1: Stratigraphy of the Al Jil Formation on the left side of the Wadi Wasit
(Fig. 39, see position on Google picture, Fig.35).

We will look at the upper part of the complete section that consists of 5 main lithologic units (Al Jil Fm.) from base up (Fig.; 39):

-Unit 1 is a thick volcano-sedimentary sequence made up of alkali pillow basalts WPB-type (Béchennec 1988, Béchennec et al., 1991, Pillevuit, 1993, Maury et al., 2003) and of tuffites with interbeds of radiolarites. These volcanic rocks are strongly enriched in the most incompatible elements and are typical of high-Ti basalts identical to plume-related alkalibasalts from intraplate continental or oceanic settings.

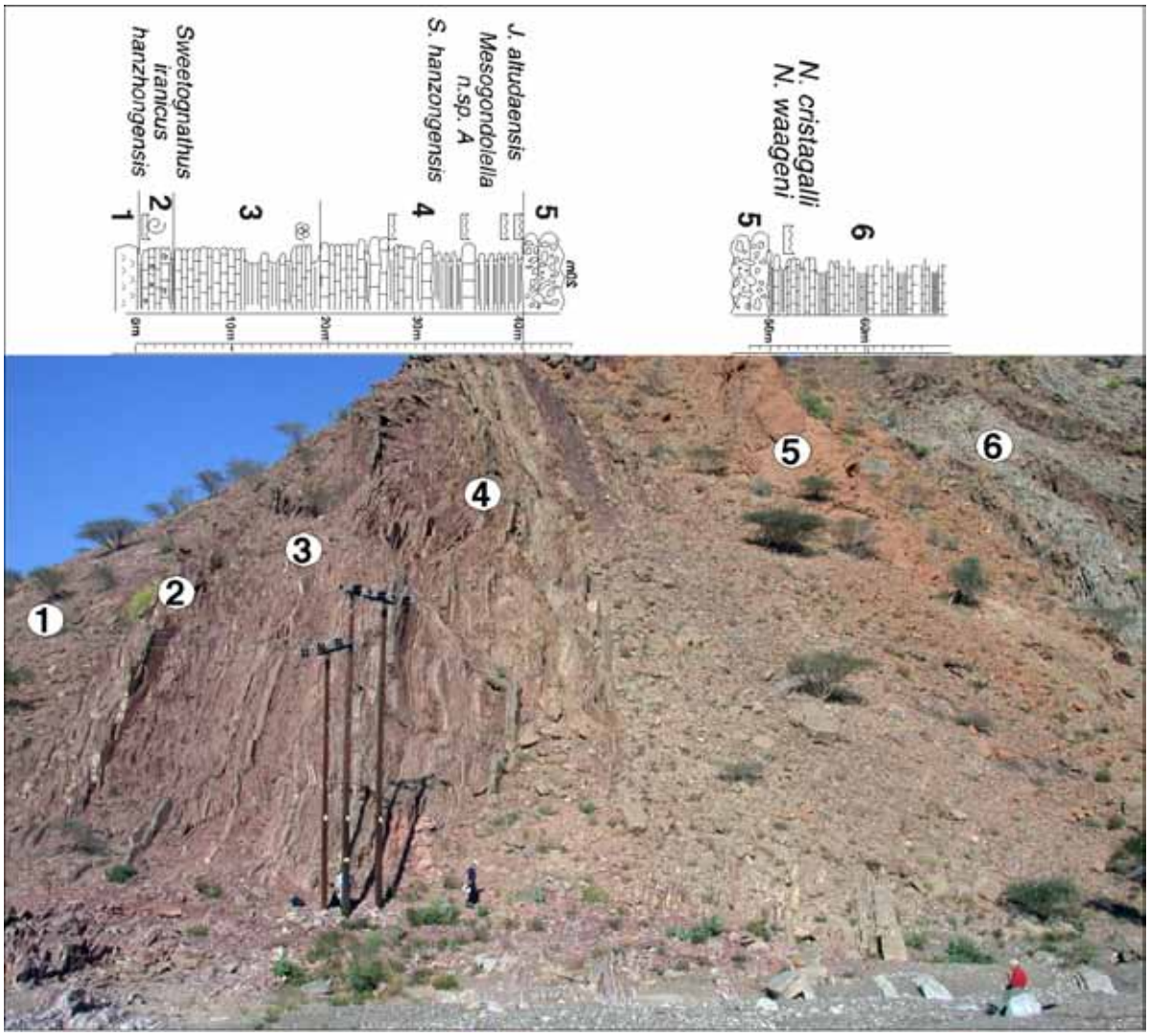

Figure 39, stop 1: View of middle part of the Wadi Wasit section. Lithological section modified from Atudorei (1999). Unit 1 to 4, conodonts recovered and determined by C. Henderson and A. Nicora. Unit 6, conodonts recovered and determined by L. Krystyn.

-**Unit 2**, 19m thick, consists essentially of medium bedded red cephalopod limestones with some levels of fine-grained resedimented limestones and red shales interbeds. Furnish and Glenister in Blendinger et al. (1992) determined the ammonoids of these limestones and gave the following list, named "Sicilian species": *Parapronorites koninckі*, *Propinacoceras beyrichi*, *Eumedlicottia bifrons, Neogeoceras marcoui*, *Adrianites elegans*, *Aricoceras ensifer*, *Tauroceras scrobiculatum, Stacheoceras sp*. and *Waagenoceras sp*. *Epadrianites beyrichi* is known from Timor and *Mongoloceras omanicum* is a new species.
L. Krystyn also collected the Guadalupian ammonoids *Timorites sp.* and *Strigogoniatites sp.*
In the same level as the ammonoid, H. Henderson and A. Nicora recovered the conodonts *Mesogondolella n.sp. A and Sweetognathus iranicus hanzhongensis (early morphotype).*

-**Units 3 and 4** (21m thick) consists of depositional sequences mainly of turbiditic lime packstones and red shales, the latter being more abundant in the upper part. The allodapic limestones are represented either by calcarenites or calcirudites and they include occasionally reddish-whitish chert nodules. The following conodonts have been recently recovered in the unit 4: *Mesogondolella n. sp.*

A, and Jinogondolella cf. shannoni and 2 metres higher Jinogondolella altudaensis (det. C. Henderson and A. Nicora) with an age of Late Capitanian.
According to Atudorei (1999), Units 3 and 4 have high $\delta^{13}C_{tot}$ values between +4‰ and +5‰ consistent with usual Late Permian values.

Below (Fig. 40) is a depositional model for the Middle Permian of the Wadi Wasit basin margin that evolves with the creation and extension of the Neo-Tethys. Reefal aggradation takes place on the shelf edge and shallow part of tilted block (after Blendinger, 1988).

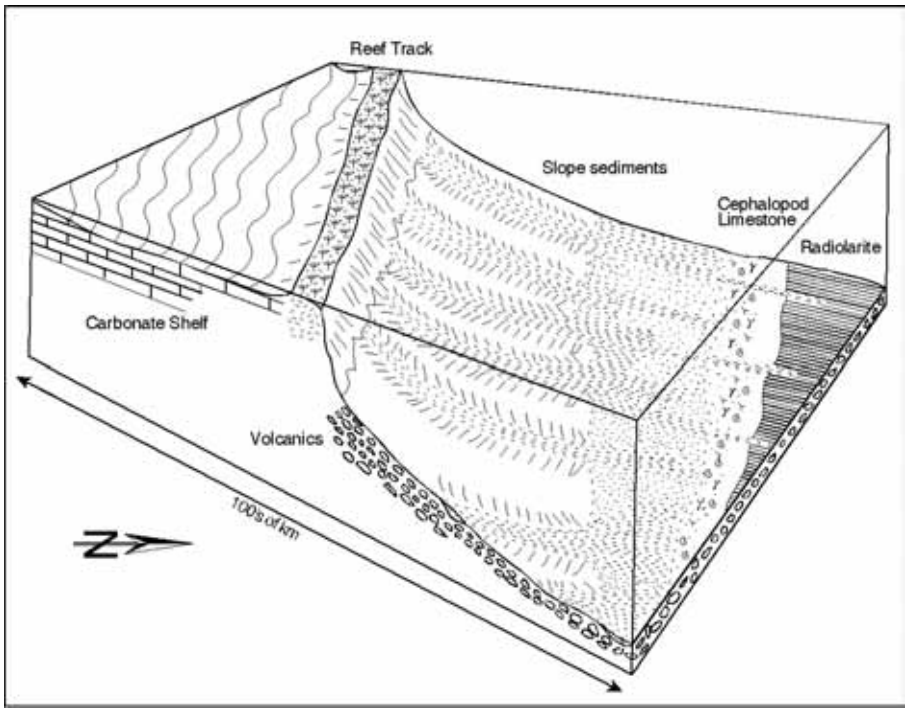

Figure 40: Depositional model for the Middle Permian of the Wadi Wasit basin margin (modified after Blendinger, 1988).

-Unit 5 from 10 to up 50m thick is represented by a massive dolomitized breccia with blocks of reefal limestones. It consists of a gravity flow deposit partly composed of reef boulders. The reef biota of the Permian reef boulders deposited in these deep water sediments have been intensively studied by a team from the Erlangen Paleontological Institution and also compared with the El Capitan reference section of W Texas (Flügel in Blendinger and Flügel, 1990, Senowbari et al., 1992; Weidlich, 1996a; Weidlich, 1996b; Weidlich et al., 1993; Weidlich and Flügel, 1995; Weidlich and Senowbari, 1996). The age of this unit, Middle-upper Dienerian, is bracketed between the youngest age of the youngest boulder (=Wasit block, stop 2) that is Early Dienerian and the age of the basal transgressive unit over the breccia (unit 5) that is Late Dienerian-Early Smithian.

-Unit 6 starts with grey platy limestones and thin shales or marlstones interbeds, over a 6 m thickness. The underlying contact with the massive dolomitized breccia is irregular and marked in some depressions by a thin layer of marly shales. Elsewhere the platy limestone unit has more than 100m in thickness, with a Late-Dienerian-Middle Smithian age (Richoz 2006). This unit is in some places overlain by a green shale/fine-grained quartz-sandstone sequence, 12 m thick, and then by a green/red radiolarian chert series (Ladinian) which is the base of the overlying Matbat Fm.

Stop 2: Stratigraphy of Wasit block above the right side of the middle part of the Wadi Wasit Valley (see position on map, Fig.35).
From the parking place on the right side of Wadi Wasit, we will move up the hill, crossing the Al Jil units we have seen at stop 1 and find below the top of the hill the so-called Wadi Wasit block with a size of about 150 m^3 within the calcareous breccia (Figs. 38 and 41).

Figure 41, stop 2: Left, view of the hill slope with the position of the Wasit block. Right, close view of the block.

This block consists of three main litho-units. The basal 6 m thick unstratified grey reefal limestone is developed as rudstone rich in various reef-building organisms (rugose corals, calcareous sponges, stromatoporoids). The finer grained top of the reefal limestone has been dated by rare conodonts (*M.* cf. *slovenica*) as Middle Permian (Wordian). Three microfacies are shown below (Fig., 42)

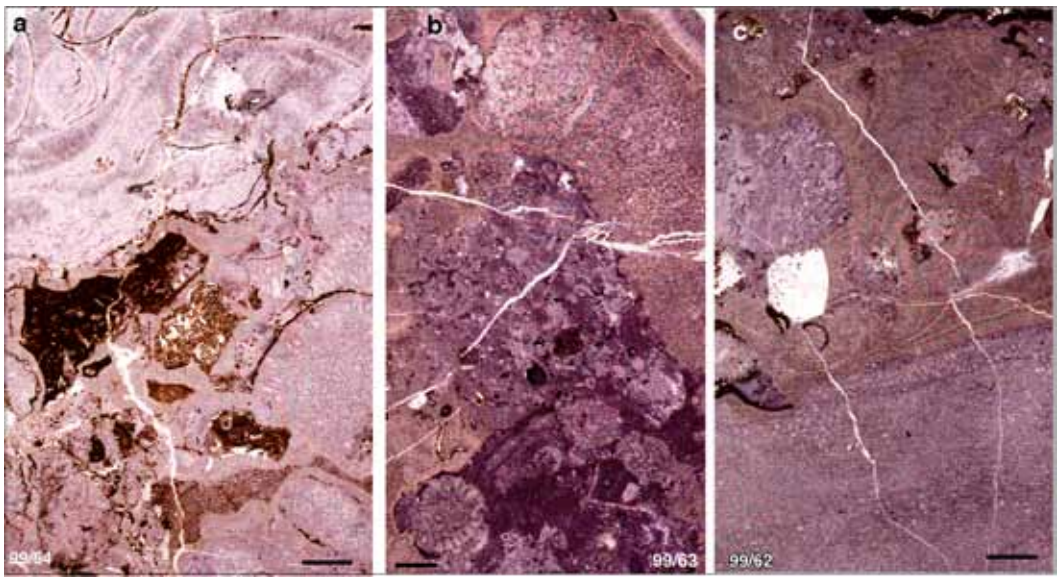

Figure 42: Microfacies of the basal reefal limestone. a- top of the reef lime-rudstone showing the sharp microcarstic relief (stylolithe, left up) with the basal Triassic bivalve floatstone. b and c- reef lime-rudstone. Scale bar = 5mm.

It is disconformably overlain with sharp relief (Fig. 42a and 43 right) by a thin laterally discontinuous peloidal packstone layer dated as lowermost Triassic by conodonts (*H. parvus*). The documented hiatus represents therefore a time break of more than 10 million years.

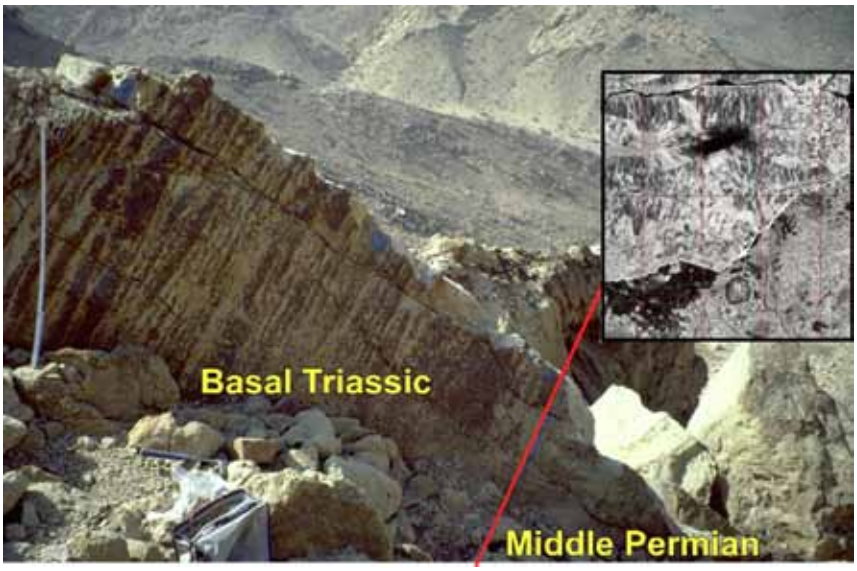

Figure 43: Close view of the block with at right the microfacies with the contact between the Permian reefoidal limestone and the basal Triassic bivalve floatstone.

Description of the section and biofacies (after Krystyn et al., 2003, Figs. 44, 46).
Section follows upward by 4 m of well- and thinly stratified light grey to yellowish coloured limestones rich in molluscs. Two main lithologies (Coquina Limestone resp. Bioclastic Limestone unit) characterize the shelly limestone, their contact seems gradual and records changes in microfacial and faunistic composition. The lower 2.5 m are developed as Coquina Limestone of mostly 10 to 20 cm thick planar or, rarely, lenticular-bedded bivalve layers. Sediment-free, spar-cemented densely packed, well sorted shells with predominantly oblique orientation dominate between 0.2 and 1.5 m above the boundary. Below and above are beds with poor shell sorting, more parallel shell orientation (mixed convex-up and -down) and mud-filled shelter porosity. The bivalve fauna is of low diversity and dominated by the genus *Promyalina* with less frequent *Claraia* and rare *Eumorphotis*.

In terms of biofacies the Coquina Limestone is thus called the *Promyalina* beds. Other fossil groups are rare; small ammonoids occur in filled cavities. Towards the top part shell accumulations become less dense and *Eumorphotis* more frequent. With a further decrease in bivalve shells, the lithofacies is changed to the Bioclastic Limestone unit. Shell concentrations are now restricted to thin layers in irregularly stratified beds within the lower metre of the unit. The bivalve composition changes remarkably owing to the disappearance of *Promyalina* and its replacement by *Eumorphotis* and *Claraia*.

The upper part of the Bioclastic Limestone consists of a single 1 m thick bed with a rich and, for the respective time interval, astonishingly diverse invertebrate fauna. It consists predominantly of grain- and packstone with microgastropods, echinoderms (crinoid ossicles, "*Cidaris*" spines), bivalve debris, ostracods and less common juvenile ammonoids, and rather rare bioclastic wackestone.

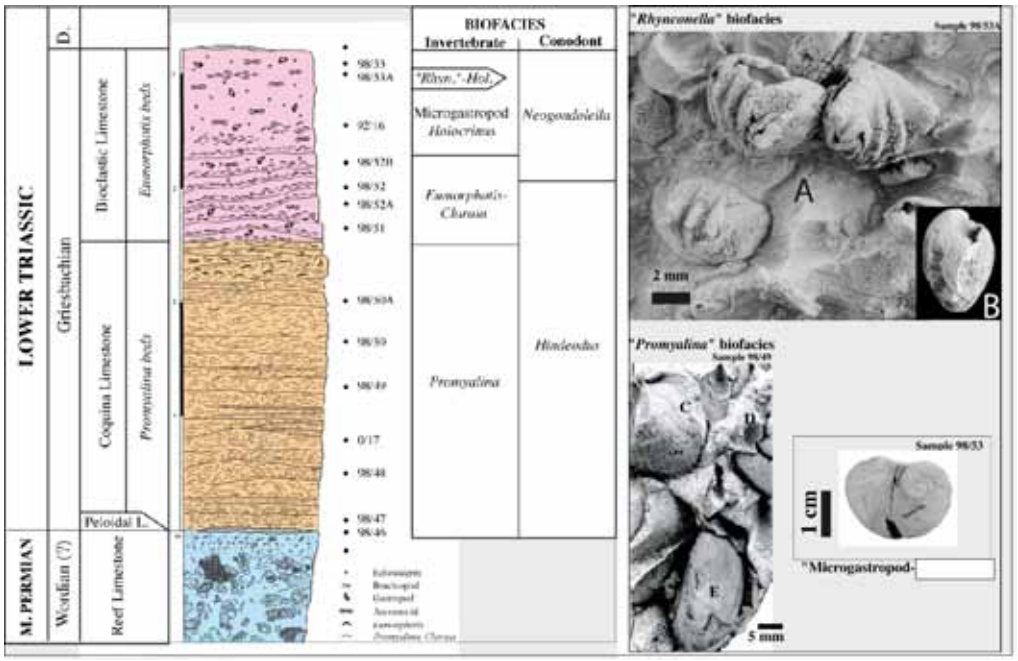

Figure 44: Stratigraphy and biofacies of the Wadi Wasit block (after Krystyn et al., 2003). A= rhynchonellids, B =spiriferid brachiopod, B=Eumorphotis, C=Claraia, E=Promyalina.

Other megafossils are very common and represented by a diverse ammonoid fauna (Fig. 45) (ophiceratids, *Pseudoproptychites*, *Pseudosageras* and two new genera related to *Pseudogyronites* and *Kymatites*, resp.), spiriferid and rhynchonellid brachiopods, the most diverse Griesbachian gastropod fauna including *Bellerophon, Ananias, Coelostylina, Naticopsis, Worthenia*, and *Omphaloptycha* (Wheeley and Twitchett, 2005) as well as *Claraia* and *Eumorphotis* bivalves. The crinoids are a new Lower Triassic taxon (Oji and Twitchett, ms in prep).

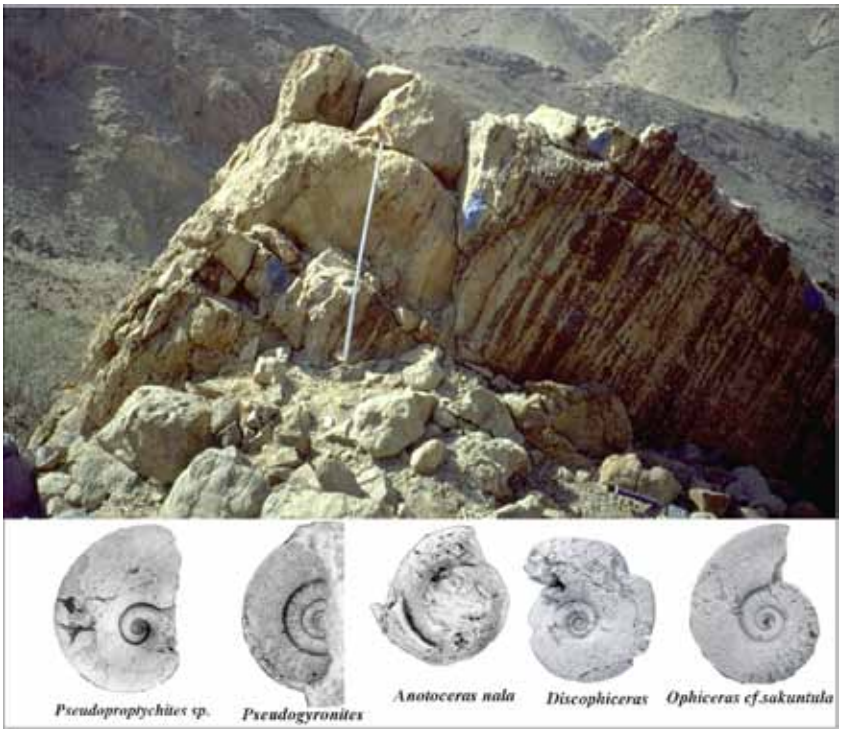

Figure 45: The ammonoid fauna of the Wadi Wasit block (after Krystyn et al., 2003).

Microfacies (after Krystyn et al., 2003, Fig. 46).
The microfacies of the *Promyalina* Beds (0-2,5 m; Figs. 44, 46) consists of sediment-free spar-cemented densely packed, well-sorted bivalve shells with predominantly oblique orientation dominate the lower half of the interval.
Above are beds with poor shell sorting and more parallel shell orientation in both convex-up and –down positions (fig. 32, 98/50). Geopetal fills of fine-grained mud- and ostracod-bearing wackestone in convex-down orientated shells become frequent in this part and are interpreted as relictic primary matrix.

The interval of the Lower *Eumorphotis* Beds (2,5-3,2 m; Fig. 46) consists of beds with two contrasting microfacies: 1) a lower coquina layer similar to those in the top-Promyalina beds but with increasing geopetal fills of fine-grained sediment (fig. 46, 98/51) overlain with gradational contact by 2) bioclastic pack- and wackestone rich in microgatropods, ostracods, broken bivalve shell debris, echinoderms (slender echinid spines); complete single shells, crinoid ossicles and often fragmented cephalopods are comparably rare (fig. 46 98/52b).

The microfacies of the Upper *Eumorphotis* Beds (3,2-4,2 m; Fig. 46, 98/53) consists of grain- and packstone with often geopetally filled microgastropods (=A), echinoderms (disarticulated crinoid ossicles =B, slender "*Cidaris*" spines), subangular fragmented bivalve shells (=C), ostracods and, less common complete bivalve (=D) and juvenile ammonoid shells. Local wackestone concentrations may result from burrowing.

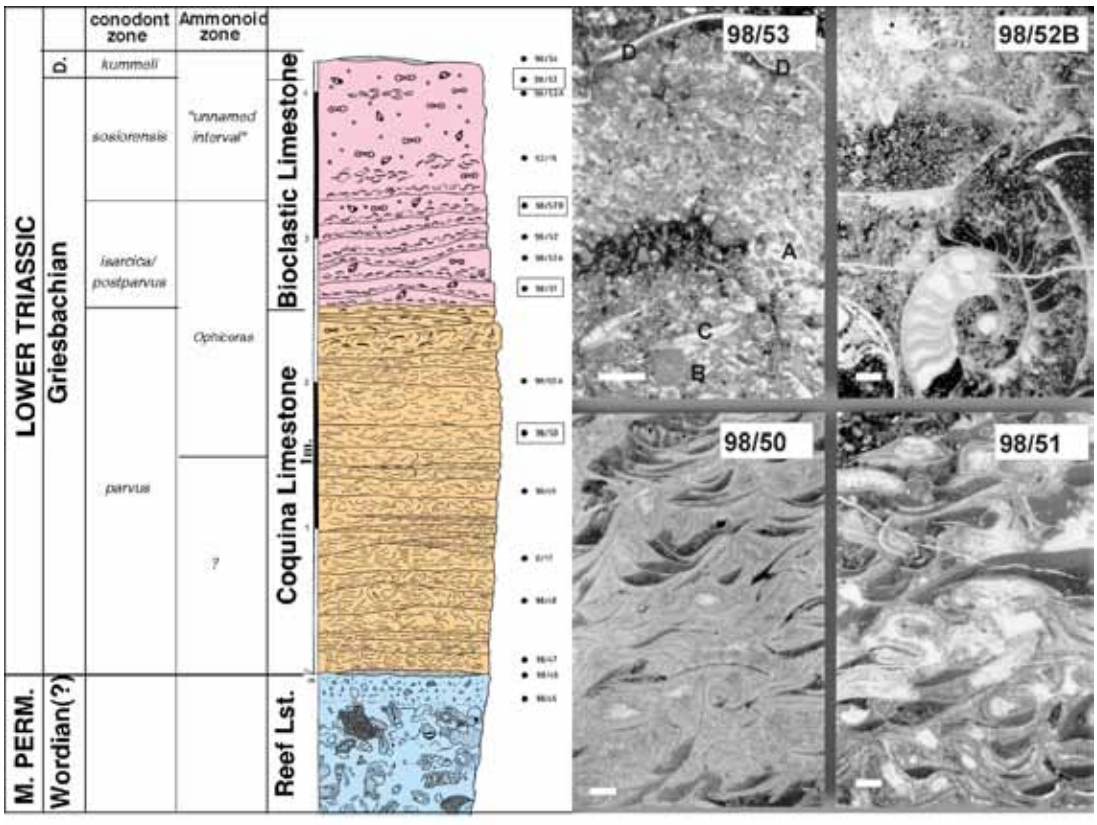

Figure 46: Stratigraphic sketch and microfacies of the Wadi Wasit block (after Krystyn et al., 2003); 98/53: *bioclastic grain- and packstone with often geopetally filled microgastropods (= A), echinoderms (disarticulated crinoid ossicles= B), subangular, fragmented bivalve shells (=C), ostracods and less common unbroken bivalve shells (=D); upper Eumorphotis beds. 98/52B: bioclastic pack- to wackestone, rich in skeletal debris (bivalves, echinoderms, ostracods, rare*

ammonoids); lower Eumorphotis beds. 98/50: Densely packed, spar-cemented bivalve shells with rare geopetal infill of ostracods-bearing mud; Promyalina beds. 98/51 Bivalve coquina with increased geopetal infill overlain by bioclastic wackestone (upper left); lower Eumorphotis beds. Scale bar is 1 mm.

Conodonts (after Krystyn et al., 2003, Fig. 47)**.**
A diverse conodont association (Fig. 47) constitutes an important part of the microfauna with several hundred specimens per kilogram. This gondolellid dominated fauna with extremely rare *Hindeodus* in the upper Bioclastic Limestone. contrasts well with the pure *Hindeodus* assemblage below.

The Bioclastic Limestone, is disconformably overlain by an only locally preserved 1 cm thin layer of megafossil free, grey, marly fine-grained limestone, dated by conodonts as Dienerian (e.g. *Sweetospathodus kummeli*). Both the mud-supported fabric and the high terrigeneous insoluble residue of this peculiar bed indicate a pronounced change of the sedimentary environment from relatively shallow carbonate-rich to deeper and siliciclastic-influenced depositional regime at the final stage of the block's history.

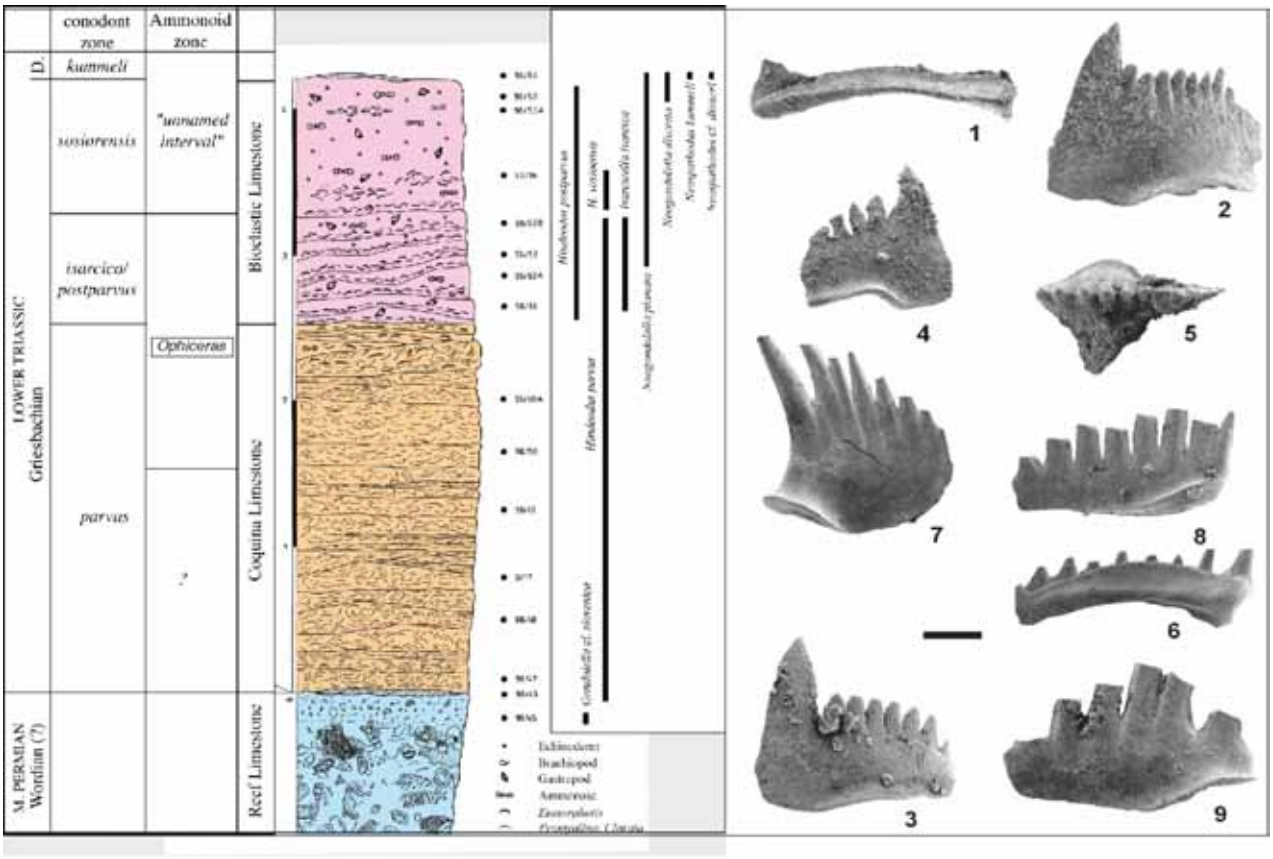

Figure 47: Stratigraphy with conodont ranges and conodonts of the Wadi Wasit block (after Krystyn et al., 2003); 1: Mesogondolella sp., 98/45. 2-3: Hindeodus parvus (KOZUR and PIATAKOVA), 2=98/46, 3=98/52A. 4: Hindeodus postparvus KOZUR, 98/53. 5: Isarcicella staeschei (DAI and ZHANG), 98/52A. 6: Neoclarkina discreta ORCHARD and KRYSTYN, 98/53. 7: Neospathodus dieneri SWEET, 92/17. 8: Sweetospathodus kummeli SWEET, 98/54. 9: Neospathodus cristagalli (HUCKRIEDE), 92/17.

The section can be divided into a lower *Hindeodus* (samples 98/46 – 98/52) and an upper gondolellid biofacies (98/52B – 98/54). The separation is very distinct and could indicate a pronounced environmental change otherwise undocumented in the sedimentary record.

The rather monotonous *Hindeodus* biofacies of samples 98/46 – 98/50A is formed by 100% *Hindeodus*. Rare specimens of *Isarcicella* and *Clarkina* reduce the *Hindeodus* abundance to 99% (98/51) and 97% (98/52) up-section.

At the base of the gondolellid biofacies (sample 98/52B), 80% of the p-elements are assigned to *Clarkina*. The relative abundance of *Clarkina and Neoclarkina* rapidly increases to 90% (92/16) and finally to 100% (0/11). *Hindeodus* elements make up 20% of the fauna in sample 98/52B, 10% in 92/16 and finally just 1% in 98/53.

A conodont study of Chinese P-T boundary sections has led Lai et al. (2001) to the conclusion that *Clarkina* and *Hindeodus* occupied different life habitats. They interpret *Clarkina* as a nektobenthic genus living in oxygenated deeper water, whereas *Hindeodus* is considered as a nektic taxon inhabiting the uppermost (shallowest) parts of the water column from near shore to pelagic environments.

This model explains the absence of *Clarkina* in the storm-generated shallow-water layers of the *Hindeodus* biofacies (see below). It does not, however, explain the decline and disappearance of *Hindeodus* in the upper part of the block.

Biochronology (after Krystyn et al., 2003, Figs 47, 48).
The Reefal Limestone unit is dated as Middle Permian (Guadalupian) by the presence of the conodont *Mesogondolella* sp. (Fig. 47/1).

The overlying Coquina Limestone and Bioclastic Limestone units are Griesbachian in age, and three conodont zones (Figure 31) are recognized:
(1) a basal Parvus Zone, 2.5 m thick;
(2) the Staeschei (or Isarcica) Zone, < 1 m thick;
(3) the Sosioensis Zone, <1 m thick.
The latter zone is herein defined from the first appearance datum (FAD) of *H. sosioensis* until the FAD of *Sweetospathodus kummeli* (Fig. 47/8), and corresponds to the *Neoclarkina discreta* Zone of Spiti (Orchard & Krystyn, 1998). Comparison with other Tethyan Griesbachian age sections (Meishan, Spiti, Abadeh) suggests that *Isarcicella staeschei* (Fig. 47/5) appears rather later in this section than elsewhere, and may not indicate the full range of the zone. The Marly Limestone unit contains *Sweetospathodus kummeli* (Fig. 47/8), indicative of a basal Dienerian age.

Ammonoids are fairly common in the upper part of the block and allow the identification of two zones (Figure 46). Firstly, the *Ophiceras tibeticum* Zone, here represented by a single and very evolute *Ophiceras* species similar to the holotype of *O. connectens* Schindewolf and by *Ophiceras* cf. s*akuntula* Diener (Fig. 46). Secondly, a zone that corresponds to the so-called "unnamed interval" first described by Orchard & Krystyn (1998) from the Himalayas. This interval is characterized by a rich and hitherto undescribed fauna composed of many genera with an intermediate ophiceratid-gyronitid morphology, together with the last true ophiceratid (*Discophiceras*, Fig. 46).

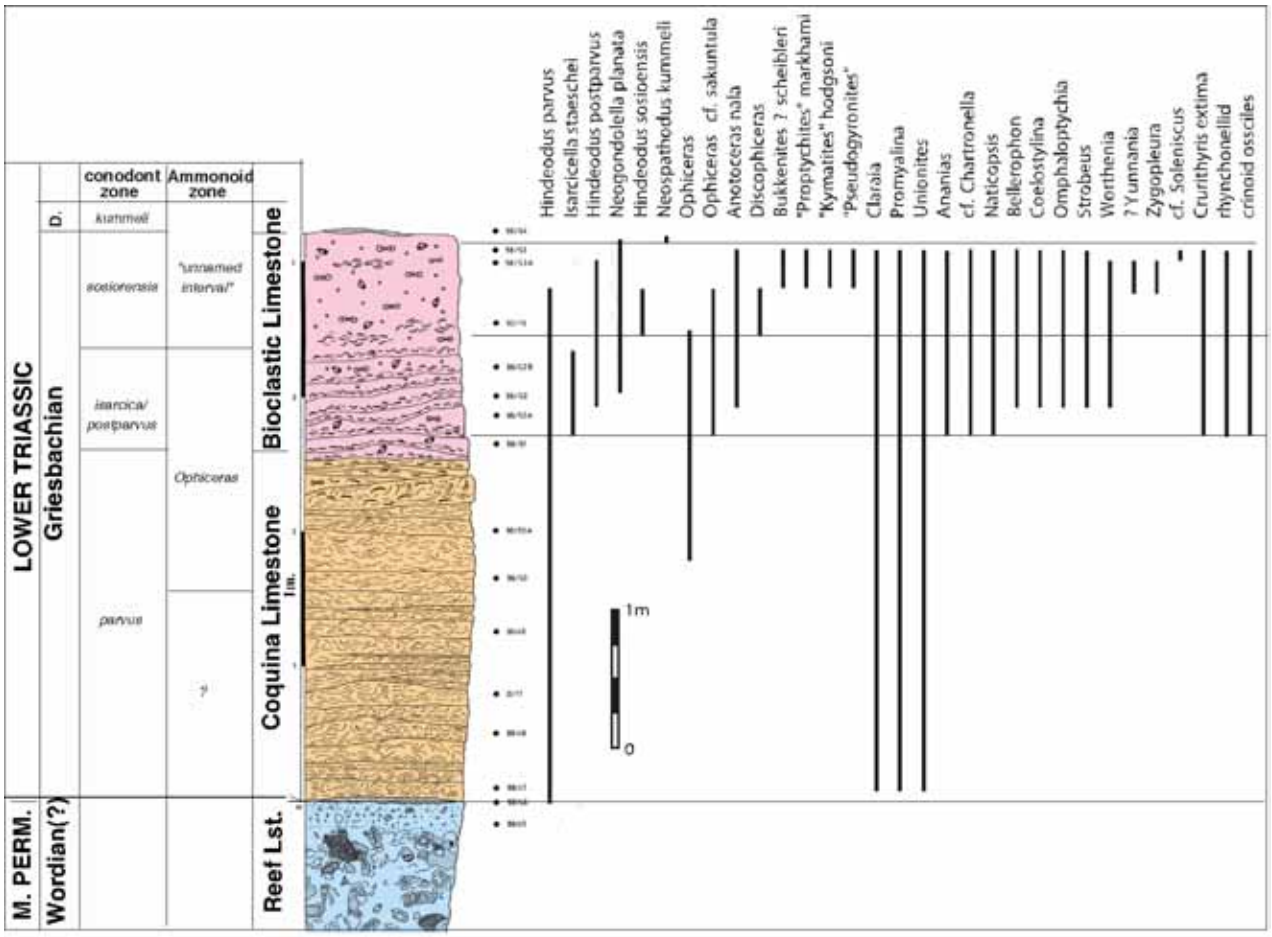

Figure 48: Stratigraphy and biochronology of the Wadi Wasit block (after Krystyn et al., 2003) with ranges of the main fossils and biota.

Chemostratigraphy (after Krystyn et al. 2003 and Richoz 2006).
In this study, δ13Ccarb isotopic analyses of the Wasit block were performed on selected micrite samples, wherever possible, which were drilled with a dental burr. Five samples (99/65-OMO64) from the Coquina Limestone unit have no micrite thus the analyses have been performed both on the early diagenetic sparry-cement and on bulk rock, which gave similar results; however the results of these analyses must be taken with caution.

The Reefal Limestone unit yields typical marine Permian values of around 4 ‰ (e.g. Atudorei, 1999; Richoz 2006). The more unstable values in the last metre can be attributed to dissolution effects during an interval of non-deposition or subaerial exposure at the boundary. Such a gap is supported by rare karstic cavity fills and the biostratigraphic data, above.

The base of the Coquina Limestone unit (lowest 10 cm) gives low values (0.4‰), typical of the very base of the Griesbachian (e.g. Richoz 2006). A shift to more positive values happens very quickly above the boundary and the remainder of the Coquina Limestone shows stable isotopic values around 2‰, with a very slight negative shift in the middle part of the Coquina Limestone. A positive shift occurs at the base of the Bioclastic Limestone unit between 98/52 and 98/52B where values increase from 2‰ to 3‰. It corresponds to the change in conodont biofacies, suggesting that there is an environmental change undetected in the sedimentary record at this level. The few isotopic values obtain on organic matter confirm the same trend.

Isotopic results confirm the biostratigraphic data, which suggest that there is no significant gap in the basal Triassic record, at least between the Coquina and Bioclastic Limestones and between the Bioclastic and Marly Limestone units. The isotopic curve (Fig. 49) follows the typical values for this time interval (e.g. Baud et al., 1989; Richoz 2006). There is a rapid recovery after the boundary, relative stability during the interval dominated by Promyalina, and a rise of δ13Ccarb and δ13Corg in the Eumorphotis beds. Thus, the changes in isotopic values closely parallel the changes in faunal diversity and suggest that the δ13C curves reflects primary productivity.

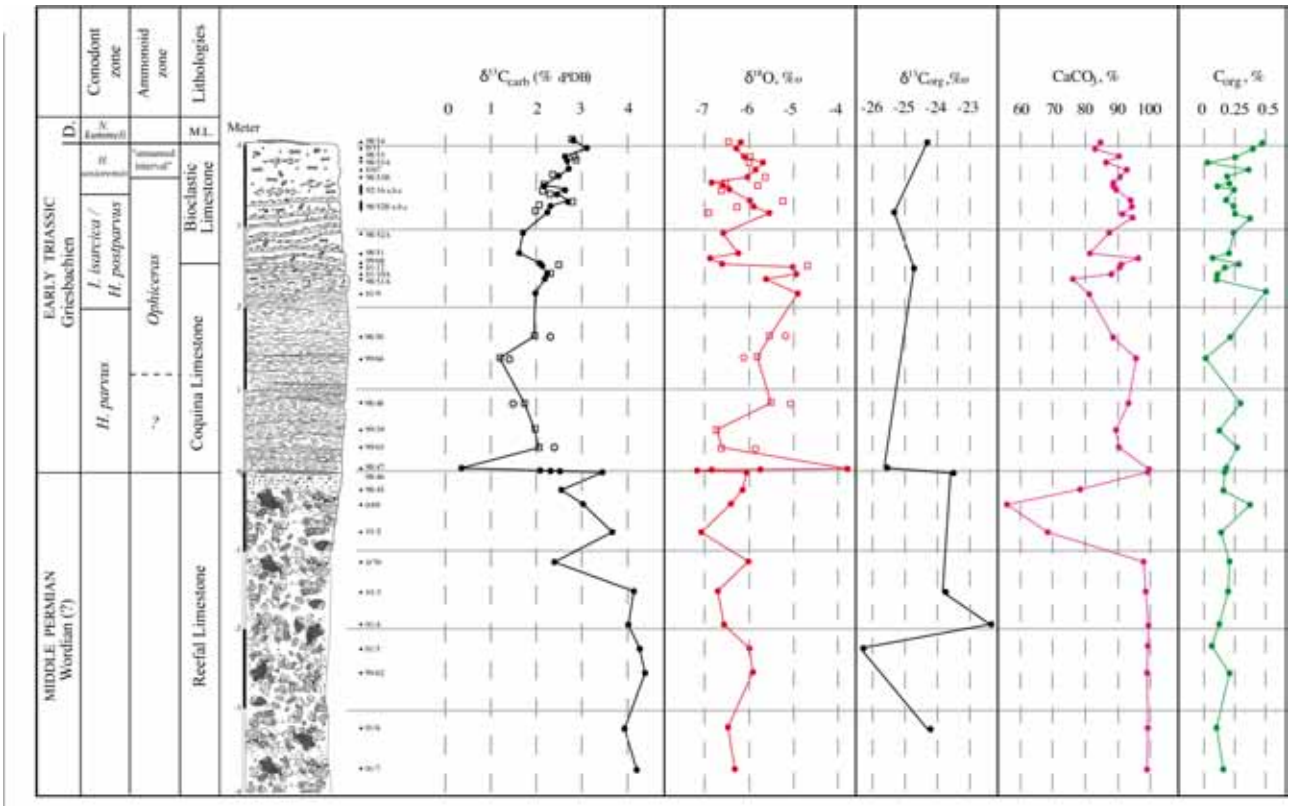

Fig.49: Chemostratigraph in Wadi Wasit block (Richoz 2006): M.L: Marly limestone, D. Dienerian. For $\delta^{13}C_{carb}$ and $\delta^{18}O_{carb}$ analyses have been made on selected micrite (filled circle), selected spar-cement (open circle) and bulk rock (open square). % in $CaCO_3$ and Corg have been obtained by coulometry.

Discussion (after Krystyn et al., 2003).

Basal Triassic depositional environment

The overall sequence is characterized by storm-influenced bivalve shell concentrations with increasing matrix support section upward. The latter could have resulted from decreasing storm influence due to a continuous deepening of the sea floor. The sharp base of the coquina layers supports an hydraulic concentration origin. Well preserved, mostly unbroken and not abraded or bioeroded shells exclude a wide lateral transport and are interpreted as evidence for rapid deposition. The nearly complete matrix loss in the *Promyalina* beds gives grounds to interpret them as proximal, very shallow neritic, local storm concentration layers. A slightly deeper palaeoenvironmentmay be inferred for the lower Eumorphotis beds due to the interfingering of the coquinas with bivalve-poor skeletal biogenic sediment containing a diverse and in part deeper marine fauna. This explains the incompletely removed micritic matrix of the bivalve shell concentrations, which are interpreted as proximal tempestites.

Storm-induced event beds are missing in the upper *Eumorphotis* beds and are conclusive of a more offshore position of the facies in increased water depth well in agreement with their pelagic influenced fauna (ammonoids, platform conodonts).

The significance of the Griesbachian bivalve beds.
Bivalve beds of Griesbachian age occur in a variety of environmental settings. In the basal Werfen Formation of the Dolostone, northern Italy, two main types of bivalve beds are encountered. Firstly, thick (0.5 to 1 m), matrix-supported, sharp-based slump units occur in the basal Mazzin Member during the early stages of transgression (Wignall and Twitchett, 1999). Secondly, much thinner (15 cm to <1 cm) bioclastic tempestites, which characterize the later stages of transgression and contain a fauna of bivalves (dominated by *Claraia*), microgastropods, conodonts and ophiuroid ossicles. The background sediment is a thinly bedded to laminated grey lime mudstone that was deposited under low-oxygen conditions in a distal ramp setting (e.g. Wignall and Twitchett, 1996; Twitchett 1999).

Bivalve beds from the Takashiho seamount, which represents a very different, ocean island type setting, were described by Kanmera and Nakazawa (1973) and more recently by Sano and Nakashima (1997) with new biochronological data. Regarding the basal Triassic as in the Wasit block, the lithofacies comprise massive, up to 4m thick, gastropod and bivalve accumulations, of Griesbachian to Dienerian age, containing *Eumorphotis* and pteriid species. The great thickness also suggests a multi-event composite origin, similar to the Wasit shell beds. One slight difference is that a gastropod biofacies appears near the base (*parvus* Zone) of the Takashiho succession, while a bivalve biofacies occurs higher up.

One of the most interesting aspects of the Wasit shell beds is the very high diversity of benthic taxa (at least, in the *Eumorphotis* beds). The Wasit bivalve beds were clearly deposited under normally oxygenated conditions, unlike the vast majority of other Griesbachian assemblages. Wignall and Twitchett (2002) concluded in their review that the shelf settings of the southern (Peri-Gondwanan) margin of Tethys (which includes present-day Oman) were the only parts of the ocean free of benthic oxygen restriction in the Early-mid Griesbachian. In this region, the deepest slope and basinal settings became oxygen restricted by the Early Griesbachian, whereas the shallower shelf settings were oxygenated until Late Griesbachian or Early Dienerian times (Wignall and Twitchett, 2002). The reason for this is unclear, although it was presumably controlled by regional ocean circulation patterns.

The Wasit bivalve beds show us that when oceanic conditions (*e.g.* oxygenation, productivity) are favourable, a much greater diversity of taxa will be present than would otherwise be the case, as it is in Griesbachian Tethyan carbonate platforms (c.f. Baud et al. 1996). Beatty et al. (2008) also showed an oxygenated "habitable zone" in shoreface siliciclastic succession on the northwestern margin of Pangea. This supports the hypothesis that the apparently slow faunal recovery after the P-Tr event was due to the long-lived and widespread unfavourable environmental conditions at least in Griesbachian (c.f. Erwin, 1993, p. 263; Twitchett, 1999). Moreover, despite the lack of evidence of anoxia, there is no Permian fauna in the basal Griesbachian (Parvus Zone), but opportunistic postextinction fauna. This challenges the hypothesis of anoxia on-set as the kill mechanism (Twichtett et al. 2003).

In Summary.
The Wasit block is a unique geological archive that contains evidence of an extraordinarily rapid faunal recovery after the P-Tr crisis with, at the same time, an increase of $\delta^{13}C_{carb}$ isotope values

from +1.2‰ in the basal Triassic transgression to 3.1‰ at the end of the Griesbachian (signifying probably an increase in productivity?).
It contains also the most diverse Griesbachian assemblage known to date, which has a community structure not normally recorded in pre-Spathian (Early Triassic) rocks and which was living under well oxygenated conditions.
This shows us that where conditions of oxygenation and productivity are favourable, a diverse fauna will be recorded. The impoverished faunas and the apparently slow recovery of the Early Triassic marine ecosystem are therefore the result of widespread unfavourable environmental conditions.

<u>February 25, 2010</u> -The Permian-Triassic transition in the Buday'ah area.

(A. Baud, S. Richoz, B. Beauchamp, F. Cordey, S. Grasby, C. Henderson, L. Krystyn).

Routing (Fig. 50): Starting at 8 a.m., February 25, from Hotel Ibis (Muscat), we will move to Buday'ah following first the Muscat-Sohar highway up to Al Khabura roundabout and then take left the paved road in direction of Wadi Hawasina -Ibri up to Buday'ah (Figs. 50 and 51)

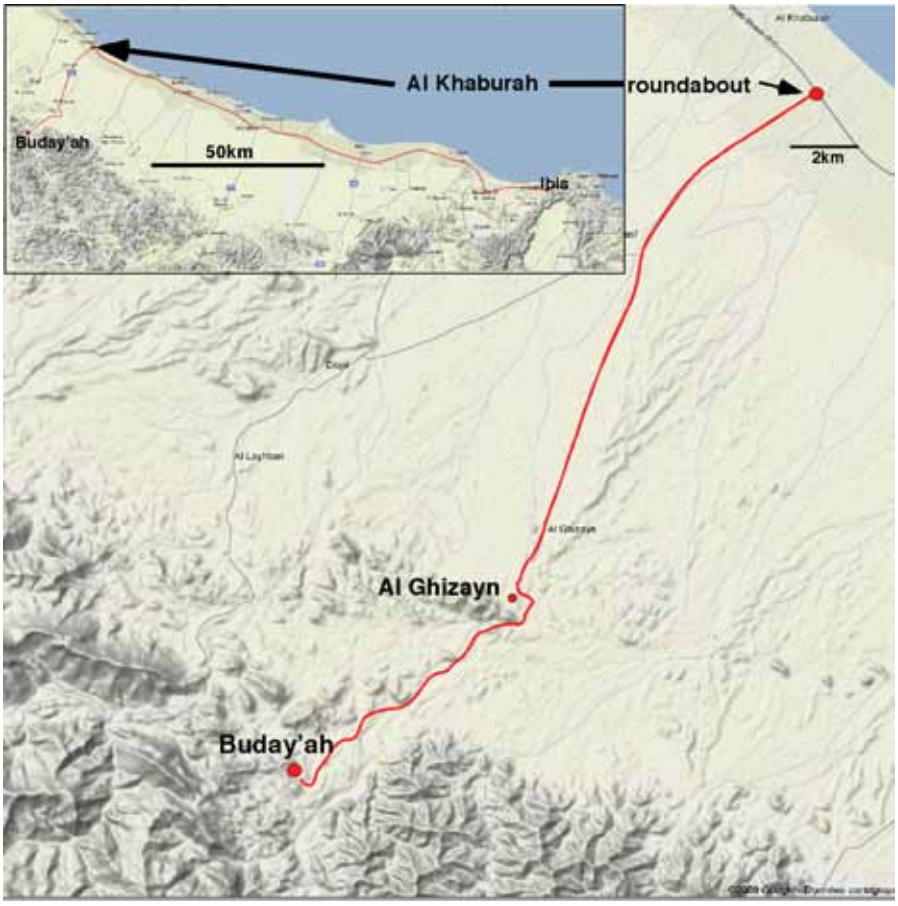

Figure 50: Google Map with detailed road itinerary from Al Khabura roundabout in red and left up a complete itinerary from Muscat to Buday'ah (coord.: N 23° 44' 43'' E 56° 54' 21'').

Introduction

The Oman Mountains expose the Middle Permian to Lower Triassic Buday'ah section of oceanic sediments belonging to the south margin of the Tethys. Located in the northeast part of the Hawasina Window (fig. 52, Ibri map, Béchennec et al., 1992c), this locality is among the very few places of real Tethyan Permian radiolarites. With previous data, this locality has been described in previous field guide-books (Baud et al., 2001b, Richoz et al, 2005) and by S. Richoz, 2006.

Compared with other Hamrat Duru successions (Wadi Wasit, Nakhl, Rustaq) the Buday'ah locality (Fig. 53) is the most distal and probably deepest Permian depositional sequence of the basin as it has, above the basal red limestones only minor carbonatic influx and misses any shallow water debris input (reefal slump blocks, calciturbites) known from the other sections. In this sense this lithological unit differs considerably from the Al Jil Formation as defined by Béchennec, 1987,

Figure 51: Google Earth oblique view of the Buday'ah area road itinerary from Al Ghiayin in red.

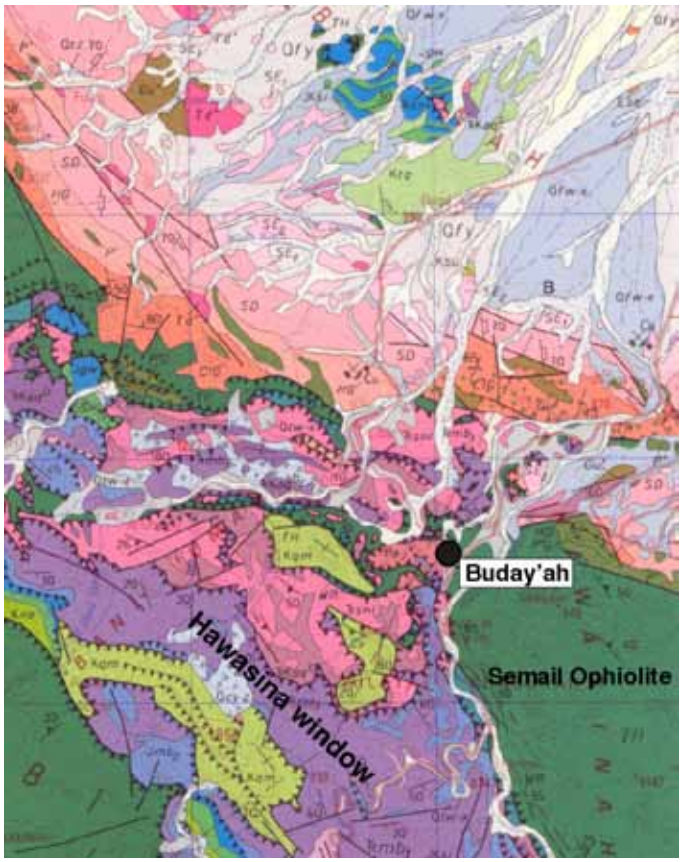

Figure 52: Geological map of the area (from Ibri map, Béchennec et al., 1992c).
at the foot of Djebel Misht and around Taw in the central west Oman Mountains (Seeb map area) and partly redefined in the same area during 1:250,000-scale mapping (Béchennec *et al*., 1992a). It is why we are proposing here the name of Buday'ah Formation that is informally subdivided in 8 minor litho-units numbered from 1 to 8 (Fig. 54).

The truncated substratum of the sedimentary succession consists of pillow basalts. These basaltic pillow lavas forms two hills, one roughly 1 km across and the other several kilometres across. The basal volcanic sequence is composed of dark-green to brown, slightly amygdaloidal, pillow basalt in which the pillows range in diametre from 20 cm to 1 m and have aphyric cores and rims which locally contain plagioclase phenocrysts.

According to Maury in Baud et al. (2001b) and Maury et al. (2003), the basalt has microlitic texture, is generally spherulitic and locally porphyritic; it is composed of plagioclase mainly as sheafs of skeletal microlites but also in spherulites and in places as phenocrysts, rare clinopyroxene as fine prisms and phenocrysts replaced by carbonate and oxides, Fe- Ti oxides occurring interstitially and as elongate skeletal crystals, and carbonate in small amygdales. Data on rare earth elements (REE), Th and high field strength elements on two basalt samples at Buday'ah show transitional and enriched MORB signatures (Maury et al., 2003, Lapierre et al. 2004); such association erupted in the Hawasina basin far away from the continent, from truly oceanic settings, but located near hot spots (Lapierre et al. 2004).

In different parts of the pillow lava succession, inter-pillow cavities are filled up with red lime-mudstone yielding conodonts, particularly near the top.

Figure 53: View of Buday'ah locality from the parking place, looking N. Overturned succession of MORB-type lavas (Buday'ah unit 1, top of the front hill) and Upper Permian radiolarian chert and shales below (Buday'ah units 3-4). Stops 1 and 2 right behind the hill (photo J. Marcoux).

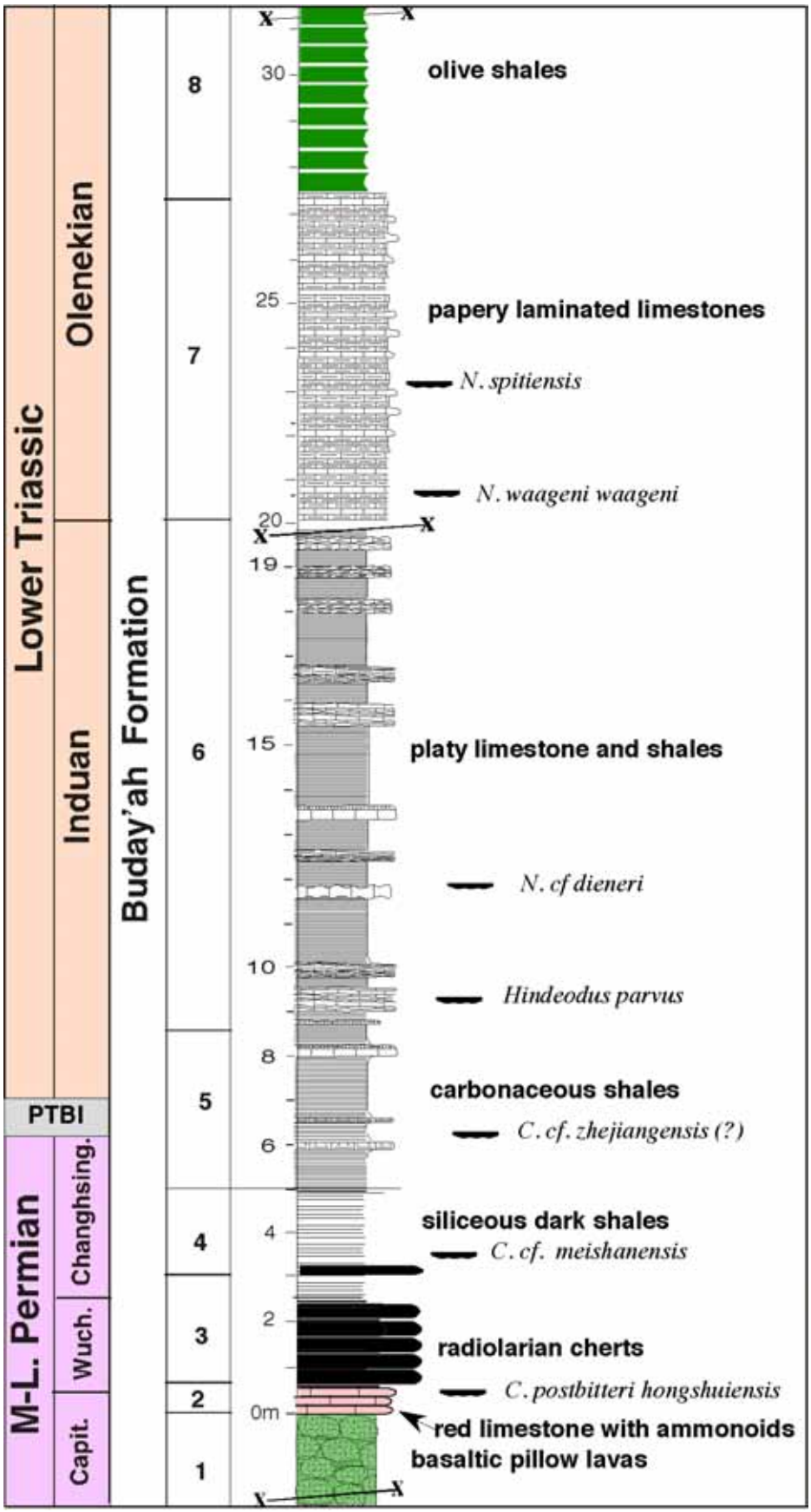

Figure 54: Stratigraphy of the Buday'ah composite section with the new conodont finding by Alda Nicora and Charles Henderson (except of H. parvus and N. dieneri reported in Richoz, 2006).

Stop 1: stratigraphy of the lower Buday'ah Formation
Details of the outcropping area are shown in the Google Earth oblique view with the situation of the three stops of the day (Fig. 55).

From the parking place we will move to stop 1 (Fig. 55) that is situated just on the other side of the hill shown on photo Fig. 53.

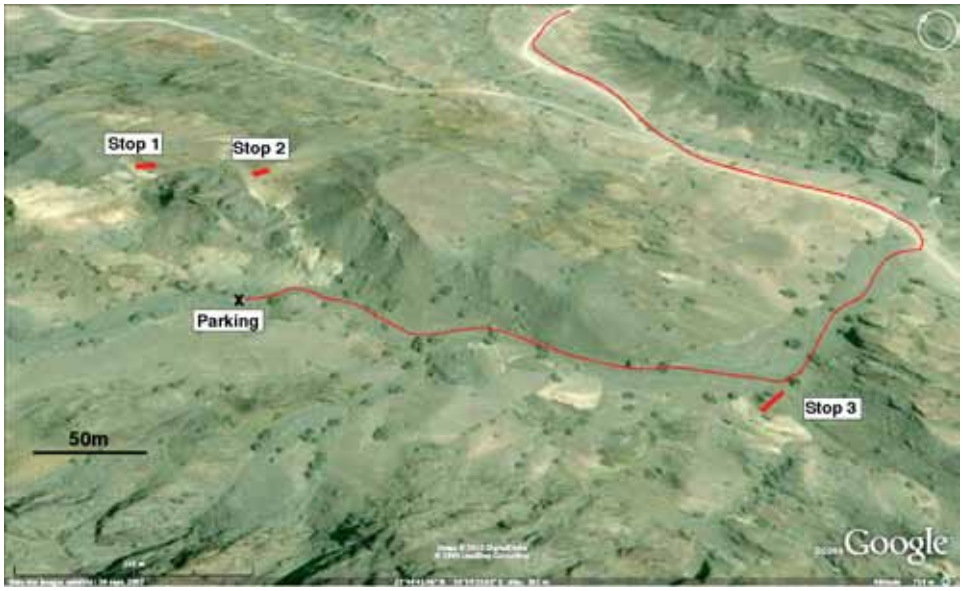

Figure 55: Google Earth oblique view of the Buday'ah area with place of the 3 stops of the day.

We will look first at the **spectacular pillow lava of the Unit 1** and at the red nodular cephalopod limestones that filled the irregular upper surface of the pillows (Fig. 56). The following **Unit 2**, dm thick **red ammonoid- limestones** (with lateral variation of thickness 0.2m-1.2m), are typical condensed cephalopod pelagic limestones known in the Triassic of Eastern Alps as the Hallstatt limestone.

Figure 56: Overturned section of the basal part of the Buday'ah Formation with the contact between units 1, 2 and 3. Arrow: lenses of limestone between pillows

Thin coatings of black manganese oxide minerals are lining the shells (Fig.57a).

Figure 57: a- surface of red limestone containing large ammonoids with thin coatings of black manganese oxide minerals lining the original shells. b- hammer on the upper limestone bed overlain by red and brownish siliceous shale and mm bedded radiolarites with left up well-bedded red radiolarites.

The ammonoids *Timorites* sp. and *Waagenoceras* cf. *mojsisovicsi* (det. L. Krystyn, Fig. 58) have been recovered in the red lime mudstone interval between lavas and indicate a Late Wordian - Capitanian age for the infilling of volcanic sequence.

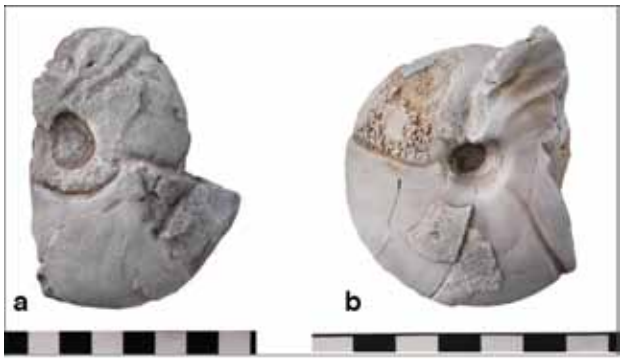

Figure 58:Ammonoids from Unit 2 of the Buday'ah Formation. Photo and det. L. Krystyn. a- Timorites sp.; b- Waagenoceras cf. mojsisovicsi GEMM.

Near the top of the limestones, A. Nicora and C. Henderson have recovered a new *Clarkina* fauna with *C. postbitteri hongshuiensis* of latest Capitanian.
When outcropping there is a 0.5 to 2m thick interval of siliceous shale and mm bedded radiolarites between the red limestones and the dm thick bedded red radiolarites (Fig. 57b)

The red radiolarian cherts (*F. Cordey, Figs. 59, 60*).
The next **unit 3** of the Buday'ah Formation consists of a succession of thin nodular brownish mudstone, siliceous shale and **red radiolarian cherts (Fig. 61)** resting conformably on the red limestone and laterally directly on the basalt and was dated as Wordian on the basis of radiolarians (Béchennec, 1987; De Wever *et al*, 1988). A separate overturned section B directly in contact with the pillow lava without limestones is illustrated in Fig. 59 (Cordey's section).

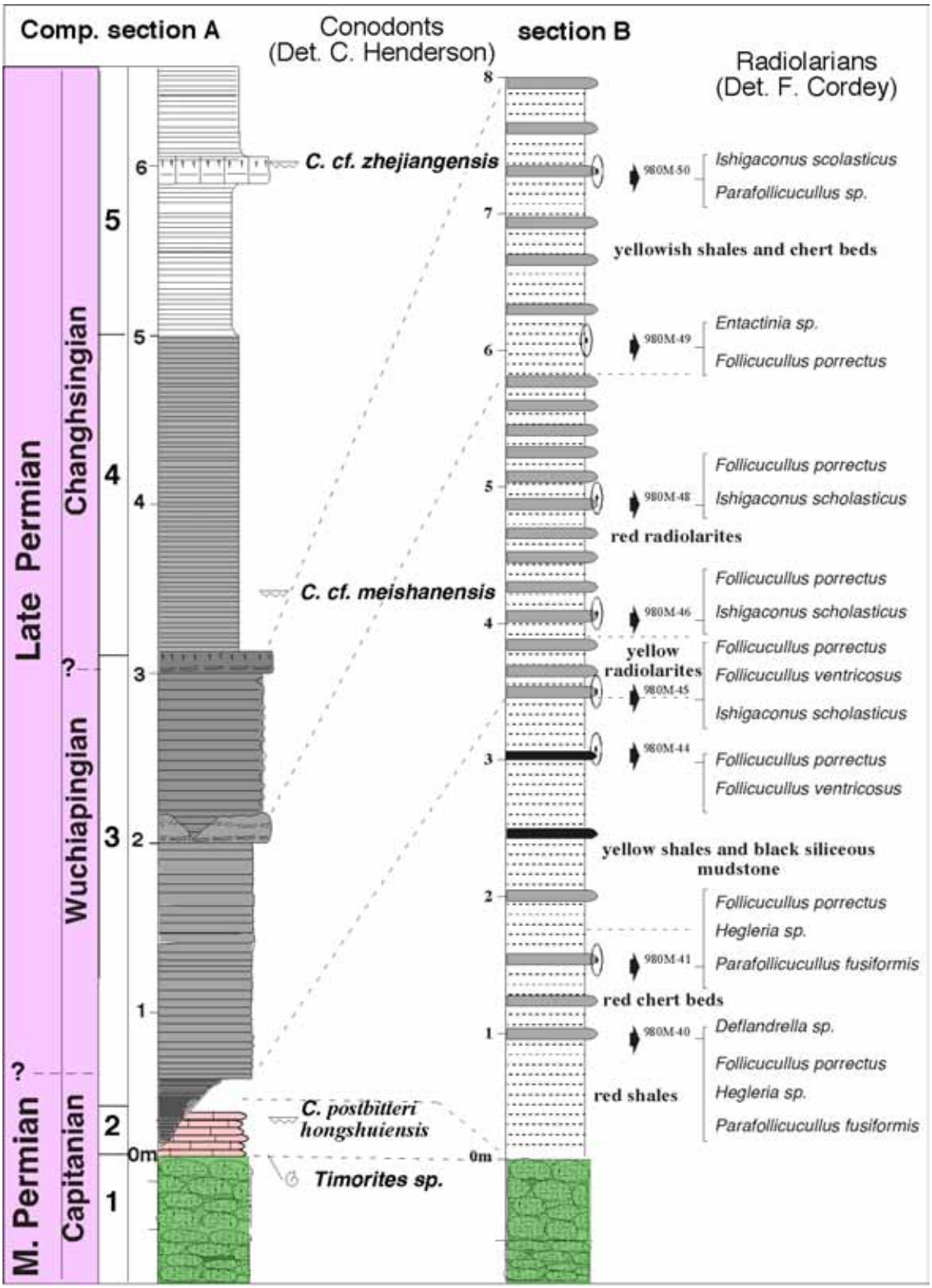

Figure 59: Stratigraphy of the Lower Buday'ah Formation (Unit 1 to 4) with the correlation between sections A and B. Section B has been presented by F. Cordey (fig. 17 in Baud et al., 2001b).

This section was sampled earlier by F. Cordey (*in* Baud et al., 2001) and consists of the following lithologies (Fig. 59): red shales and red chert beds (2 m), yellow shales and black siliceous mudstone (2 m), yellow radiolarites (0.5 m), red radiolarites (2 m), yellowish shales and chert beds (2 m). In previous publications, the radiolarians were assigned an age range from Wordian to

Capitanian on the basis of 9 associations correlated with *Parafollicucullus fusiformis* - *Parafollicucullus globosus* and *Follicucullus ventricosus* - *Ishigaconus scholasticus* assemblage zones (Fig. 59). However, according to the fact that the radiolarites (Unit 3) overlie the level with *C. postbitteri hongshuiensis* of latest Capitanian, the radiolarian assemblage zones must be latest Capitanian to Wuchiapingian in age. The extinction event is recorded at the top of the radiolarites. Some key radiolarians are illustrated below (Fig. 60, F. Cordey)

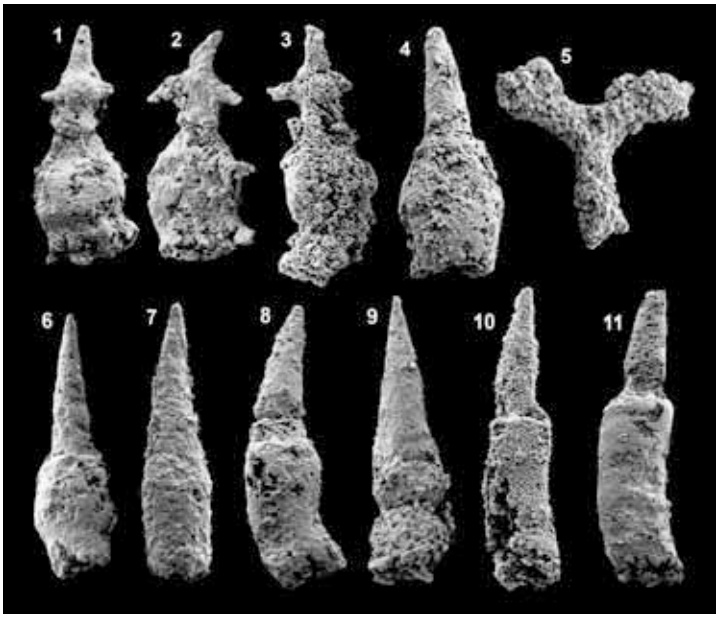

Figure 60: Radiolarian from the Unit 3 of the Buday'ah Formation, section B, photos and det. F. Cordey. 1-3. Pseudoalbaillella fusiformis HOLDSWORTH & JONES, 1 : OM98-40, 370 µm ; 2-3 : OM98-41, 400 µm. 4. Follicucullus ventricosus ORMISTON & BABCOCK, OM98-44, 350 µm. 5. ?Cauletella sp. cf. manica (De WEVER & CARIDROIT), OM98-40, 350 µm. 6. Follicucullus sp. aff. ventricosus ORMISTON & BABCOCK, OM98-40, 340 µm. 7. Follicucullus scholasticus ORMISTON & BABCOCK, OM98-41, 320 µm. 8. Follicucullus porrectus RUDENKO, OM98-46, 400 µm. 9-11. Follicucullus sp., OM98-41, 400 µm.

Figure 61: Photo of the red radiolarites (part of Unit 3); scale=hammer.

Stop 2, the middle part of the Buday'ah Formation and the PTBI (Fig. 62).

Figure 62: Stop 2, view of the studied profile. 1- Overturned succession of MORB-type lavas (Unit 1); 3- Middle to Late Permian radiolarian chert; 3=siliceous shales (part of the Unit 3); 4-siliceous shales (Unit 4); 5- carbonaceous shales (Unit 5); 6 brown weathered platy limestones and shales (Unit 6). The Permian-Triassic boundary interval (PTBI) is within Unit 5.

From stop 1, we will move over the hill up to stop 2 (situation in Fig.55 and view, Fig. 62). Overlying the red radiolarites is **the Unit 4** with monotonous **dark grey siliceous shales** about 2 m thick. Near the base (Fig. 62), a conodont sample provided *C. cf. meishanensis* (det. C. Henderson) of latest Changhsingian age.

A sudden subtle lithological change occurs at the base of the **Unit 5** (about 3m thick) with the appearance of **light calcareous shales** with 2-3 thin limestone beds. 1.2m above the base a conodont sample provided a fragment attributed to C. *zhejiangensis*(?) (det. C. Henderson) that spans the Permian-Triassic boundary.

Chemostratigraphy (S. Grasby, B. Beauchamp).
According to the $\delta^{13}C_{org}$ curve (Fig. 63), we consider that the first shift at 6.1m can be correlated with the shift found at the Permian-Triassic Boundary as it immediately overlies the single occurrence of the conodont *C. zhejiangensis(?)*.The second shift at 9.5m is just above the finding of *H. parvus* reported by S. Richoz, 2006.
Geochemical data across the Buday'ah section are shown in Fig. 64 (Units 1 through 5) are relatively consistent with no significant variation in geochemical parametres. The contact between units 5 and 6 shows slight enriched redox sensitive trace elements, increases total organic carbon content (TOC) and the highest d13C organic values in the section. The $\delta^{13}C_{org}$ values drop at the extinction boundary (base of the first carbonate), associated with a second spike in redox sensitive elements.

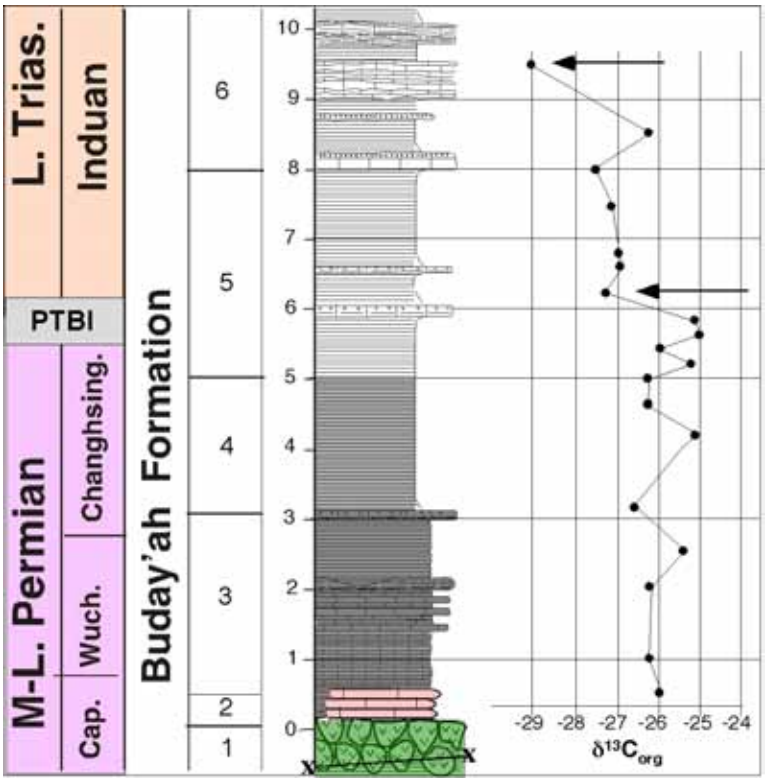

Figure 63: The lower Buday'ah Formation with $\delta^{13}C_{org}$ curve of S. Grasby and B. Beauchamp. Arrows for the 2 main negative shifts.

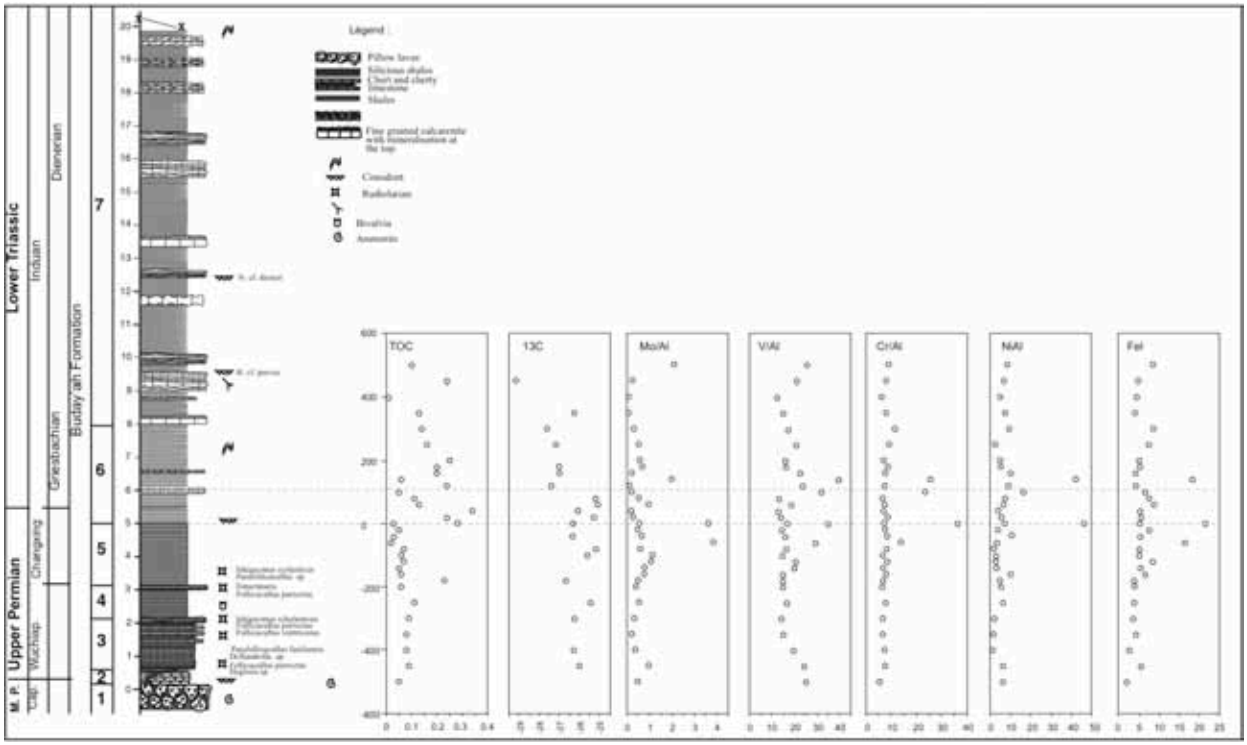

Figure 64: Chemostratigraphy of the lower part of the Buday'ah section (S. Grasby and B. Beauchamp)

The next **Unit 6,** about 11m thick (Fig. 65), start with a micritic grey limestone bed, 20cm thick (microfacies -a bioturbated and laminated lime mudstone, Fig. 65 B) followed by 80cm of light calcareous shales. The following platy limestones with calcispheres contain a badly preserved conodont *Hindeodus* cf. *parvus* and 3m higher *N. dieneri* (Richoz, 2006). The main part of this unit consists of alternating yellow marly shales, cm thick platy limestones and thicker (dm) marly limestones (Fig. 65A). Bedding and turbidite facies are shown in Fig. 65B and 65C.
Only laterally we can observe the contact with the next unit

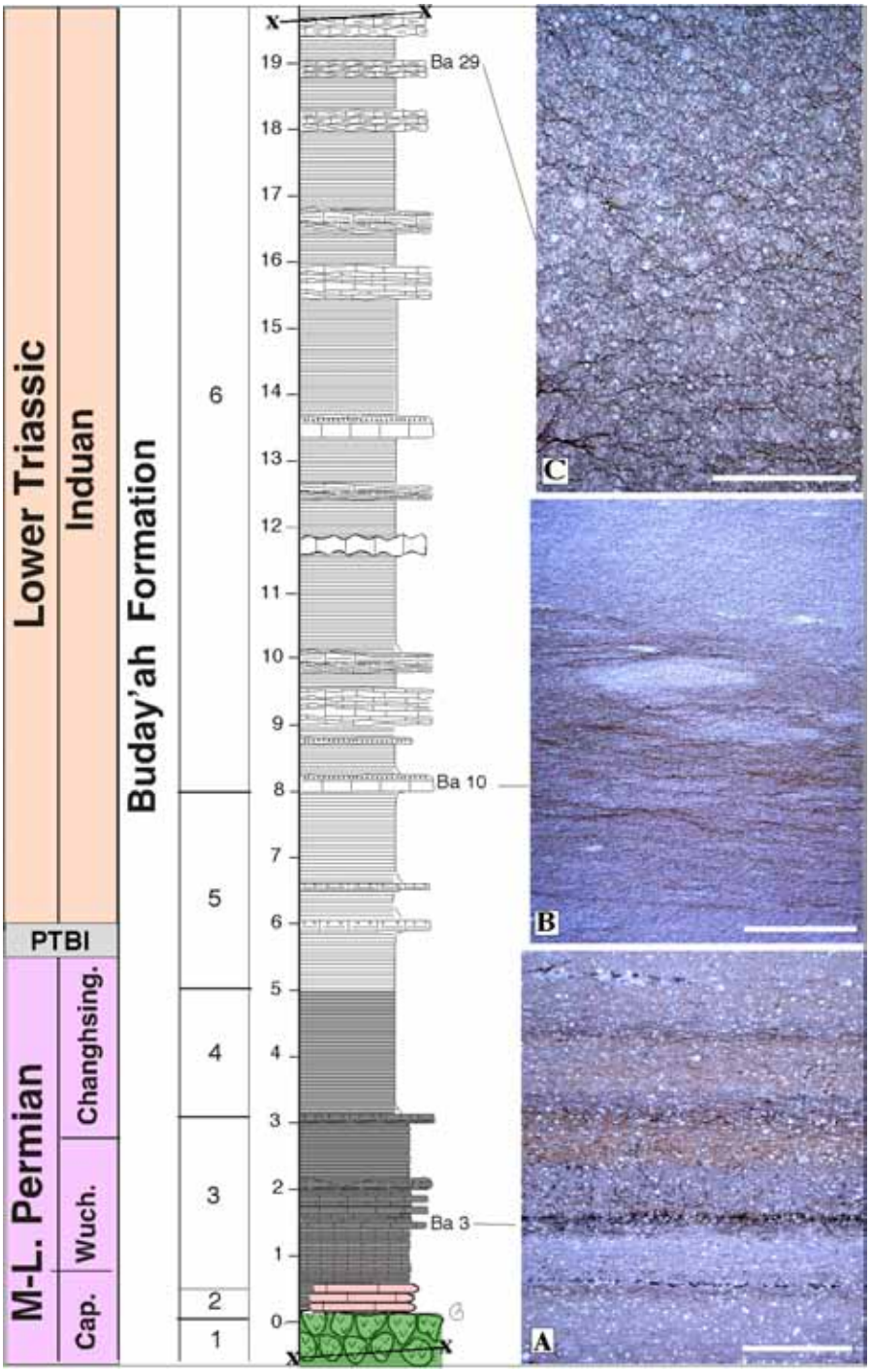

Figure 65: Microfacies of the lower and middle Buday'ah Formation (Unit 1 to 6). A: laminated lime siltstone with radiolarian (Wuchiapingian); B: lime mudstone with trace fossils (Griesbachian); C: lime packstone-siltstone with calcispheres (Griesbachian). Scale bar 5mm.

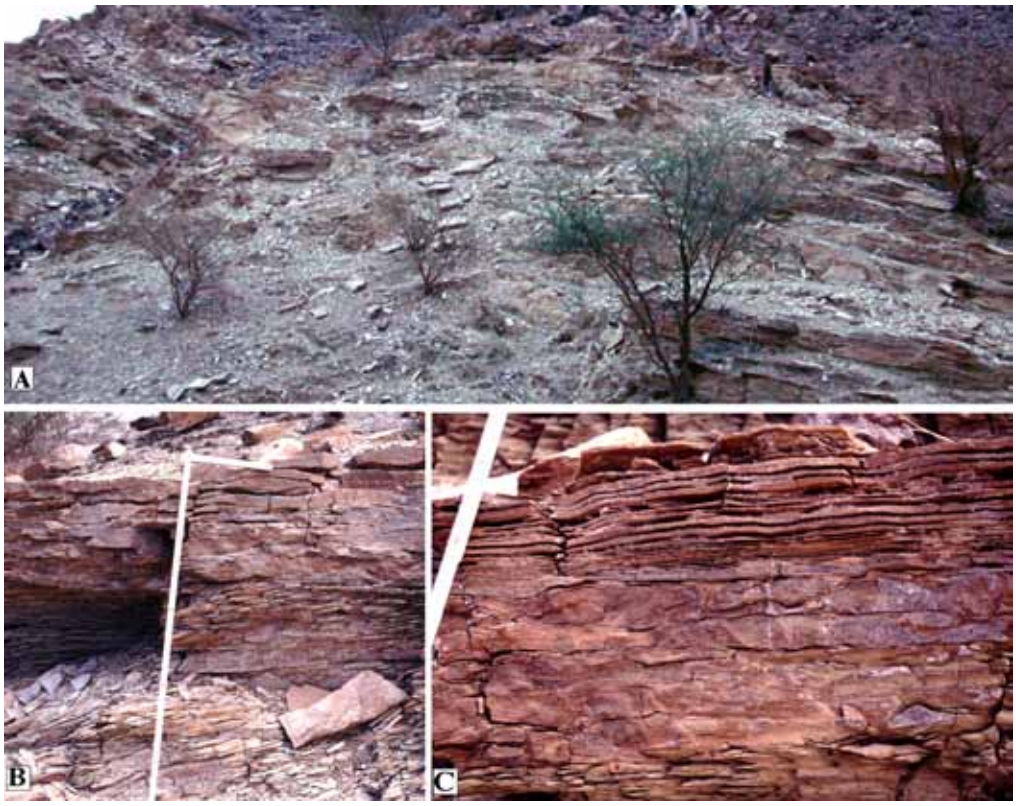

Figure 66: Platy limestone and shales of Unit 6. A- general outcrop picture; B- close view on the limestone bedding (vertical scale 60cm); C- detailed view on thinning upward bedding (distal lime mud silty turbidite (vertical scale 20cm).

Stop 3, the papery limestones and overlying shales (upper part of the Buday'ah Formation)
From stop 2, we will move down the hill and walk up to stop 3 (situation in Fig.55 and view, Figs. 67 - 68).

Figure 67: Stop 3 with overview of the upper part of the Buday'ah Formation and relationships between the top part of unit 6, Unit 7 and a truncated lower part of Unit 8.

The **Unit 7** consists of a very thin bedded grey limestone unit (**papery limestones**, Figs. 67-68) is completely devoid of macrofossils, without any trace fossils but provided the conodont *N. waageni waageni* (det. C. Henderson and A. Nicora, Plate 2) near the base and *N. spitiensis* near the middle of the unit. Both species are typical of the ammonoid *E. romunderi* Zone (Smithian, Orchard and Zonneveld, 2009).

Figure 68: left, the typical papery limestone facies: right, detailed view of finely laminated lime mudstone. White scale bar =10cm.

This facies has some similarities with the basal Triassic limestones of Wadi Maqam (we will look at and compare next February 26 stop 2).

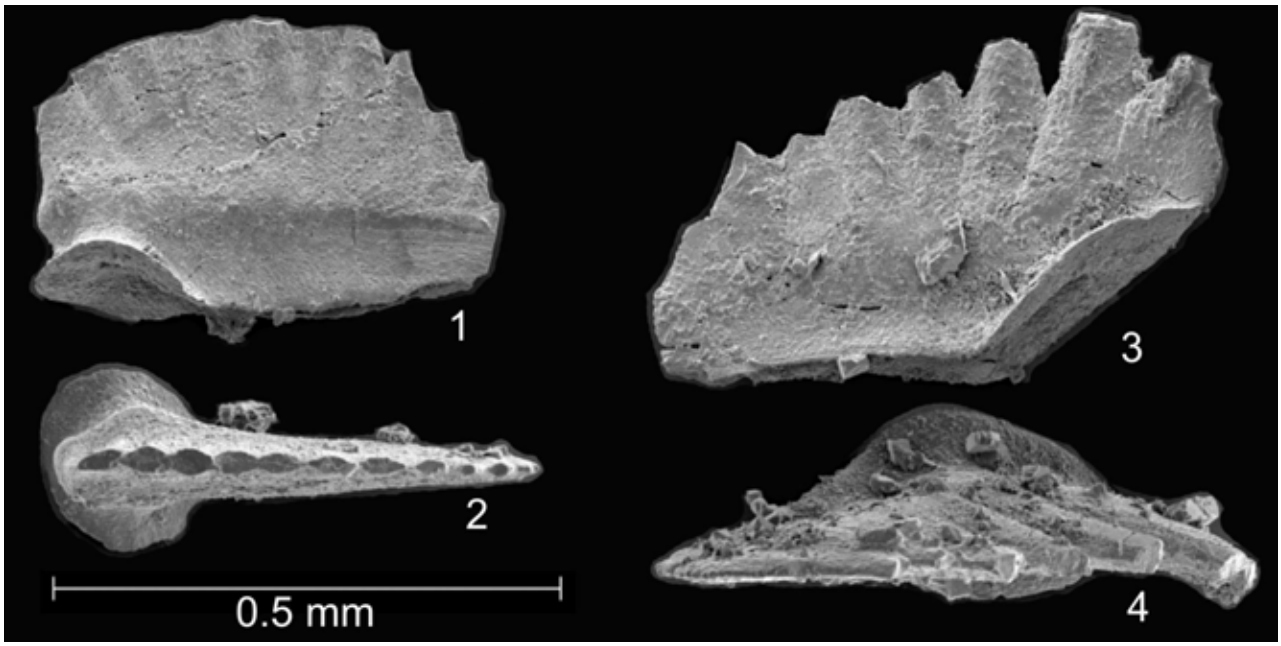

Plate 2: 1, 2, Novispathodus waageni waageni (waageni sensu lato) from base of unit 7. No 3, 4, N. spitiensis from middle of unit 7.

Until now, there are no detailed investigations on the overlying **olive shales** of **Unit 8**.

Discussion

A significant decrease of siliceous bioproductivity is recorded in the Late Permian but more researches is needed to evaluate the exact duration of this decrease. Actually we place the extinction event at the top of the bedded radiolarites. Casts of radiolarian and sponge spicules are present in the overlying platy limestones.

Comparing our Tethyan oceanic section with published Panthalassa sections shows that all localities display radiolarian cherts as the dominant type strata in the lower Late Permian. Up section, successions grade into "boundary shales" and/or black shales of various thicknesses. Did this change occur earlier in the Tethys (Early Changhsingian?) than in Panthalassa oceanic sections? We have not yet an answer. But it is only in southern Panthalassa that the chert deposition is continuous. The chert gap is of longer duration in the Tethys (15 My?) than in Panthalassa Mino-Tamba terrane (8 My) or Cache Creek terrane (12My). There is no chert gap in the Southern Panthalassa.

What is unique is that during the Early Triassic, the Tethyan margin included microbial carbonate close to the oceanic realm (platy to papery limestones) during Induan and at least part of the Olenekian. The Panthalassa oceanic sections are devoid of carbonate and biogenic siliceous sedimentation reappears progressively up section.

<u>February 26, 2010</u> -The Permian-Triassic transition in the Sumeini area.

(S. Richoz, A. Baud, B. Beauchamp, S. Grasby, C. Henderson, L. Krystyn, R. Twitchett).

Routing (Fig. 69, 70):

Starting at 8 a.m, from Holiday Arabian Resort Hotel (about 10km west from Hatta, UAE, 1, Fig. 69) we will follow the Dubai Highway for about 5km and then turn left on a side truck road. We will follow this road and then a side road according to the Google map (Fig. 70) up to the entrance of Wadi Maqam and parking place.

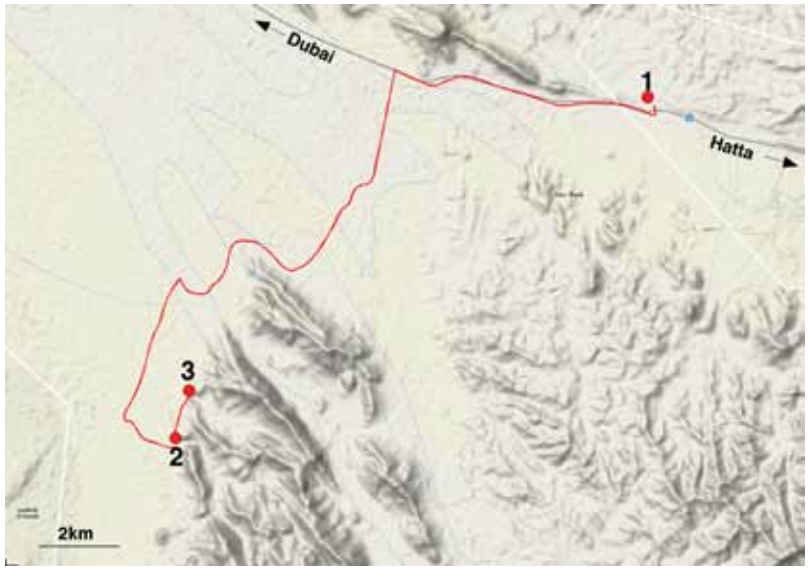

Figure 69: Google Map with detailed road itinerary from 1- Holiday Arabian Resort Hotel to 2- parking near the entrance of Wadi Maqam (coord.: N 24°46'30'' E 55°51'43''). 3- Wadi Shu'yab entrance.

Figure 70: Google Earth oblique view of the Sumeini area with the road from the Dubai Highway up to the entrance of the Wadi Maqam gorge in red.

Introduction

The Oman Mountains expose the Middle Permian to Cretaceous Sumeini group belonging to the south margin of the Tethys. The Sumeini Group, as defined by Glennie et al. (1974) is represented by a thick sequence (about 2500 m) of slope carbonate deposits and crops out (Searle et al., 1990; Le Métour et al., 1992) near the border between Oman and the United Arab Emirates (geol. map, Fig. 71). A comprehensive sedimentologic study of the Sumeini Group has been carried out by Watts (1987, 1990) and by Watts and Garrison (1986). Detailed mapping and stratigraphical studies were done by Le Métour et al, (1991), Béchennec et al., (1993), Pillevuit (1993), Baud et al., (2001), Richoz (2006) and Richoz et al, (2005).

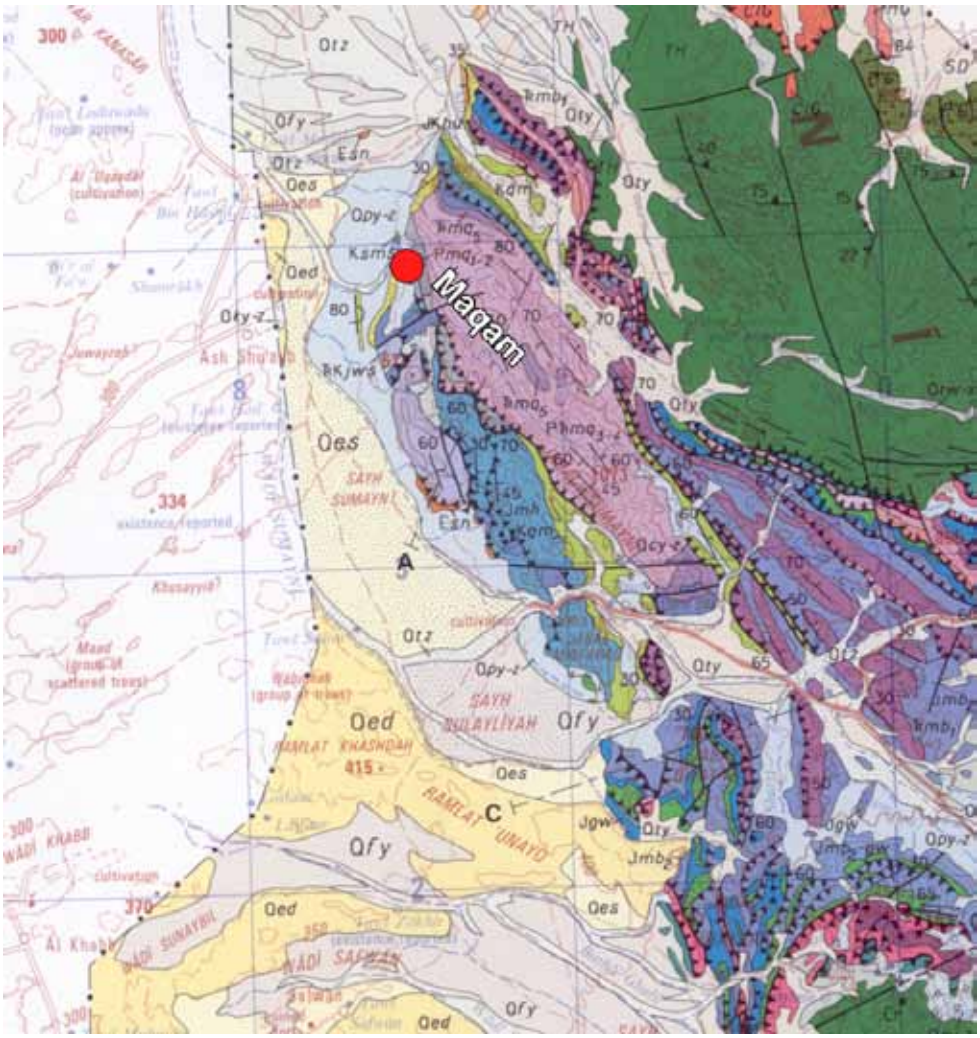

Figure 71: Geological map of the Sumeini area (Map Buraymi, Le Metour et al., 1992).

The Sumeini Group tectonically overlies autochthonous Eocene limestones and is overlain by sediments from the Hawasina nappes. This group is also described as para-autochthonous with a 5 to 30 km displacement in regards of the "autochthonous". The Sumeini Group includes 4 formations: Maqam Formation (Middle Permian to Lower Jurassic), Mayhah Formation (Middle and Upper Jurassic), Huwar Formation (Uppermost Jurassic to Cretaceous) and Qumayrah Formation (Upper Cretaceous).

The lower part of the Sumeini Group (about 1700 m thick) is included in the Maqam Formation (Middle Permian to Lower Jurassic), further subdivided into 6 members, A, B, C, D, E and F (Fig. 72 left), according to Watts and Garrison, 1986.

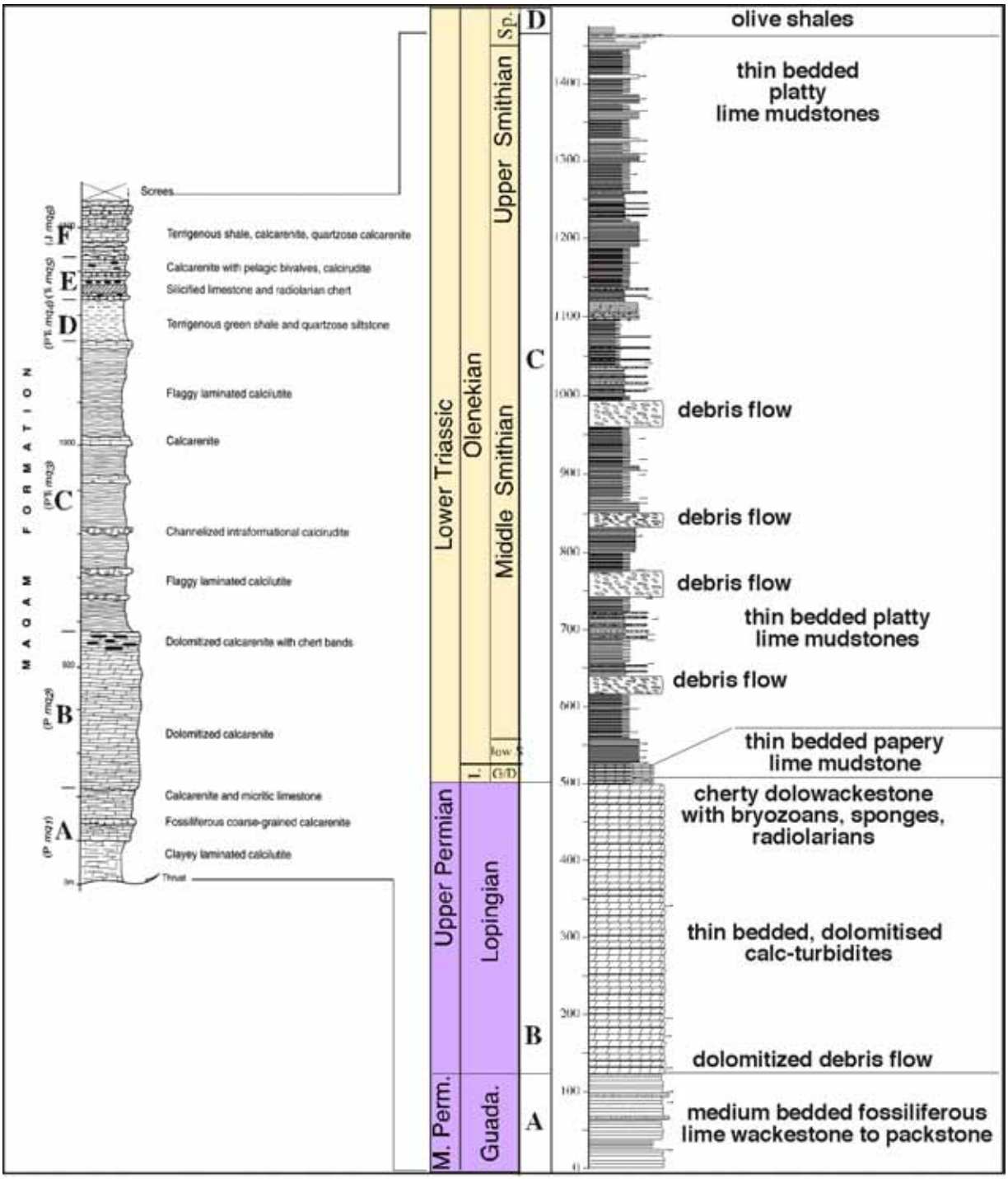

Figure 72: On the left: Stratigraphic section of the Maqam Formation from Le Métour et al., (1992a). Members A-F according to Watts and Garisson (1986). On the right: stratigraphic section of the Maqam Formation, member A, B, C after Richoz et al., 2005, modified.

General overview of the Maqam Formation (Fig. 72).

The following descriptions are based on previous guidebooks (Baud et al., 2001, Richoz et al., 2005) and new data in Richoz et al. (2010 and in prep.).

Member A of the Maqam Formation (Figs. 72 and 73), here about 80 m thick, (but laterally up to 250m) is tectonically truncated at the base and its substratum remains unknown. Its base is made of

an unknown thickness of multicoloured shales with accessory tectonized thin-bedded limestone or dolostones and the upper part consists of outer shelf fossiliferous limestones.
A Wordian age was proposed by Pillevuit (1993) for the lower part (A1-A2) on the basis of the ammonoids *Stacheoceras sp., Adrianites?*, *A. isoniorphus, Aghathiceras sp.* (Det. from W.W. Nassichuck), of the trilobites *Néoproetus indicus,* Tesch, n. subsp. Ditomopyginae (Becq-Giraudon and Pillevuit, 1995) and of the ostracods *Bairdia sp., Aurigerites sp., Healdianella sp., Acratia sp.* (Det. S. Crasquin Soleau).

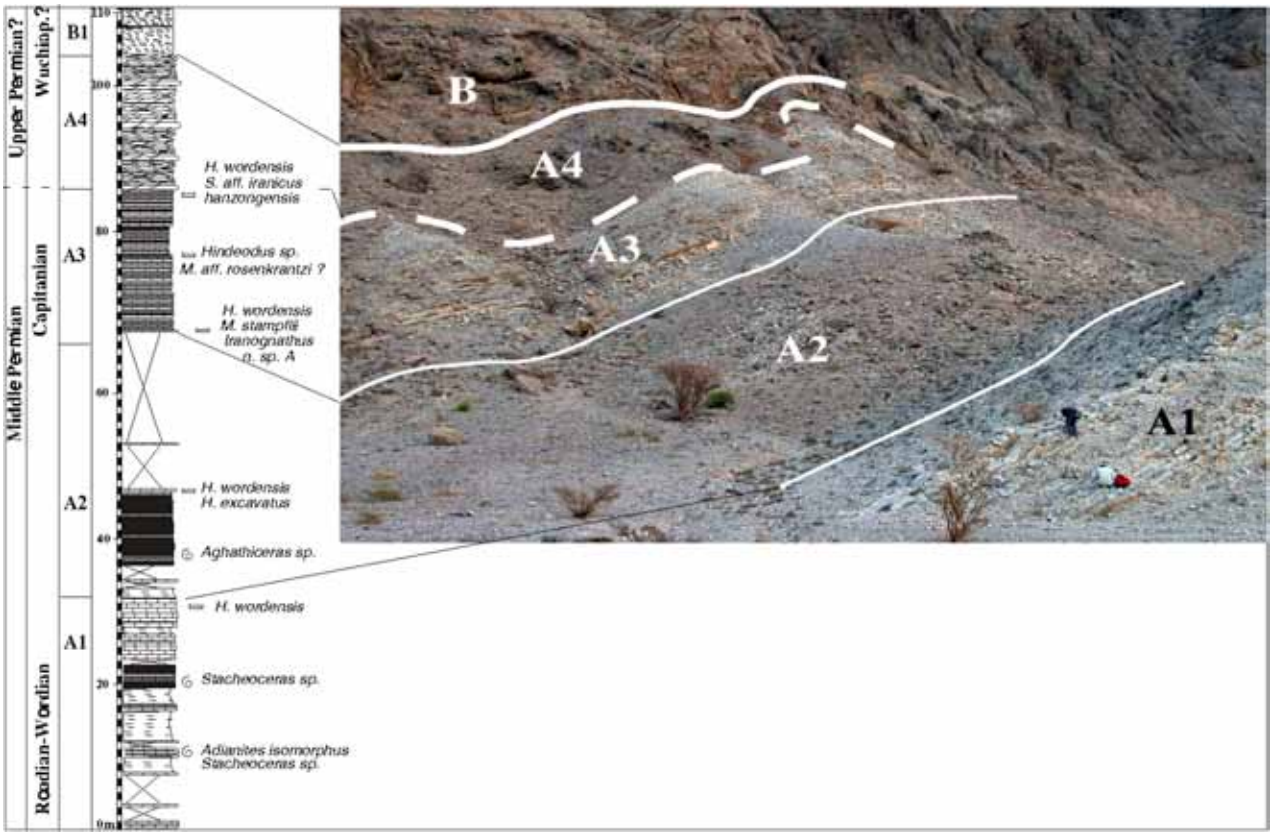

Figure 73: Stratigraphic section with the new conodont finding of C. Henderson and A. Nicora with, right, view on Member A of the Maqam Formation. A1 –shale and limestones unit; A2 – mainly hidden shale unit: A3 – upper limestone unit separated from A4 by an irregular front of dolomitization. B –base of the dolomitized B unit with a thick dolorudite, clast supported bed.

Recently C. Henderson and A. Nicora recovered *Hindeodus wordenis* at the top of Unit A1 and the conodonts (Plate 3) *Sweetognathus. aff. iranicus hanzhongensis*, *Hindeodus wordensis*, and *Mesogondolella* (or *Jinogondolella*) n.sp. A (with some affinity to *M. rosenkrantzi*) at the middle of unit A3 and *Iranognathus n. sp*. A, *Hindeodus wordenis, M. cf. stampflii* at the base of unit A3 (position on Fig. 73). Both the *Iranognathus* and *Sweetognathus* species indicate an Upper Capitanian age close to the Guadalupian-Lopingian boundary (Mei et al., 2002). It means that the overlying Member B of the Maqam Formation is uppermost Capitanian and Lopingian and not simply Capitanian as thought before (Watts and Garrison, 1986) on the basis of pieces of irregular coral genera *Wentzellites* and *Lonsdaleiastraea* reworked in the basal dolomitized mass flow.

Plate 3: 1, 2: Lateral and upper surface views of Clarkina cf. zhangi (near top of unit B; B6a base, OMO 83A). 0.20mm scale bar.
3: Upper surface view of Sweetognathus aff iranicus hanzhongensis (advanced form). Sample M4 at middle of Unit A3. 0.10mm scale bar.
4, 5: Lateral and upper surface view of Mesogondolella n.sp. A (or Jinogondolella n.sp. A). Sample M4 at middle of Unit A3. 0.20mm scale bar
6.:Hindeodus wordensis lateral view. Sample M4 at middle of Unit A3.
7, 8: Iranognathus n.sp. A. Sample M3 (base of Unit A3). (7 use .10mm scale bar; 8 use .20mm scale bar).
9: Hindeodus wordensis. Sample M3 (base of Unit A3). 0.20mm scale bar.
10, 11: Mesogondolella cf. stampflii. Sample M3 (base of Unit A3). 0.20mm scale bar.

The member B consists of a 415 m thick sequence of predominantly thin-bedded to massive dolostone with numerous dolorudite intervals and locally abundant breccia in the lower part and cherty in the upper part. This thick dolostone succession is formed in a deep-marine environment. Overlying the synrift units this succession record the break-up and the early development of the Oman continental margin, subsidence and possible tectonic flexure or faulting. At the same time the former rift shoulder (Djebel Akdhar) is flooded by the open marine transgression (Late Middle Permian).
The upper part of member B consists of 50m of dm-sized bed of cherty dolostone and cherts rich in sponge spicules. It must be emphasized that a silica rich interval is widesprad on NW Pangea margin and also known in the Lopingian carbonate of the Tethys. Biogenic silica factories collapsed near the end of the Permian Period throughout the world (Beauchamp & Baud, 2001). C. Henderson reports *C. cf. zhangi* near the top of unit B (base of B6a unit, Fig. 73b).
The top part of the B Member and the transition to C Member records the end Permian events that will be seen at stop 1 of the day.

The Member C comprises a thin (25m) Griesbachian-Dienerian part and a thick (up to 900m) Smithian part.

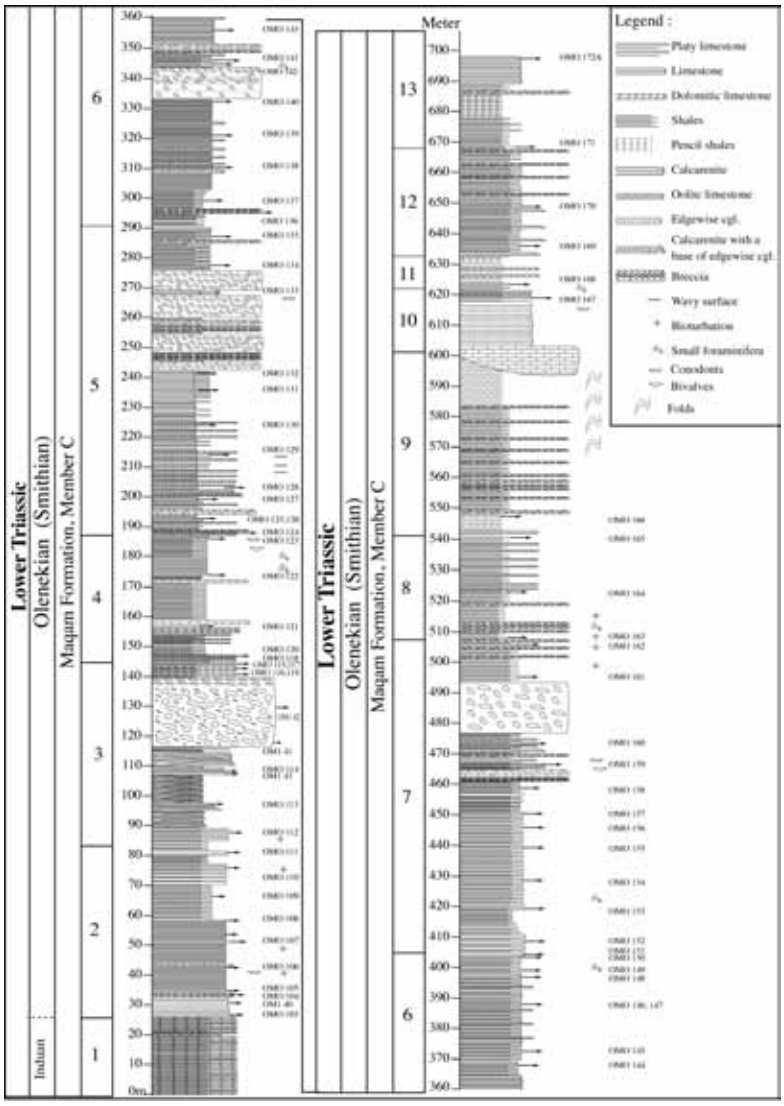

Figure 74: Lithology and stratigraphy of the lower 700 metres of Member C in Wadi Maqam (after Richoz et al., 2005, Richoz 2006).

The base consists of thin-bedded platy dolostone, corresponding to thin-bedded lime mudstone, NW of the dolomitization front. These platy dolostone display numerous large-sized slumps. The thin Lower Smithian (7m) is characterized by vermicular limestones. The incredibly thick Middle and Upper Smithian sediments mark the onset on the base of slope of a basin in which the carbonate submarine fan deposits developed This very thick unit consists essentially of platy limestones, calcarenites and calcirudites. It comprises mainly grey-beige calcilutite, laminated and flaggy, interbedded with sparse beds of fine-grained calcarenite in cm beds. Channelizing beds of intraformational calcirudite are also part in this succession, which constitutes the great part of the outcrops of the Sumeini Group. A detailed sedimentologic survey and depositional model of carbonate submarine fans have been presented and discussed by Watts (1987). Carbonate sedimentation of the C Member ended abruptly in the Early Spathian.

The overlying **Member D** is characterized by deposition of 10m brown shale with rare mm-thick sandstone and marls beds, follow by a 75m thick sequence of green terrigenous siltstone. There are no age diagnostic fossils (Spathian-Anisian?).

The Member E, around 90m thick, comprises mainly radiolarian chert, calcarenite and calcirudite. This succession is Ladinian to Carnian in age dated by radiolarians, bivalves, and foraminifers.
A metric channel bed of calcirudite with a calcarenitic matrix crops out at the base, containing elongated clasts 5-30cm in diametre of grey micritic limestone. Above, a 20 m thick succession consists essentially of grey-brown radiolarian chert in regular cm beds with interbeds of clayey shale and in places, fine-grained calcarenite with horizons of accumulations of pelagic bivalve shells of the genus *Daonella sp*. The top 2 m of this siliceous succession are made up of red radiolarian chert, which is overlain by a carbonate succession approximately 35 m thick with abundant brown patina cherts. Above, an irregular interval, 3-6 m thick, is made up of poorly defined metre-thick beds of matrix-supported calcirudite and coarse-grained calcarenite with sub-angular and tabular clasts of grey micritic limestone ranging from 5 to 40 cm in diametre. This interval is overlain by a 20 m-thick succession made up of light grey micritic limestone with horizons of accumulations of pelagic bivalve shells, and of fine-grained, dark grey calcarenite in beds 20-60 cm thick at the base and 1-15 cm thick elsewhere. In places, the intraformational calcirudite contains slump-structures. At the top of the member E is a channeling interval 1-8 m thick of calcirudite with a reduced or absent matrix, containing reworked sub-angular clasts of micritic limestone, calcarenite, and reef limestone

The Member F (Carnian-Norian) is made of calcirudites and calcarenites with, in addition to the reworked lithoclasts of limestone, in places chert and of brownish shales. It also contains a biota of Late Triassic age including debris of algae, crinoids, pelagic bivalve shells and benthic foraminifera: *Trochammina* sp., *Endothyra* sp. or *Endothyranella* sp., duostominids, lituolids (Béchennec et al., 1993b). The discovery in this upper carbonate succession of an *Aulacoceras sp.* and *Heterastidium sp.* allowed correlations with the Early and Late Norian (Baud et al., 2001).

General overview of the carbon isotope stratigraphy in Wadi Maqam (by S. Richoz).
The present $\delta^{13}C_{carb}$ isotopic curve (Fig. 75) is a compilation of data from Richoz et al. (2005) for top Member B and Member C and from Atudorei (1999) for values on Member A and B. No covariance in the $\delta^{18}O$-$\delta^{13}C_{carb}$ plot and good correlation with time equivalent sections allow us to consider this isotopic curve as primary. Isotopic values were measured in some beds from Member A, both side of the dolomitization front. δ13Ccarb values show identical values, whereas the δ18Ocarb values are strongly affected (Richoz unpublished data).

The highest $\delta^{13}C_{carb}$ values (+5.5‰) are recorded in members A and B and correspond to the high Middle - Late Permian values recorded in the Tethys (Baud et al., 1989, Richoz 2004).
Values are around +4.9‰ in Member B4, around +3,5‰ 10m below the top of the Member B and drop to around +2,5‰ in the last grey limestone beds of Members B (fig. M4, M8). The shaly interval record a drop of 3.3‰ followed by a positive shift of 1.0‰ in the first platy limestones beds of Members C. The minimum (-1.2‰) is reached here at the level of the first appearance of *H. parvus* (Fig.). The overall drop of around 6‰ in the $\delta^{13}C_{carb}$ values is one of the largest known within the PTBI in the Tethys. The isotopic values increase to +2,8‰ then in the first 20m of platy dolostone and fall to +1‰ after the first breccia to shift again in the vermicular limstones to reach a peak at 1.7‰ at the level of the Smithian *N. waageni* conodont zone. Values decrease to stay globally negative (between –0.9‰ and –2.5‰) during most of the Member C in Wadi Maqam and Wadi Shu'yab. 20m below the top of Member C, values are around –1.6‰ and shift down to -2.5‰ in the last metres of platy limestones.
Values shift rapidly to positive values (2,1‰) in the base of the marly orange limestone interval ending Member C. At the top of this orange interval and in the more calcareous beds at the base of Member D, values are again very negative (around –2.5‰). This short peak is believed to be equivalent to the one at the Smithian-Spathian boundary in some other sections (Atudorei, 1999; Payne et al., 2004; Richoz 2006, Horacek et al 2007, 2009).
$\delta^{18}O$ curves have values from -3.2‰ to -4.0‰ for Member A and B, shifting at the beginning of Member C down to -5.2‰ and then staying stable between -5.4‰ and -6.9‰. If this shift corresponds to the Permian-Triassic boundary, it corresponds also to the dolomitization front and is certainly affected.

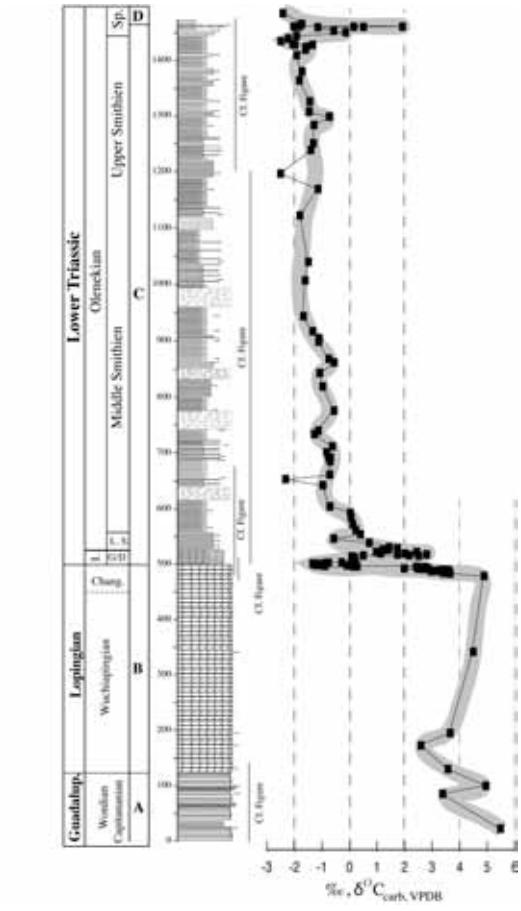

Figure 75: Carbon isotope profile of the Maqam Formation, member A, B, C. (Data from Atudorei, 1999, for the Members A and B and from Richoz, 2004, for the Member C).

Stop 1 (Fig. 76): stratigraphy of upper Member B and basal Member C of the Maqam Formation

From the parking place we will move on the hill inside a small gully (Fig. 77) up to stop 1 area looking at the cherty upper part of Member B.

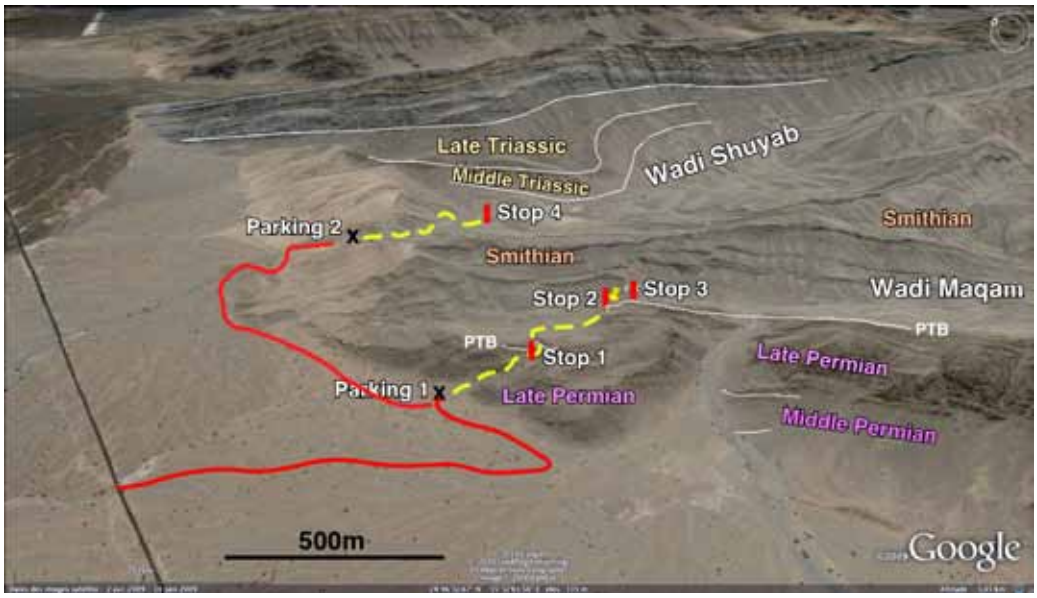

Figure 76: Google Earth oblique view of the Sumeini area with place of the 4 stops of the day. The red line is the itinerary with cars and the yellow line is the walk up to the stops.

Climbing the gully, we will see the onset of the cherty dolostone and its development of dm-sized bed of cherty dolostone and cherts rich in sponge spicules (Fig. 77).

Figure 77: stop 1 area with good exposure of the Wuchiapingian cherty dolostone (Upper Member B of the Maqam Formation) and the basal Triassic platy dolostone.

Due to the instability of the slope deposits at the end of the Permian, the Permian-Triassic transition record is very variable from one outcrop to the others. In this guidebook we will illustrate three

types of Permian-Triassic transition outcrops and two different types will be shown during the excursion (stops 1 and 2).
The model of deposition is that of a scalloped margin. A good record is given on the right slope of the gully (Fig. 78) with a large channel in the cherty dolostone and the onlap of the uppermost Permian and basal Triassic units

Figure 78: Scalloped margin with strong erosion of cherty dolostone (B4) and progressive onlap filling by transgressive latest Permian-earliest Triassic carbonates and shales (Unit B6 and C1a).

The upper part of the Unit B4 is mainly constituted of cherty dolomudstone rich in sponge spicules and with increasing yellow to violet shale intercalations section upwards. Some beds show concentrations of bryozoans or crinoids, slumping and intraformational breccias are also frequently observed.
The cherty dolostone B4 is topped by a silicified hard ground indicating a submarine break of unknown duration (section and view, Fig. 79). An outcrop view of a lateral Permian Triassic transition section (Benoit' section) is given in Fig. 80a.

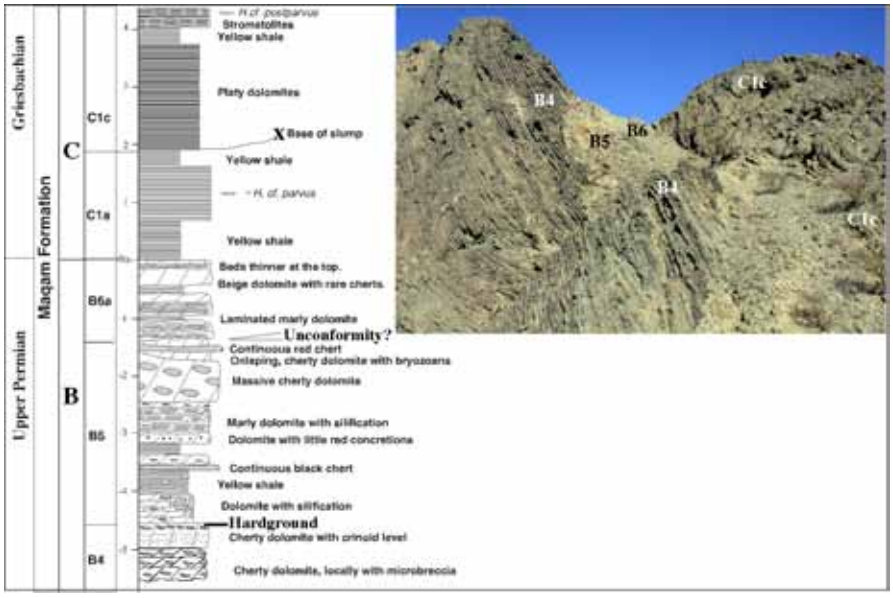

Figure 79: The Permian Triassic transition section about 500m SE of stop 1, with a dolomitic overprint and a similar lithology as seen at stop 1.

Chemostratigraphy (S. Grasby and B. Beauchamp)**.**
Geochemical data for Permian-Triassic transition in Wadi Maqam (Beauchamp's section) are shown in Figure 80b. These data show an initial onset and gradual decrease in δ13C values marked by a sudden significant drop of ~6‰ at the extinction boundary. Contrary to most sections that show an onset of carbonate deposition right after the extinction event, this location shows a significant drop in total carbon content suggesting disruption of carbonate sedimentation associated with the extinction event. Organic carbon content is very low, and unlike other areas where there tends to be a degree of correspondence, δ13C values of organic carbon do not show any strong relationship with carbonate-carbon.

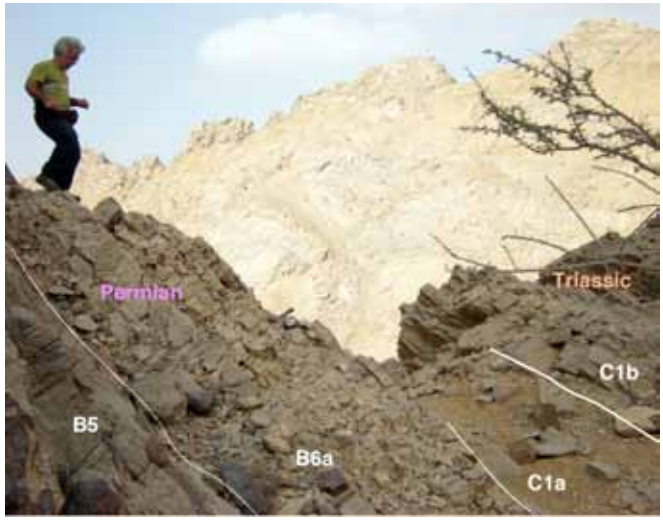

Figure 80a: Close view to the Permian Triassic transition in a new locality found by Benoit Beauchamp (scale). Coord: N 24°46'09'' E 55°52'14''

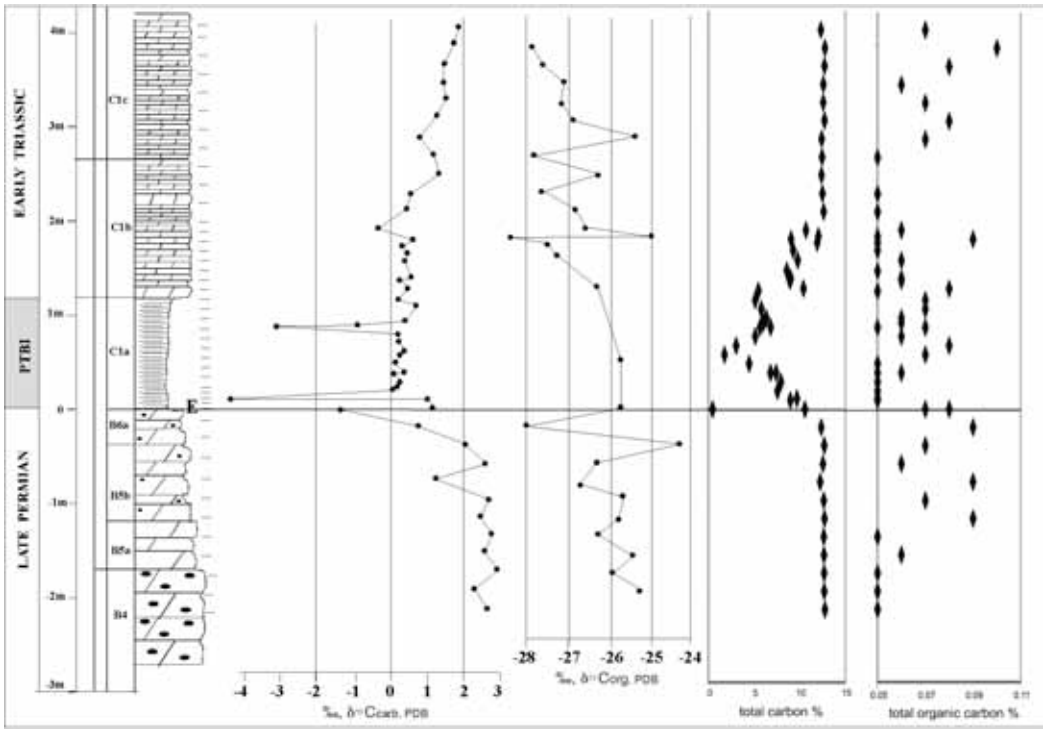

Figure 80b: Chemostratigraphy of the Permian-Triassic transition at the new locality (Fig. 80a) found by Benoit Beauchamp (after S. Grasby and B. Beauchamp).

Stop 2: The Permian Triassic transition above the dolomitization front.

From the upper part of the gully (stop 1) we will move up to the open space of a small valley and walk to the stop 2 about 200m on the right. Here the Permian Triassic transition beds are just above the front of dolomitization and escaped to the late dolomitic diagenesis. A fault separates the uppermost Permian carbonates (Fig. 81) from the overlying boundary clay and thin bedded marly limestones. The Fig. 82 is a composite section from both sides of the fault.

Figure 81: the most complete uppermost Permian succession at stop 2. The Unit B6 with grey limestones escaped to late diagenetic dolomitization. On the right, we can see the hardground at the top of B4 unit. A. Baud for scale!

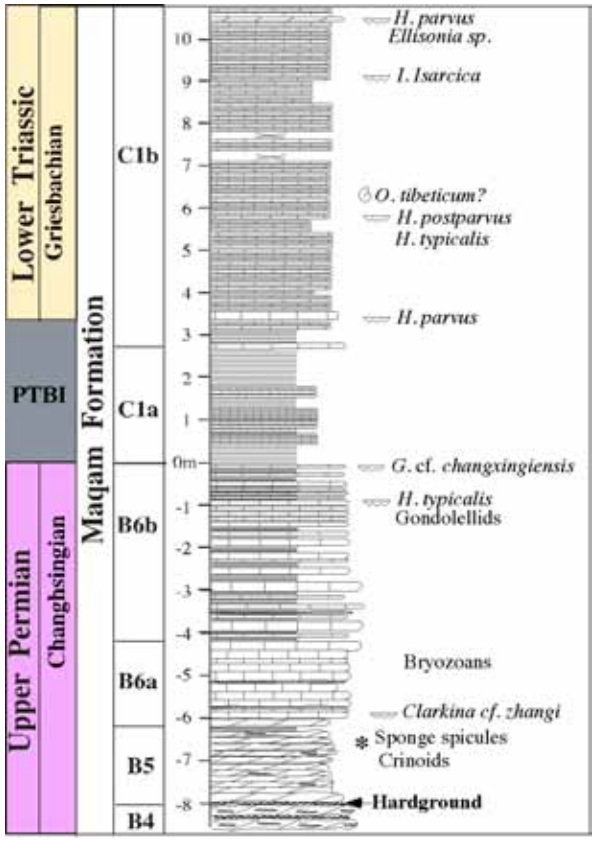

Figure 82: Stratigraphy of the Permian Triassic transition section at stop 2 with the conodonts finding of L. Krystyn and C. Henderson. Description of the lithology in the text (after Richoz et al., 2005, modified).

The upper part of Member B (Fig. 82), above the thick hard ground at the top of the cherty dolostone (B 4), has two units B5 and B6. The Unit B5, between 1 and 3m thick consits of brown weathered dolomitic limestones with rare rounded cherts.

The Unit B6, 6-7m thick is made of 5-15cm thick grey limestone beds having some red shaly intercalation. Conodonts *H. typicalis*, Gondolellids and *Clarkina cf. zhangi* (det. L. Krystyn and C. Henderson, Plate 3/1-2, p. 83) at the base gave an Upper Changhsingian age to this Unit (Fig. 82).

Ichnotaxa at stop 2 (R. Twitchett in Richoz et al., 2005).
The topmost part of Member B (B6a and b in Figs. 81 and 82) with well bioturbated beds is indicating a well-oxygenated palaeowater column and a diverse infauna (Fig. 83/1 to 4)). The ichnotaxa include *Chondrites*, *Palaeophycus*, *Thalassinoides, Rhizocorallium* and possibly *Zoophycos*. The *Thalassinoides* burrows (Fig. 83/2) are often cast by the diagenetic chert, in a similar fashion to that which occurs in the Cretaceous chalks of Western Europe.

Crosscutting relationships may be observed in places, indicating that *Thalassinoides* burrows were emplaced at a shallow depth within the sediment, with *Chondrites* and ?*Zoophycos* occupying deeper tiers. This tiering relationship is also reminiscent of the Upper Cretaceous chalks of western Europe (e.g. Bromley and Ekdale, 1986). *Thalassinoides* burrows are typically 10-16 mm in diametre (mean = 14.3). The bedding planes of the well-bioturbated, uppermost beds of Member B (B6b in Figs. 81 and 82), contain a diverse and large-sized ichnofauna. Prominent are the dramatic and beautiful *Rhizocorallium* burrows (Fig. 83/4), which range from 11 to 28 mm in diametre (mean = 20.0 mm). Rarer, large, *Thalassinoides* (Fig. 83/2) are also present (mean diametre = 17.2 mm; range = 12-21 mm).

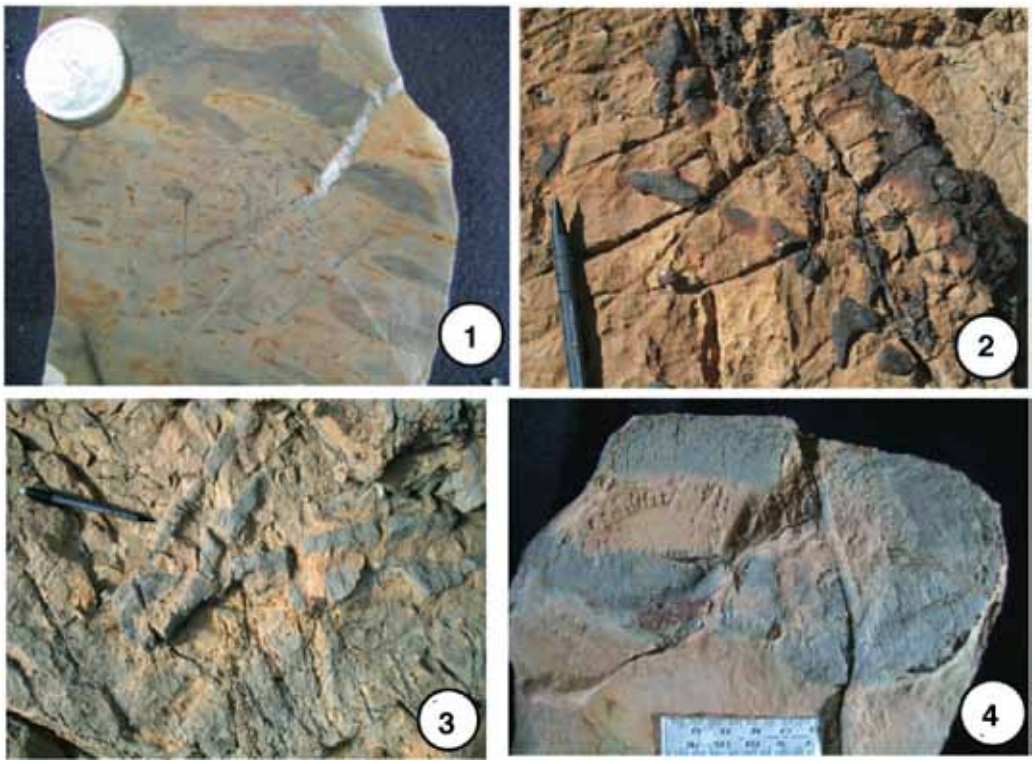

Figure 83: Selected trace fossils and ichnofabrics of the Unit B6b, Maqam Formation from R. Twitchett (in Richoz et al., 2005). 1- Well bioturbated (ii5) ichnofabric, less than 1 m below P/Tr boundary. Coin =20mm diametre; 2- Thalassinoides; 3- Rhizocorallium; F: large Rhizocorallium.

The Member C starts with 3m of red shales and siltites, one 10cm-thick calcarenite bed and 20cm of yellow shale (Fig. 84). This succession is overlain by platy lime and then dolo- mudstone more or less marly comprising several slump levels. The first lime mudstone bed gave the conodont *H. parvus*, *H. postparvus* is present in stromatolites levels, 9m above the red shales is *I. isarcica*, index of the second Griesbachian conodont zone and 16m above the Griesbachian conodont *H. parvus* (Fig. 84).
In sharp contrast to the well-bioturbated Member B, the overlying basal metres of Member C (C1b in Fig. 84) are well laminated (A, fig. 85) with no evidence of bioturbation. This dramatic loss of the burrowing infauna indicates the appearance of oxygen-poor waters. A similar loss of bioturbation is recorded in many sections worldwide (Twitchett and Wignall, 1996; Twitchett et al., 2001; Wignall and Twitchett, 2002).

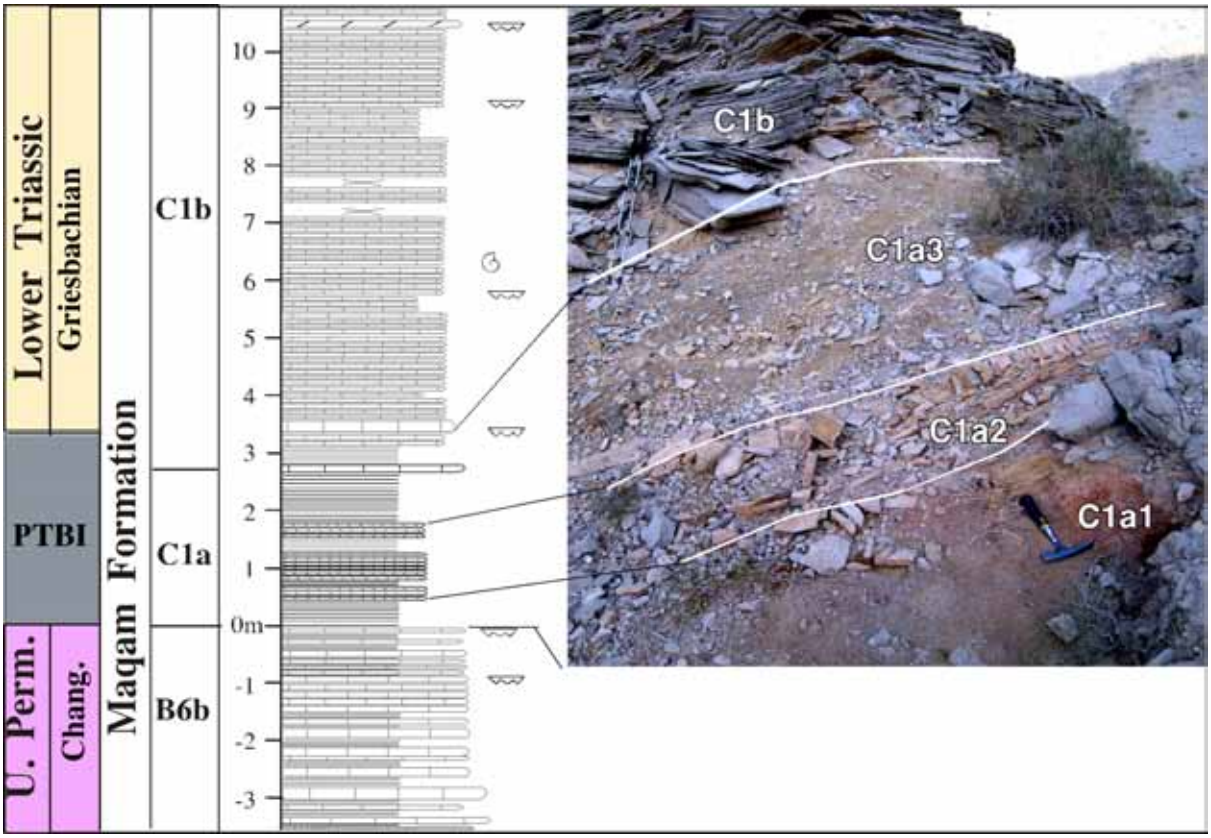

Figure 84: Close view to the boundary clay at stop 2. At the top are the platy to papery limestones (Unit C1b).

There is a dramatic decrease in the size of marine animals, and their associated trace fossils, through the Permian-Triassic extinction interval (e.g. Twitchett, 1999; Twitchett and Barras, 2004). This "Lilliput effect" (Twitchett, 2005) is observed at many, if not all, extinction crises and is probably caused by environmental stress such as the loss of primary productivity and decreased oxygenation. Globally, *Rhizocorallium* and *Thalassinoides* do not return to its pre-extinction sizes (diametres in excess of 20mm) in any depositional setting until the Anisian (RJT, unpublished data). Similar size changes in these ichnotaxa are also recorded through the Triassic-Jurassic extinction-recovery interval (Twitchett and Barras, 2004).

Figure 85: The overlying basal metres of Member C (C1b) showing a typical papery to platy lime mudstones devoid of bioturbation (right, closer view).

It is interesting to note that laterally stromatolite levels are recognizable as shown by the Fig. 86.

Figure 86: Microbial laminations and plastic deformations from the basal part of Member C (C1b) in Wadi Maqam.

Detail of the Carbon isotope stratigraphy at stop 2 (by S. Richoz).
The typical negative shift at the Permian-Triassic boundary, display here several step (Fig. 75 and 87). A first shift of 1.3‰ occurs in Member B4, Member B having values around 4,8‰, Top of B4 and B5 having values around 3,5‰. A second one of 1,1‰ amplitude is in the last 3m of the grey Changhsingian limestone.

The last one (2,1‰ in amplitude) occurs between the last limestone bed of Member B and the first platy limestone of Member C above the shale interval. Its sharp design could represent a gap, difficult to estimate whithout isotopic data from the first shale interval. A small peak of 1‰ amplitude occurs just below the FAD of *H*. parvus. The increase of the isotopic values starts in the *O. tibeticum* ammonoid zone and *I. isarcica* zone as in other well dated sections in Oman (Wasit block, Krystyn et al., 2003; Richoz 2006), Iran and Turkey (Richoz 2006, Richoz et al. 2010), Salt Range in Pakistan (Baud et al., 1996; Atudorei, 1999) and south China (Tong et al., 2002; Krull et al., 2004; Payne et al., 2004).

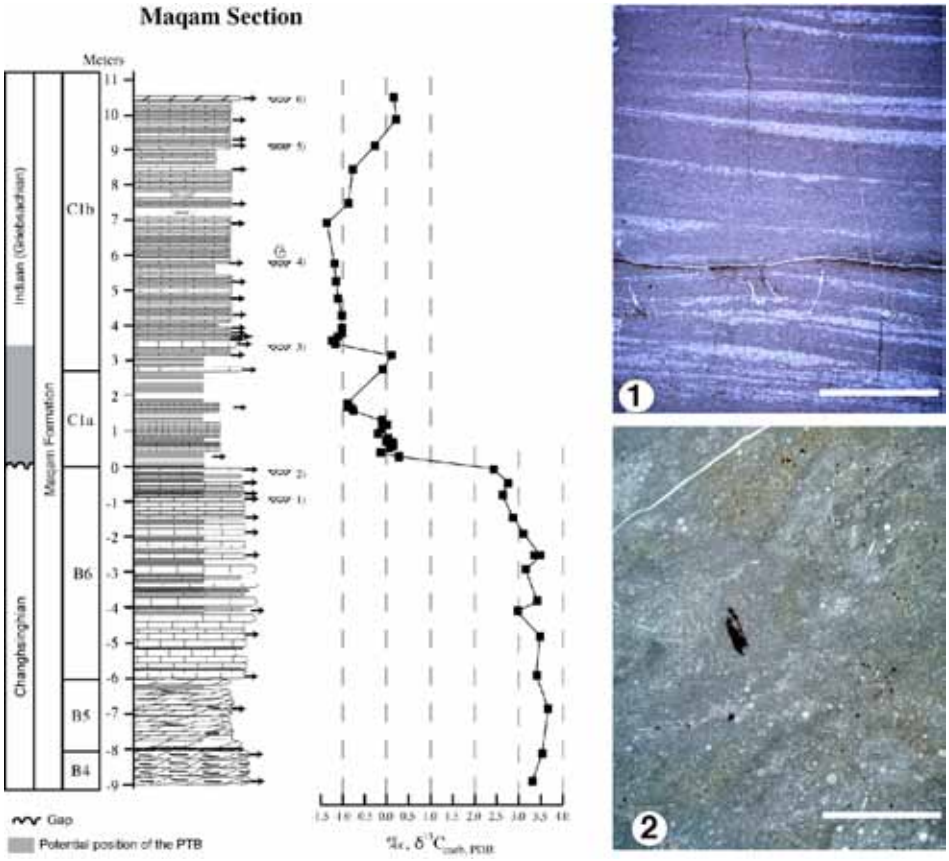

Figure 87: statigraphic sketch of the Permian-Triassic transition with Carbon isotope profile (S. Richoz) at stop 1. Microfacies -1: laminated calcisiltite of the basal Triassic C1b unit. 2: bioturbated lime mudstone with calcitized radiolarian, Changhsingian B6a unit. Scale bar A and B: 5mm.

Stop 3: the Induan platy limestone succession.

Crossing the bedding we will observe the next 35m of the platy limestones development, laterally platy dolostone. Several slump levels are visible (Fig. 88/1) but probably the 35m are one big slump. These levels have given a mix of Griesbachian and upper Dienerian conodonts: *N. dieneri, N. cristigalli, Ng. planata, H. parvus* and *I. isarcica* (det. L. Krystyn). The isotopic curve is as well not well recognizable, showing probably a mixed signal.

Figure 88: 1-slump beds in unit C1 (Griesbachian); 2-monogenic flat pebble conglomerate bed in platy limestones (unit C3, Lower Smithian)

10m above occurs the first 2m thick clast supported calcirudite with reworked Late Permian with *Colaniella sp.* and basal Triassic shallow water pebbles. This succession is overlain by 2m of platy lime mudstone, 4 to 6m of vermicular limestone and 4m of alternance of clast-supported (edge-wise) conglomerate beds (Fig. 89) and vermicular limestone. One of the conglomerate beds contain the conodonts *N. dieneri, N. cristagalli* and *N. waageni* (det. L. K.) index of the first conodont zone of the Smithian (Fig. 89).

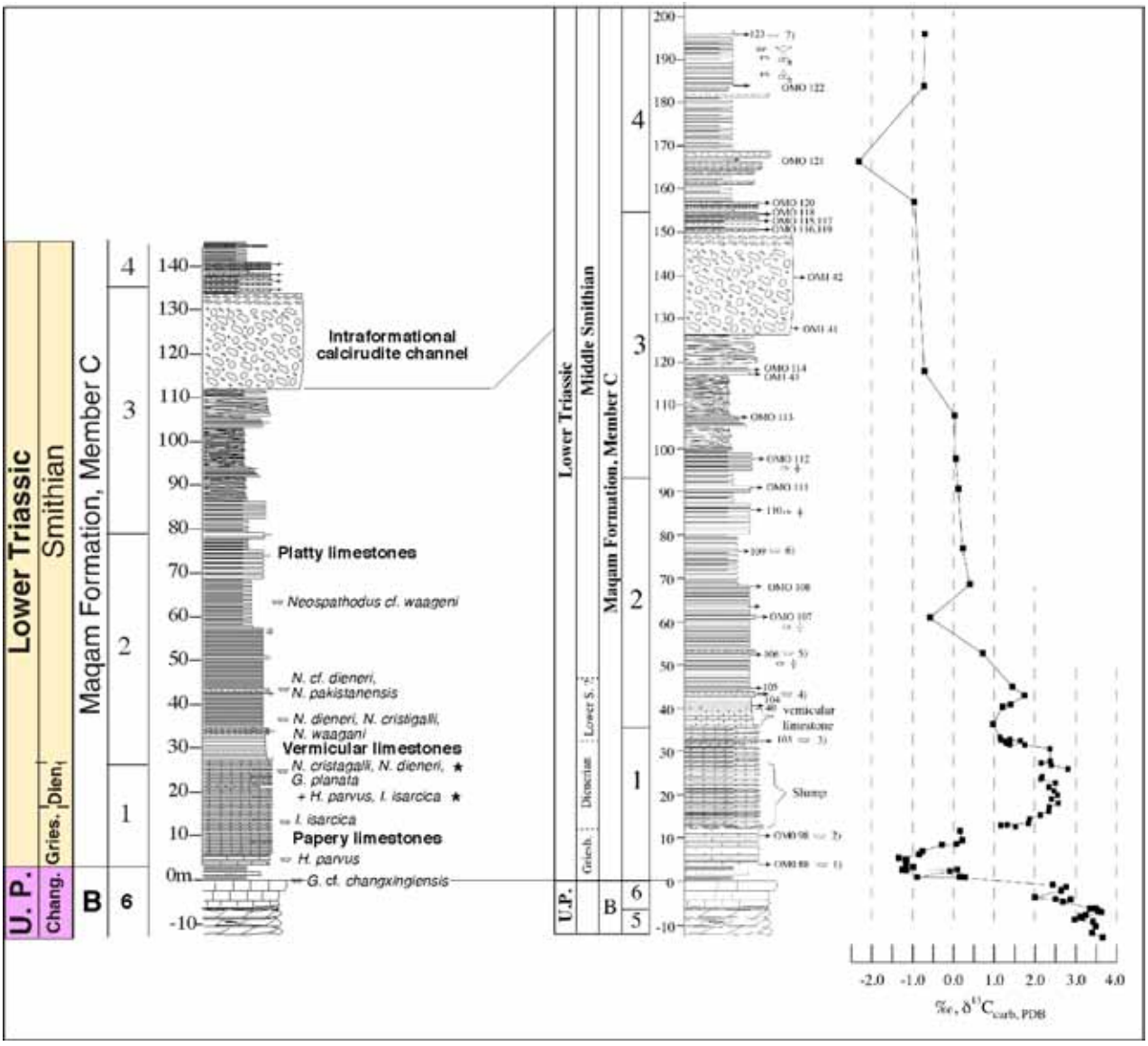

Figure 89, left: stratigraphy of the lower part of Member C, (conodonts, L. Krystyn); right, Carbon and Oxygen isotope curves with corrected lithological column (additional slump, S. Richoz).

Detail of the Carbon isotope stratigraphy at stop 3 (by S. Richoz).
The isotopic curve in the lower part of the Member C shows some variations (Fig. 89), but the main part of the Member has homogenous negative values (Fig. 75). After the large negative shift at the Permian-Triassic boundary, values increase of 4‰ until +2.8‰ from *I. isarcica* conodont zone up to 5m below the edge-wise conglomerate containing *N. cristagalli*, index conodont of the upper Dienerian. In this conglomerate and vermicular limestones above, values decrease 1.8‰. A second positive shift with 0.7‰ amplitude occurs in near the edge-wise conglomerate containing *N. waageni*, index conodont of the basal Smithian zone. The less positive values in between these two

peak at 1.7‰ occur in the vermicular limestone, topmost Dienerian and first conodont zone of Smithian age.
A double peak around the Induan Olenekian Boundary is also known in other Oman section (Richoz, 2006), in Iran (Horacek et al., 2007a), Northern Italy (Horacek et al., 2007b), Spiti (Atudorei, 1999, Richoz et al., 2007), south China (Tong et al., 2002; Payne et al., 2004, Galfetti et al., 2007, Zuo et al., 2006) and Japan (Horacek et al., (2008). δ13Ccarb values decrease rapidly, still in the N. waageni zone, to around 0‰ and then progressively to-2‰. Most of the Member C, until the last 20m, has negative values between –0.5‰ and –2.5‰. This shape with homogenous very negative values is also known in Turkey (Richoz 2004), Salt Range and Spiti (Baud et al., 1996; Atudorei, 1999), Northern Italy (Horacek et al., 2007b), south China (Tong et al., 2002; Payne et al., 2004) and Japan (Horacek et al. 2008).

Ichnotaxa at stop 3 (R. Twitchett in Richoz et al., 2005).
Although the lower part of Member C is almost entirely laminated, occasional horizons of bioturbation are present. The bioturbation is only weakly developed, and primary lamination may be only slightly disturbed (ii2) or more disturbed, resulting in slightly wavy bedding (ii3). Ichnodiversity is low and burrow diametres are much reduced compared to the underlying Member B. Common burrows are subhorizontal and unbranched *Planolites* and *Palaeophycus*, with burrow diametres typically between 2 and 6 mm (mean = 4.3). Rarer mm-sized *Arenicolites* and ?*Megagrapton* are also present (Fig. 90).
These bioturbated intervals presumably indicate that, occasionally, oxygen levels increased sufficiently to allow a limited benthos to colonize the substrate. Similar ichnofacies are recorded in the Induan worldwide (Twitchett and Wignall, 1996; Twitchett and Barras, 2004). It is interesting to note that *Chondrites*, thought by many to indicate dysaerobic environments in the Mesozoic (e.g. Bromley and Ekdale, 1984), is not recorded here, nor at any other Induan section

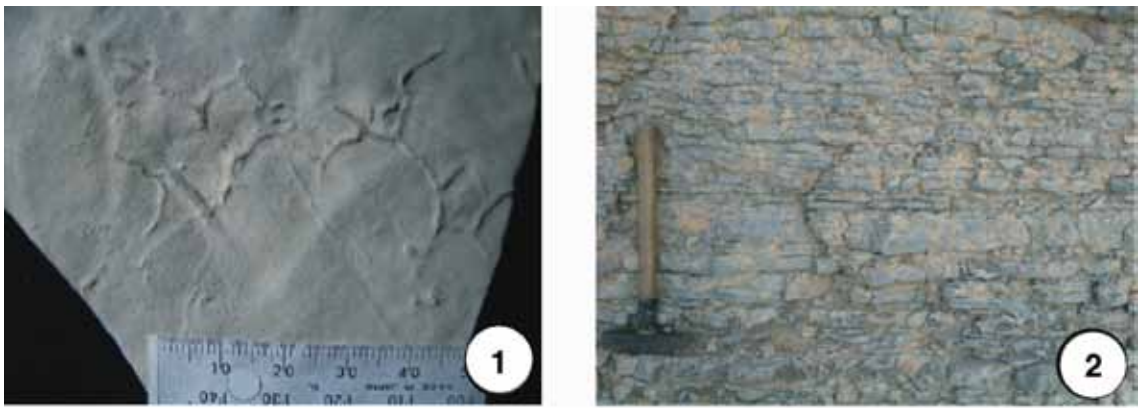

Figure 90: Selected trace fossils of the lower part of Member C (R. Twitchett in Richoz et al., 2005); 1- cf. Protopaleodictyon, 2- Rare bioturbated interval (ii3), below the vermicular limestones.

Higher up in Member C, the calcirudites, commonly clast-supported (edge-wise conglomerates), are characterized by tabular clasts representing the sub- in situ reworking of the laminated, platy calcilutite. In places, the calcarenite becomes predominant and interbedded with calcirudite in metric beds. Some levels of the calcarenite contains reworked tangential oolitic limestone clasts and a sparse biota of silicisponge spicules, mollusk debris and benthic foraminifera *Trochammina* sp. We note also the presence of typical Lower Triassic *Cyclogyra* and *Earlandia* type foraminifera found about 160m above the base (unit C4)

Figure 91 left: platy limestone with megabreccia (calcirudite bed) at the top (unit C5, Middle Smithian); right: monogenic flat pebble conglomerate bed (unit C5, Middle Smithian).

Stop 4: upper part of Member C in Wadi Shu'yab

From stop 3 we will move back to the car and drive to the entrance of Wadi Shu'yab (parking 2, Fig. 76) and walk inside the wadi to cross the upper part of the Member C (Smithian) and look at the spectacular development of the ichnofauna.

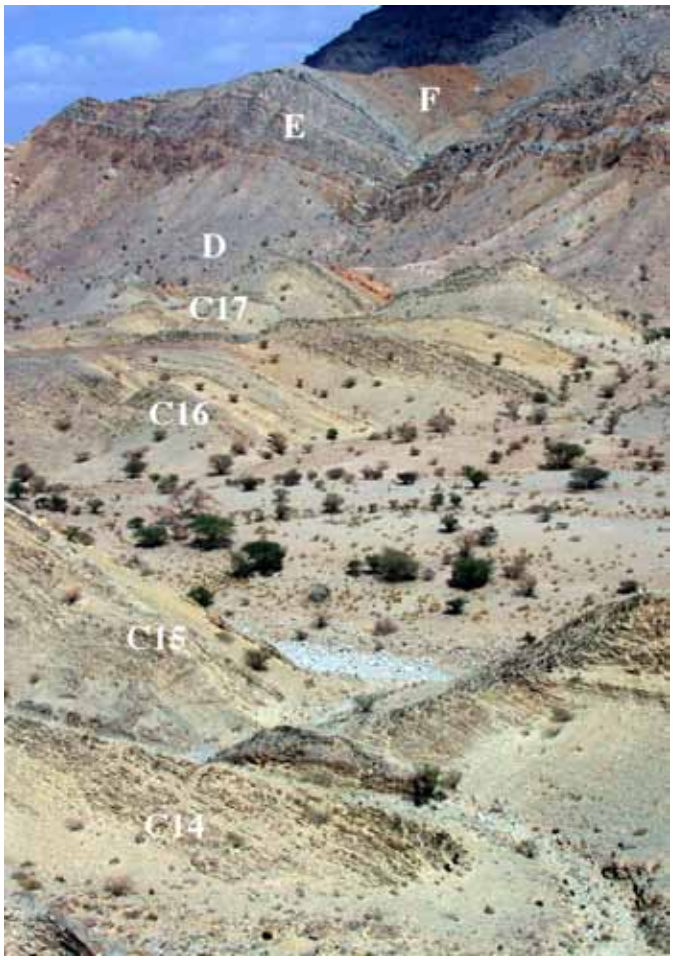

Figure 92: View of the upper part of Member C in Wadi Shu'yab, area of stop 4; Members D, E and F (Middle-upper Triassic) are in the ground.

This part is still a thick succession of platy calcilutite more or less marly, with locally abundant edge-wise conglomerate, oolitic calcarenite become rare and calcirudite absent. Unidentified Smithian ammonoids imprints are frequent (Guex, oral communication). A Smithian conodont is

present 10m below the last platy limestone. Traces (*cf. Paleodictyon)* and ripples are frequent in this upper C Member (Fig. 93).

Figure 93 left: Ripples and traces cf. Paleodictyon at the top of a calciturbidite megabreccia (upper part of Member C in Wadi Shu'yab); right: Cross-ripples from the same outcrop.

Above the last platy calcilutite, there are 10m of olive shale and with minor tectonic discordance 5m of yellow-orange marly limestone, well visible in the landscape (above C17 in Fig. 92). This orange sequence, that can be laterally tectonically truncated, is made of 2m of platy laminated marly limestone, a 1m thick channelized turbiditic breccia with numerous crinoids and conodonts *Icriospathodus collinsoni*, *Neogondollela elongata*, *Neospathodus* n.sp. (det. L. Krystyn), index of the second zone of the Spathian. This turbdite is overlain by 50cm of marly orange limestone and 1.5m of grey-orange limestone.

The upper (Olenekian) part of Member C (Fig. 92) records a gradual change in palaeo-oxygen levels as the "Superanoxic Event" begins to wane and the substrate becomes oxygenated for longer periods than it was during the Induan. However, the levels of bioturbation recorded in Upper Permian Member B (i.e. ii4) are never recorded in Member C, indicating suboptimal environments for at least the duration of the Early Triassic. Alternating packages of unbioturbated (ii1) and bioturbated (ii2-3) strata are typically 5-20m thick. Thus, at times the substrate was anoxic, whereas at other times it was dysoxic with slightly elevated, fluctuating, oxygen levels.

Ichnotaxa at stop 4 , Fig. 94 (R. Twitchett in Richoz et al., 2005).
Ichnodiversity is low. Typically, only one or two ichnotaxa (predominantly subhorizontal burrows produced by a depauperate community of deposit feeders) are present in any given bed. Occasionally, vertical *Arenicolites* are observed, indicating the presence of suspension feeders. From ca. 140m (Figure x), the bioturbated intervals begin to show an increase in ichnodiversity. *Arenicolites* and *Chondrites* are recorded at this level. However, the straight-branched form of *Chondrites* present in the upper Member C is clearly showing an unusual habit, compared to more 'typical' forms that branch downwards through the sediment. Here, *Chondrites* is largely subhorizontal (Fig. 94/2) in habit, possibly because the deeper levels of the substrate were completely anoxic or lacked sufficient food resources.
From ca. 155 to 180m, the platy limestones are reasonably well bioturbated (ii3) and contain an ichnofauna comprising *Chondrites*, *Palaeophycus* and *Phycodes*. The *Phycodes* burrows are particularly well preserved (Fig. 94/3) and locally common and characterise the remaining metres of Member C. The relative abundance of these ichnotaxa is variable. Rare crosscutting relationships indicate that the tracemakers all occupied the same, shallow, tier within the sediment. From ca. 190

to 215 m the platy limestones are less well bioturbated (ii1-2), but where the bioturbation does occur, *Chondrites* and *Phycodes* typically dominate, with occasional *Planolites* (Fig. 94/1).

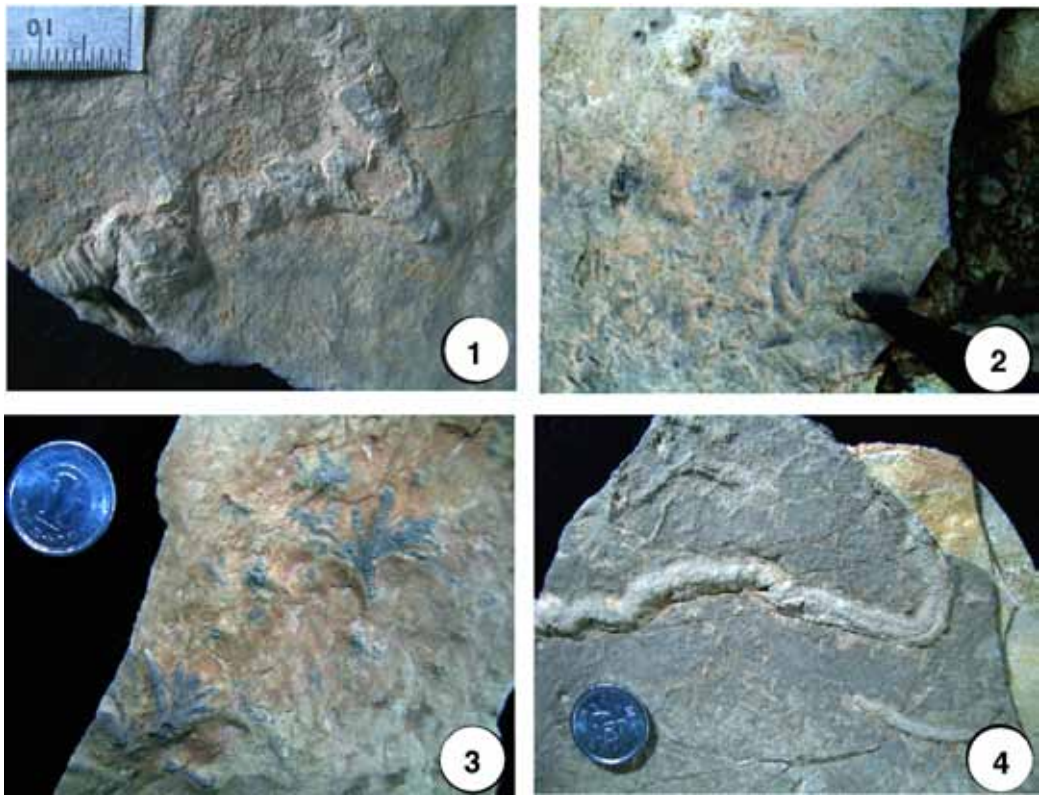

Figure 94: Selected trace fossils of the upper part of Member C (R. Twitchett in Richoz et al., 2005); 1- ?Planolites with annular backfill; 2- subhorizontal Chondrites; 3-Phycodes; 4- cf. "Scolicia". Scale coin 0 20mm diametre.

The uppermost parts of Member C (from 225 to 235 m) are fairly well bioturbated (ii3) and contain the most diverse trace fossil assemblage of the Lower Triassic part of the Maqam Formation. Here, *Arenicolites*, *Chondrites*, *Palaeophycus*, *Planolites* and *Phycodes* are all recorded. Rare, subhorizontal trails ("*Scolicia*", Fig. 94/4) are also present in loose slabs at this approximate level. However, the ichnofauna is still clearly different to that of the Upper Permian. *Rhizocorallium* and *Thalassinoides* are not present, the sediments are less well bioturbated and burrow diametres are typically less than 10mm (usually 2-3 mm). Environmental conditions near the end of the Early Triassic were clearly very different to those of the latest Permian.

Details of the Carbon isotope stratigraphy at stop 4 (by S. Richoz, Fig. 95).
Around 20m below the top of Member C, carbon isotope values are around –1.6‰ and decrease to -2.5‰ in the last metres of platy limestones. Values shift rapidly to less negative values values (-0,1‰) in the base of the marly orange limestone interval ending Member C, before decreasing again at -1,5‰ just below the breccias niveau and to reach a short lived strongly positive peak (2,1‰) just above it. At the top of this orange interval and in the some marly beds at the base of Member D, values are again quite negative (around -2.0‰ and –2.5‰). This positive peak occurs some centimetres below the conodont *I. collinsoni*, index of the second zone of the Spathian (Fig. 95).
This short strong peak is believed to be equivalent to the one around the Smithian-Spathian boundary in some other sections in Oman and Turkey (Richoz 2006), Salt Range and Spiti (Baud et

al., 1996; Atudorei, 1999), Southern Alps (Italy), Iran (Horacek et al., 2007a,b) and south China (Tong et al., 2002 and Payne et al., 2004).

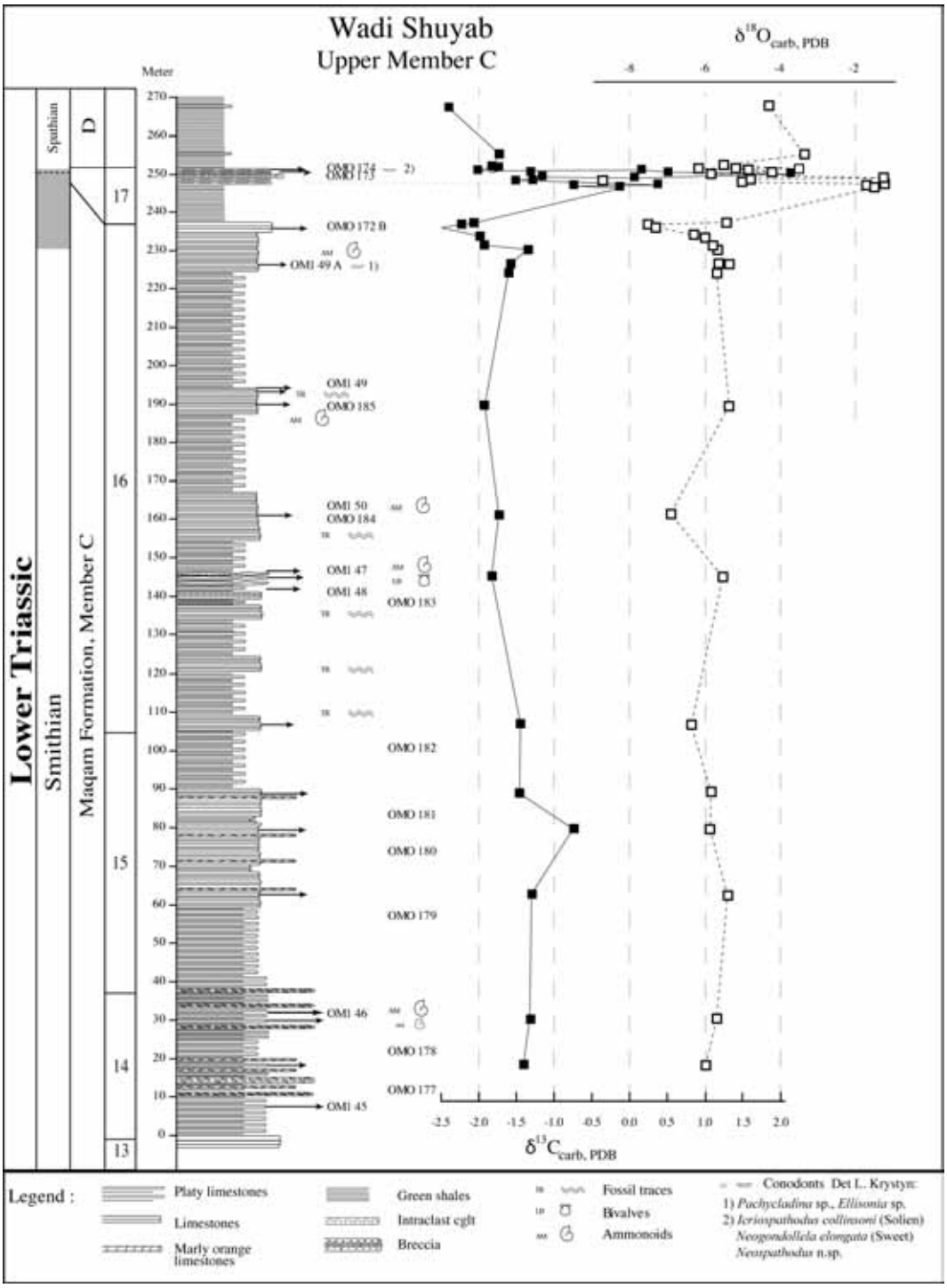

Figure 95: Lithology and stratigraphy of the upper part of Member C in Wadi Shu'yab with the Carbon and Oxygen isotope curve. The 0 metre is corresponding to the 700 metre of Fig. 74.

If we have time, we will have a look up to the Ladinian radiolarites and then go back to the cars and drive back to the Holiday Arabian Resort Hotel. Some participants will go directly to Muscat and other participants will stay there.

Acknowledgements

The Workshop Organizing Committee thanks the University Council, especially the Deputy Rector for Academic Affairs Dr. Barbara Stauble and the Public Relation Department Dr. Judith Rauhut and Manuela Gutberlet for their kind support.

The generous financial support of the Omani Reasearch Council and IGCP-UNESCO is kindly acknowledged.

We are particularly grateful to Dr. Hilal bin Mohammed Al-Azri, former Director General of Minerals, for his kindness, his interest and encouragement to our past fieldwork and research in Oman. Some of us (A.B., B.B, L.K., S.G., C.H., J.M., and S.R.) are very grateful to Dr. Jean-Paul Breton and Françoise his wife, for their generous hospitality and their valuable help to resolve many logistic problems, to prepare the fieldwork and to organize sample shipment.

A. Baud and S. Richoz appreciate the hospitality of the Geological Museum in Lausanne, of the Institute of Mineralogy and Petrography and the Institute of Geology and Paleontology, University of Lausanne for their Laboratory works. C. Henderson acknowledges support from a NSERC Discovery Research Grant.

References

Al-Husseini, M., 2006, Permian Arabian Tectono-Stratigraphy Chart: GeoArabia v. 11, p. 95-102.

Angiolini, L., Balini, M., Garzanti, E., Nicora, A., and Tintori, A., 2003a, Gondwanan deglaciation and opening of Neotethys: the Al Khlata and Saiwan Formations of Interior Oman: Palaeogeography, Palaeoclimatology, Palaeoecology, v. 196, p. 99-123.

Angiolini, L., Balini, M., Garzanti, E., Nicora, A., Tintori, A., Crasquin, S., and Muttoni, G., 2003b, Permian climatic and paleogeographic changes in Northern Gondwana: the Khuff Formation of Interior Oman: Palaeogeography, Palaeoclimatology, Palaeoecology, v. 191, p. 269-300.

Angiolini, L., Crasquin, S.S., Platel, J.P., Roger, J., Vachard, D., Vaslet, D., and Al, H.M.I., 2004a, Saiwan, Gharif and Khuff Formations, Haushi-Huqf Uplift, Oman: GeoArabia (Manama), v. 9, p. 163.

Angiolini, L., Nicora, A., Bucher, H., Vachard, D., Pillevuit, A., Platel, J.P., Roger, J., Baud, A., Broutin, J., Hashmi, H.A., and Marcoux, J., 1998, Evidence of a Guadalupian age for the Khuff Formation of southeastern Oman: preliminary report: Rivista italiana di Paleontologia e Stratigrafia, v. 104, p. 329-340.

Angiolini, L., S., Platel, J.-P., Roger, J., Vachard, D., Vaslet, D., and Al Husseini, M., 2004b, Saiwan, Gharif and Khuff formations, Haushi-Huqf Uplift, Oman: Geoarabia, v. Special Publication, p. 149-183.

Atudorei, N.-V., 1999, Constraints on the upper Permian to upper Triassic marine carbon isotope curve. Case studies from the Tethys [PhD thesis]: Lausanne, Geological Museum, Switzerland.

Baud, A., Atudorei, V. N., and Marcoux, J., 1999, The Permian-Triassic boundary interval (PTBI) in Oman : Carbon isotope and facies changes, in Yin, H., and Ton, J., editors, International Conference on Pangea and the Paleozoic-Mesozoic Transition: Wuhan (China), China University of Geosciences Press, p. 88-89.

Baud, A., Atudorei, V., and Richoz, S., 2005, Sea-floor carbonate fans and calcimicrobial mound in the Lower Triassic red limestone of the Alwa Formation, Baid Exotic, Eastern Oman Mountains, in IAS, ed., 24th IAS meeting of Sedimentology, Volume Abstract Volume: Muscat, Oman, p. 31.

Baud, A., Atudorei, V. & Sharp, Z. D., 1996, Late Permian and Early Triassic evolution of the Northern Indian margin: carbon isotope and sequence stratigraphy. Geodinamica Acta, v. 9, p. 57-77.

Baud, A., Béchennec, F., Cordey, F., Krystyn, L., Le Métour, J., Marcoux, J., Maury, R., and Richoz, S., 2001a, Permo-Triassic Deposits: from the Platform to the Basin and Seamounts, Conference on the Geology of Oman, Field guidebook, Excursion A01: Muscat, Oman, 54pp.

Baud, A., Béchennec, F., Cordey, F., Le Métour, J., Marcoux, J., Maury, R., and Richoz, S., 2001b, Permo-Triassic Deposits: from shallow water to base of slope, Conference on the Geology of Oman, Field guidebook, Excursion B01, Muscat, Oman, 40 pp.

Baud, A., Droste, H., Guillocheau, F., Razin, P., and Robin, C., 2005, Mesozoic Evolution of the Tethyan margin of Oman, 24th IAS regional Meeting, Pre-Conference Excursion BF 4: Muscat, Oman, 61 pp.

Baud, A., Marcoux, J., Guiraud, R., Ricou, L.E., and Gaetani, M., 1993, Late Murgabian (266 to 264 Ma), *in* Dercourt, J., Ricou, L.E., and Vrielynck, B., eds., Atlas Tethys Palaeoenvironmental Maps. Explanatory Notes: Paris, Gauthier-Villars, p. 9-20.

Baud, A., Richoz, S., and Pruss, S., 2007, The Lower Triassic anachronistic carbonate facies in space and time: Global and Planetary Change, v. 55, p. 81-89.

Beatty, T. W., Zonneveld, J-P, and Henderson, C.M., 2008, Anomalously diverse Early Triassic ichnofossil assemblages in northwest Pangea: A case for a shallow-marine habitable zone. Geology, v. 36, no.10, p. 771-774

Beauchamp, B., and Baud, A., 2002, Growth and demise of Permian biogenic chert along NW Pangea: evidence for northern sea ice, thermohaline circulation and end-Permian global warming: Paleogeography, Paleoclimatology, Paleoecology, v. 184, p. 37-63.

Beauchamp, B. and Desrochers, A., 1997. Permian warm- to very cold-water carbonates and cherts in northwest Pangea. In: N.P. James and J.A.D. Clarke (Editors), Cool-water carbonates, Tulsa, pp. 327-347.

Béchennec, F., 1988, Géologie des nappes d'Hawasina dans les parties orientales et centrales des montagnes d'Oman: Orléans, France, Bureau de Recherches Géologiques et Minières, 474 pp.

Béchennec, F., Beurrier, M., Hutin, G., and Rabu, D., 1986, Geological map of Bahla, sheet NF 40-7A, scale 1/100 000: Orléans, France, Sultanate of Oman, Ministry of Petroleum and Minerals, Directorate of Minerals.

Béchennec, F., Le Metour, J., Rabu, D., Beurrier, M., Bourbillon-Jeudy-de-Grissac, C., De Wever, P., Tegyey, M., and Villey, M., 1989a, Geologie d'une chaîne issue de la Tethys: Les montagnes d'Oman: Bull. Soc. Geol. de France, v. Vol. 2, p. 231-240.

Béchennec, F., Le Métour, J., Rabu, D., Beurrier, M., Bourbillon-Jeudy-de-Grissac, C., De Wever, P., Tegyey, M., and Villey, M., 1989b, Geologie d'une chaîne issue de la Tethys: Les montagnes d'Oman: Bulletin de la Société géologique de France, v. 2, p. 231-240.

Béchennec, F., Le Métour, J., Rabu, D., Beurrier, M., Bourdillon-Jeudy-De-Grissac, C., De Wever, P., Beurier, M., and Villey, M., 1990, The geology and tectonics of the Oman mountains., in Robertson, A.H.F., Searle, M.P., and Ries, A.C., eds., Volume 49, Special Publications of the Geological Society of London, p. 213-224.

Béchennec, F., Roger, J., Le Métour, J., and Wyns, R., 1992, Explanatory notes to the Geological map of Seeb, Sheet NF40-03: Muscat, Oman Ministry of Petroleum and Minerals, 104 pp.

Béchennec, F., Tegyey, M., Le Métour, J., Lemière, B., Lescuyer, J.L., Rabu, D., and Milési, J.P., 1991, Igneous rocks in the Hawasina Nappes and the Hajar supergroup, Oman mountains: Their significance in the birth and evolution of the composite extentional margin of Eastern Tethys, in al, T.P., ed., Ophiolite genesis and evolution of the oceanic lithosphere, Volume 1, Ministry of Petroleum and Minerals, Sultanate of Oman, p. 593-611.

Becq-Giraudon, J-F., and Pillevuit, A., 1995, Trilobites du Permien supérieur (Murgabien/Midien) du Nord de l'Oman. Eclogae geologicae Helvetiae, v. 88, p. 761-775.

Bernecker, M., 1996a, Upper Triassic coral communities from the Oman Mountains; occurrence and distribution pattern: Special Publication The Paleontological Society, p. 8; Pages 31.

—, 1996b, Upper Triassic reefs of the Oman Mountains - data from the south Tethyan margin: Facies, v. 34, p. 41-76.
—, 1996c, Upper Triassic reefs of the Oman Mountains - data from the south Tethyan margin: Facies, v. 34, p. 41-76.
—, 2007, Facies architecture of an isolated carbonate platform in the Hawasina Basin: The Late Triassic Jebel Kawr of Oman: Palaeogeography, Palaeoclimatology, Palaeoecology, v. 252, p. 270-280.
Bernecker, M., and Weidlich, O., 1994, Attempted reconstrucsion of Permian and Triassic skeletonization from reefbuilders (Oman Turkey): Quantitative assement with digital image analysis: Abh. Geol. Bundesanstalt, v. 50, p. 31-56.
Berthelin, M., Broutin, J., Kerp, H., Crasquin-Soleau, S., Platel, J.P., and Roger, J., 2003, The Oman Gharif mixed paleoflora: a useful tool for testing Permian Pangea reconstructions: Palaeogeography Palaeoclimatology Palaeoecology, v. 196, p. 85-98.
Beurrier, M., Béchennec, F., Rabu, D., and Hutin, G., 1986, Geological map of Rustaq. Sheet NF 40-3A. Scale 1/100 000: Orleans, France, Sultanate of Oman, Ministry of Petroleum and Minerals, Directorate General of Minerals.
Blendinger, W., 1988, Permian to Jurassic deep water sediments of the Eastern Oman Mountains: Their significance for the evolution of the Arabia margin of south Tethys: Facies, v. 19, p. 1-32.
—, 1991, Upper Triassic (Norian) cephalopod limestones of the Hallstatt-type, Oman: Sedimentology, v. 38, p. 223-242.
—, 1995, Lower Triassic to Lower Jurassic cephalopod limestones of the Oman Mountains: N. Jb. Geol. Paläont. Mh., v. 10, p. 577-593.
Blendinger, W., Furnish, W.M., and Glenister, B.F., 1992, Permian cephalopod limestones, Oman Mountains: evidence for a Permian seaway along the northern margin of Gondwana: Palaeogeography, Palaeoclimatology, Palaeoecology, v. 93, p. 13-20.
Bromley R. G. & Ekdale, A. A. 1984. Chondrites: a trace fossil indicator of anoxia in sediments. Science, v. 224, p. 872-874.
Broutin, J., Roger, J., Platel, J.P., Angiolini, L., Baud, A., Bucher, H., Marcoux, J., and Hasmi, H.A., 1995, The Permian Pangea. Phytogeographic implications of new discoveries in Oman (Arabian Peninsula): Comptes Rendus de l'Académie des Sciences de Paris, Série II a, v. 321, p. 1069-1086.
Chauvet, F., 2007, La marge continentale sud-téthysienne en Oman : structure et volcanisme au Permien et au Trias. Thesis, Grenoble I University. 362 p.
Chauvet, F., Lapierre, H., Bosch, D., Guillot, S., Mascle, G., Vannay, J.C., Cotten, J., Brunet, P., and Keller, F., 2008, Geochemistry of the Panjal Traps basalts (NW Himalaya): records of the Pangea Permian break-up: Bulletin de la Société géologique de France, v. 179, p. 383-395.
Cordey, F., Baud, A., Béchennec, F., Gorican, S., Krystyn, L., Marcoux, J., Robin, C., and Richoz, S., 2001, Permian-Triassic deep water sediments of the Wadi Wasit revisited, Geology of Oman, Pangea Symposium, Volume Abstract Vol.: Muscat, Oman.
Corsetti, F.A., Baud, A., Marenco, P.J., Richoz, S., 2005. Summary of Early Triassic carbon isotope records. Comptes Rendu Palevol 4, 405–418.
Coy, G.A., 1997, Dolomitisation of the Akhdar Group: the Arabian platform of Oman, Thesis, Cambridge University, U.K., 217 pp.
Coy, G.A., 2004, Geological excursion tho the Saiq Plateau, in Oman, G.S.o., ed., Field Guide, Volume 008, p. 10.
Crasquin-Soleau, S., Broutin, J., Besse, J., and Berthelin, M., 2001, Ostracods and palaeobotany from the Middle Permian of Oman: implications on Pangaea reconstruction: Terra Nova, v. 13, p. 38-43.

De Wever, P., Bourdillon-De-Grissac, C., and Bechennec, F., 1988, Découverte de radiolaires permiennes au bord Sud de la Tethys (nappes d'Hawasina, Sultanat d'Oman): C. Acad. Sci. Paris, v. 307, serie II, p. 1383-1388.

Erwin, D.H., 1993. The great Paleozoic crisis: life and death in the Permian. Columbia University Press, New York, 327 pp.

Fluegel, E., and Bernecker, M., 1996, Upper Triassic reefs of the south Tethyan margin (Oman): Goettinger Arbeiten zur Geologie und Palaeontologie, p. Sonderband.

Fluegel, E., and Senowbari Daryan, B., 1996, Evolution of Triassic reef biota; state of the art: Goettinger Arbeiten zur Geologie und Palaeontologie, v. Sonderband, p. 285-294.

Gaillot, J. and Vachard, D., 2007. The Khuff Formation (Middle East) and time-equivalents in Turkey and South China: biostratigraphy from Capitanian to Changhsingian times (Permian), new foraminiferal taxa, and palaeogeographical implications. Coloquios de Paleontología, 57: 37-223.

Galfetti, T., Bucher, H., Ovtcharova, M., Schaltegger, U., Brayard, A., Brühwiler, T., Goudemand, N., Weissert, H., Hochuli, P. A., Cordey, F., Guodun, K., 2007a. Timing of the Early Triassic carbon cycle perturbations inferred from new U-Pb ages and ammonoid biochronozones. Earth and Planetary Science Letters 258 (3-4), 593-604.

Galfetti, T., Bucher, H., Brayard, A., Hochuli, P.A., Weissert, H., Guodun, K., Atudorei, V., Guex, J., 2007b. Late Early Triassic climate change: insights from carbonate carbon isotopes, sedimentary evolution and ammonoid paleobiogeography, Palaeogeography Palaeoclimatology Palaeoecology 243, 394–411.

Glennie, K.W., Boeuf, M.G.A., Hughes Clarke, M.W., Moody-Stuart, M., Pilaart, W.F.H., and Reinhart, B.M., 1974, Geology of the Oman mountains: Verh. Konink. Neder. Mijnb. Genoot., v. 31, p. 1-423.

Haq, B.U., Hardenbol, J., and Vail, P., 1987, Chronology of fluctuating sea levels since the Triassic.: Science, v. 235, p. 1156-1167.

Henderson, C.M., and Mei, S.L., 2003, Stratigraphic versus environmental significance of Permian serrated conodonts around the Cisuralian-Guadalupian boundary: new evidence from Oman: Palaeogeography Palaeoclimatology Palaeoecology, v. 191, p. 301-328.

Henderson, C.M. and Mei, S.L., 2007. Geographical clines in Permian and Lower Triassic gondolellids and its role in taxonomy. Palaeoworld, v. 16, p. 190-201.

Horacek M., Richoz, S., Brandner, R., Krystyn, L., Spötl, C. 2007a. Evidence for recurrent changes in Lower Triassic oceanic circulation of the Tethys: The d13C record from marine sections in Iran. Paleogeography, Paleoclimatology, Paleoecology, v. 252, p. 355-369.

Horacek, M., Brandner, R. and Abart, R., 2007b, Carbon isotope record of the P/T boundary and the Lower Triassic in the Southern Alps: Evidence for rapid changes in storage of organic carbon.. Paleogeography, Paleoclimatology, Paleoecology, v. 252, p. 347-354.

Horacek, M., Wang, X., Grossman, E. L., Richoz, S., Cao, Z. 2007c. The carbon-isotope curve from the Chaohu section, China: different trends at the Induan –Olenekian Boundary or diagenesis? Albertiana, v. 35, p. 41-45.

Horacek, M., Koike, T., Richoz, S., 2009. Lower Triassic $d^{13}C$ isotope curve from shallow- marine carbonates in Japan, Panthalassa realm: Confirmation of the Tethys $d^{13}C$ curve. Journal of Asian Earth Sciences, v 36(6), p. 481-490.

Horacek, M., Povoden, E., Richoz, S., Brandner, R., in press. Exact correlation of the d13C curve and the paleomagnetic pattern across the Permian-Triassic Boundary in the Seis/Siusi section, N-Italy. Palaeogeography, Palaleoclimatology, Palaecology. doi: 10.1016/j. palaeo.2010.01.007.

Hutin, G., Béchennec, F., Beurrier, M., and Rabu, D., 1986, Geological map of Birkat Al Mawz, sheet NF 40-7B, scale 1/100 000: Orléans, France, Sultanate of Oman, Ministry of Petroleum and Minerals, Directorate of Minerals.

Immenhauser, A., Schreurs, G., Peters, T., Matter, A., Hauser, M., and Dumitrica, P., 1998, Stratigraphy, sedimentology and depositional environments of the Permian to uppermost Cretaceous Batain Group, eastern-Oman: Eclogae geologicae Helvetiae, v. 91, p. 217-235.

Insalaco, E., Virgone, A., Courme, B., Gaillot, J., Kamali, M., Moallemi, A., Lotfpour, M., and Monibi, S., 2006, Upper Dalan Member and Kangan Formation between the Zagros Mountains and offshore fars, Iran: depositional system, biostratigraphy and stratigraphic architecture: Geoarabia, v. 11, p. 75-176.

Isozaki, Y., 2009, Illawarra Reversal: The fingerprint of a superplume that triggered Pangean breakup and the end-Guadalupian (Permian) mass extinction: Gondwana Research, v. 15, p. 421-432.

Isozaki, Y., and Aljinovic, D., 2009, End-Guadalupian extinction of the Permian gigantic bivalve Alatoconchidae: End of gigantism in tropical seas by cooling: Palaeogeography Palaeoclimatology Palaeoecology, v. 284, p. 11-21.

Kanmera, K., and Nakazawa, K., 1973, Permian-Triassic relationships and faunal changes in the eastern Tethys, International Permian-Triassic conference: Calgary, Alta., Canada, p. 100-119.

Kohrer, B., Aigner, T., and Poppelreiter, M., 2009, Characterization of Khuff Geobodies in Outcrop and Subsurface of Oman: Al Ajar, Journal of the Geological Society of Oman, p. 10-13.

Krull, E.S., Lehrmann, D.J., Druke, D., Kessel, B., Yu, Y.Y., and Li, R.X., 2004, Stable carbon isotope stratigraphy across the Permian-Triassic boundary in shallow marine carbonate platforms, Nanpanjiang Basin, south China: Palaeogeography Palaeoclimatology Palaeoecology, v. 204, p. 297-315.

Krystyn, L., Richoz, S., Baud, A., and Twitchett, R.J., 2003, A unique Permian-Triassic boundary section from the Neotethyan Hawasina Basin, Central Oman Mountains: Palaeogeography Palaeoclimatology Palaeoecology, v. 191, p. 329-344.

Lapierre, H., Samper, A., Bosch, D., Maury, R.C., Bechennec, F., Cotten, J., Demant, A., Brunet, P., Keller, F., and Marcoux, J., 2004, The Tethyan plume: geochemical diversity of Middle Permian basalts from the Oman rifted margin: Lithos, v. 74, p. 167-198.

Le Métour, J., 1988, Géologie de l'Autochtone des Montagnes d'Oman : la fenêtre du Saih Hatat, Documents du Bureau de Recherches Géologiques et Minières Orléans, Volume 129: Orléans, p. 430.

Le Métour, J., Béchennec, F., Beurrier, M., Janjou, D., Roger, J., and Wyns, R., 1991, Geological map of Dank - Sheet NF40-2B . Scale 1/100 000: Orléans-France, Sultanate of Oman, Ministry of Petroleum and Minerals, Directorate General of Minerals.

Le Métour, J., Béchennec, F., Chevremont, P., Roger, J., and Wyns, R., 1992, Explanatory notes to the Geological map of Burayimi, Sheet NF40-14: Muscat, Oman Ministry of Petroleum and Minerals.

Le Métour, J., Béchennec, F., Roger, J., Wyns, R., 1986. Geological map of Muscat with explanatory notes, Sheet NF40-4, scale 1:250.000, Directorate General of Minerals, Ministry of Petroleum and Minerals, Sultanate of Oman, 76 pp..

Le Métour, J., de Gramond, X., Villey, M., and Beurrier, M., 1986a, Geological map of Masqat, sheet NF 40-4D, scale 1/100 000: Orléans, France, Sultanate of Oman, Ministry of Petroleum and Minerals, Directorate of Minerals.

Le Métour, J., Villey, M., and de Gramond, X., 1986b, Geological map of Quryat, sheet NF 40-4D, scale 1/100 000: Orléans, France, Sultanate of Oman, Ministry of Petroleum and Minerals, Directorate of Minerals.

Le Nindre, Y.-M., Manivit, J., and Vaslet, D., 1990a, Géodynamique et paléogéographie de la plate-forme arabe du Permien au Jurassique: Orléans, Documents du BRGM no 192, 280 p.

Le Nindre, Y.-M., Vaslet, D., and Manivit, J., 1990b, Le Permo-Trias d'Arabie centrale: Orléans, Documents du BRGM no 193, 290 pp.

Lys, M., 1988, Biostratigraphie du Carbonifere et du Permien en Mésogée: Documents du Bureau de Recherches Géologiques et Minières Orléans, v. 147, p. 1-315.
Maury, R.C., Bechennec, F., Cotten, J., Caroff, M., Cordey, F., and Marcoux, J., 2003, Middle Permian plume-related magmatism of the Hawasina Nappes and the Arabian Platform: Implications on the evolution of the Neotethyan margin in Oman: Tectonics, v. 22, p. art. no.-1073.
Mei, S.L., Henderson, C.M., and Wardlaw, B.R., 2002. Evolution and distribution of the conodonts *Sweetognathus* and *Iranognathus* and related genera during the Permian and their implications for climate change. Palaeogeography, Palaeoclimatology, Palaeoecology, 180, p. 57-91.
Miller, A.I. and Foote, M., 2009, Epicontinental seas versus open-ocean settings: the kinematics of mass extinction and origination. Science, v. 326, p. 1106-1109.
Minoux, L., and Janjou, D., 1986, Geological map of Ibrì, sheet NF 40-2F, scale 1/100 000: Orléans, France, Sultanate of Oman, Ministry of Petroleum and Minerals, Directorate of Minerals.
Montenat, C., Lapparent, A.F., Lys, M., Termier, H., Termier, G., and Vachard, D., 1976, La transgression permienne et son substratum dans le jebel Akhdar (Montagnes d'Oman, Peninsule Arabique): Annales de la Société géologique du Nord, v. XCVI, p. 239-258.
Niko, S., Pillevuit, A., and Nishida, T., 1996, Early Late Permian (Wordian) non-ammonoid cephalopods from the Hamrat Duru Group, central Oman Mountains: Transactions and Proceedings of the Palaeontological Society of Japan, p. New Series.
Oekentorp, K.L., Montenat, C., and Fontaine, H., 1978, Eine kleine Korallenfauna aus dem unteren Oberperm von Saiq, Oman (Arabische Halbinsel): N. Jb. Geol. Paläont. Abh., v. 155 / 3, p. 374-397.
Payne, J.L., Lehrmann, D.J., Wei, J.Y., Orchard, M.J., Schrag, D.P., Knoll, A.H., 2004, Large perturbations of the carbon cycle during recovery from the end-Permian extinction. Science v. 305, 506-509.
Orchard, M.J., 1995, Taxonomy and correlation of Lower Triassic (Spathian) segminate conodonts from Oman and revision of some species of Neospathodus: Journal of Paleontology, v. 69, p. 110-122.
Orchard, M.J. and Krystyn, L., 1998. Conodonts of the lowermost Triassic of Spiti, and new zonation based on Neogondolella successions. Rivista Italiana di Paleontologia e Stratigrafia, v. 104(3), p. 341-367.
Orchard, M.J. and Zonneveld, J-P, 2009. The Lower Triassic Sulphur Mountain Formation in the Wapiti Lake area: lithostratigraphy, conodont biostratigraphy, and a new biozonation for the Lower Olenekian (Smithian). Canadian Journal of Earth Sciences, v. 46, p. 757-790.
Pillevuit, A., 1993, Les Blocs Exotiques du Sultanat d'Oman: Evolution paléogéographique d'une marge passive flexurale: Lausanne, Université de Lausanne, Institut de Géologie et Paléontologie, 249 p.
Pillevuit, A., Marcoux, J., Stampfli, G., and Baud, A., 1997, The Oman Exotics: a key to the understanding of the Neotethyan geodynamic evolution: Geodinamica Acta, v. 10, p. 209-238.
Rabu, D., 1988, Géologie de l'autochtone des montagnes d'Oman : La fenêtre du Djebel Akdar. La semelle métamorphique de la Nappe ophiolitique de Semail dans les parties orientales et centrale des Montagnes d'Oman : une revue: Documents du Bureau de Recherches Geologiques et Minières, Orléan, v. 130, p. 1-582.
Rabu, D., Béchennec, F., Beurrier, M., and Hutin, G., 1986, Geological map of Nakhl, sheet NF 40-3E, scale 1/100 000: Orléans, France, Sultanate of Oman, Ministry of Petroleum and Minerals, Directorate of Minerals.
Richoz, S., 2006, Stratigraphie et variations isotopiques du carbone dans le Permien supérieur et le Trias inférieur de la Néotéthys (Turquie, Oman et Iran), in Guex, J., ed., Mémoires de Géologie (Lausanne), Volume 46: Lausanne, Geological Museum, Lausanne, p. 264.

Richoz, S., Atudorei, V., Baud, A., and Marcoux, J., 2001, Upper Permian to Lower Triassic carbon isotope record : review and new data in the Oman Mountains, from the shallow platform to the basin., Geology of Oman, Pangea Symposium, Volume Abstract Vol.: Muscat, Oman.

Richoz, S., Baud, A., Krystyn, L., Twitchett, R., and Marcoux, J., 2005, Permo-Triassic Deposits of the Oman Mountains: from Basin and Slope to the shallow Platform, in 24th IAS regional Meeting, Post-Conference Excursion A13: Muscat, Oman, 57 pp.

Richoz, S., Krystyn, L., Baud, A., Brandner, R., Horacek, M. Mohtat-Aghai, P., (in press). Permian–Triassic boundary interval in the Middle East (Iran and N. Oman): Progressive environmental change from detailed carbonate carbon isotope marine curve and sedimentary evolution. Journal of Asian Earth Sciences (2010), doi:10.1016/j.jseaes.2009.12.014

Ricou, L.-E., 1994, Tethys reconstructed - plates, continental fragments and their boundaries since 260 My. from central America to south-eastern Asia: Geodinamica Acta, v. 7, p. 169-218.

Sano, H., and Nakashima, K., 1997, Lowermost Triassic (Griesbachian) Microbial Bindstone-cementstone Facies, Southwest Japan: Facies, v. 36, p. 1-24.

Senowbari-Daryan, B., Bernecker, M., Krystyn, L., and Siblik, M., 1999, Carnian reef biota from a megabreccia of the Hawasina complex (Al Aqil, Oman): Rivista italiana di Paleontologia e Stratigrafia, v. 105, p. 327-342.

Stampfli, G., Marcoux, J., and Baud, A., 1991, Tethyan margins in space and time: Palaeogeography, Palaeoclimatology, Palaeoecology, v. 87, p. 373-409.

Tong, J., Qiu, H., Zhao, L. & Zuo, J., 2002. Lower Triassic inorganic Carbon isotope excursion in Chaohu, Anhui Province, China. Journal of China University of Geosciences, v. 13/2, p. 98-106

Tong J., Zuo J. and Chen Z.Q. 2007. Early Triassic carbon isotope excursions from south China: Proxies for devastation and restoration of marine ecosystems following the end-Permian mass extinction. Geological Journal, v. 42, p. 371-389.

Tozer, E.T., and Calon, L., 1990, Triassic ammonoids from Djebel Sefra and Wadi Alwa, Oman, and their significance.: Special Publications of the Geological Society of London, v. 24, p. 121-132.

Twitchett, R.J., 1999, Paleoenvironments and faunal recovery after the end-Permian mass extinction: Palaeogeography, Palaeoclimatology, Palaeoecology, v. 157, p. 27-37.

Twitchett, R.J., 2001, Incompleteness of the Permian-Triassic fossil record: A consequence of productivity decline?: Geological Journal, v. 36, p. 341–353

Twitchett, R.J., 2007, The Lillliput effect in the aftermath of the end-Permian extinction event: Palaeogeography, Palaeoclimatology, Palaeoecology, v. 252, p. 132–144,

Twitchett, R.J., Barras, C.G., 2004. Trace fossils in the aftermath of mass extinction events. In: McIlroy, D. (Ed.), The Application of Ichnology to Palaeoenvironmental and Stratigraphic Analysis, Geological Society, London, Special Publications, v. 228, p. 397– 418.

Twitchett, R.J., Krystyn, L., Baud, A., Wheeley, J.R. and Richoz, S., 2004. Rapid marine recovery after the end - Permian mass - extinction event in the absence of marine anoxia. Geology, v. 32, p. 805-808.

Vachard, D., Gaillot, J., Vaslet, D., and Le Nindre, Y.M.H., 2005, Foraminifers and algae from the Khuff formation (Late Middle Permian-Early Triassic) of central Saudi Arabia: Geoarabia, v. 10, p. 137-186.

Vachard, D., Hauser, M., Martini, R., Zaninetti, L., Matter, A., and Peters, T., 2001, New algae and problematica of algal affinity from the Permian of the Aseelah Unit of the Batain Plain (east Oman): Geobios, v. 34, p. 375-404.

—, 2002, Middle Permian (Midian) foraminiferal assemblages from the Batain Plain (eastern Oman): Their significance to Neotethyan paleogeography: Journal of Foraminiferal Research, v. 32, p. 155-172.

Vaslet, D., Le Nindre, Y.M., Vachard, D., Broutin, J., Crasquin-Soleau, S., Berthelin, M., Gaillot, J., Halawani, M., and Al-Husseini, M., 2005, The Permian-Triassic Khuff formation of central Saudi Arabia: Geoarabia, v. 10, p. 77-134.

Villey, M., De Gramont, X., and Le Metour, J., 1986a, Geological map of Sìb, Sheet NF 40-3C, scale 1/100 000: Orléans, France, Sultanate of Oman, Ministry of Petroleum and Minerals, Directorate General of Minerals.

Villey, M., Le Metour, J., and De Gramont, X., 1986b, Geological Map of Fanjah, Sheet NF 40-3F, BRGM.

—, 1986c, Geological map of Fanjah, Sheet NF 40-3F, scale 1/100 000: Orléans, France, Ministry of petroleum and minerals, directorate general of minerals.

Wardlaw, B.R., 2000. Guadalupian Conodont Biostratigraphy of the Glass and Del Norte Mountains. In: Wardlaw, B.R., Grant, R.E., and Rohr, D.M. (eds.), Smithsonian Contributions to the Earth Sciences, 32, p. 37-87.

Watts, K.F., 1987, Triassic carbonate submarine fans bounding the Arabian carbonate margin, Sumeini Group, Oman: Sedimentology, v. 34, p. 43-71.

—, 1990, Mesozoic carbonate slope facies marking the Arabian platform margin in Oman: depositional history, morphology and peleogeography, in Robertson, A., Searle, M., and Ries, A., eds., The Geology and Tectonics of the Oman Region, Special Publications of the Geological Society of London, v. 49, p. 139-159.

Watts, K.F., and Garrison, R.E., 1986, Sumeini group, Oman. Evolution of a Mesozoic carbonate slope on a south Tethyan continental margin.: Sedimentary geology, v. 48, p. 107-168.

Weidlich, O., 1996. Bioerosion in Late Permian Rugosa from reefal blocks (Hawasina Complex): Implications for reef degradation. Facies, v. 35, p. 133-142.

Weidlich, O., 2002. Middle and Late Permian reefs - distributional patterns and reservoir potential. In: Kiessling, W., Flügel, E., Golonka, J. (Eds.), Phanerozoic reef patterns, Society of Economic Petroleum Geologists and Mineralogists Special Publication v. 72, p. 339-390.

Weidlich, O., 2007, Permian reef and shelf carbonates of the Arabian platform and Neo-Tethys as recorders of climatic and oceanographic changes: Special Publications of the Geological Society, London, v. 275, p. 229-253.

Weidlich, O., 2010. Meteoric diagenesis in carbonates below karst unconformities: heterogeneity and control factors. In: F. van Buchem, K. Gerdes and M. Esteban (Eds), Mesozoic and Cenozoic carbonate systems of the Mediterranean and the Middle East: Stratigraphic and diagenetic reference models. Geological Society, London, p. 289-313.

Weidlich, O., Bernecker, M., 2003. Supersequence and composite sequence carbonate platform growth: Permian and Triassic outcrop data of the Arabian platform and Neo - Tethys. Sedimentary Geology, v. 158, p. 87-116.

Weidlich, O., and Bernecker, M., 2007, Differential severity of Permian-Triassic environmental changes on Tethyan shallow-water carbonate platforms: Global and Planetary Change, v. 55, p. 209-235.

Weidlich, O., Bernecker, M. PTB Mass Extinction and Early Triassic Recovery at the Eastern Rim of the Arabic Plate, Sultanate of Oman. Palaeogeography, Palaeoclimatology, Palaeoecology, submitted.

Weidlich, O., Bernecker, M., Flügel E., 1993. Combined quantitative analysis and microfacies studies of ancient reefs: an integrated approach to Upper Permian and Upper Triassic reef carbonates (Sultanate of Oman). Facies, v. 28, p. 115-144.

Weidlich, O., and Flugel, H.W., 1995, Upper Permian (Murghabian) Rugose Corals from Oman (Baid Area, Saih-Hatat) - Community Structure and Contributions to Reefbuilding Processes: Facies, v. 33, p. 229-263.

Weidlich, O., Kiessling, W. Flügel, E., 2003. The Permian-Triassic boundary interval as a model for forcing marine ecosystem collapse by long-term atmospheric oxygen drop. Geology, v. 31, p. 961-964.

Weidlich, O., and Senowbari, D.B., 1996, Late Permian "sphinctozoans" from reefal blocks of the Ba'id area, Oman Mountains: Journal of Paleontology, v. 70, p. 27-46.

Weldlich, O., and Bernecker, M., 2003, Supersequence and composite sequence carbonate platform growth: Permian and Triassic outcrop data of the Arabian platform and Neo-Tethys: Sedimentary Geology, v. 158, p. 87-116.

Wheeley, J.R., and Twitchett, R.J., 2005, Palaeoecological significance of a new Griesbachian (Early Triassic) gastropod assemblage from Oman: Lethaia, v. 38, p. 37-45.

Wignall, P.B., and Twitchett, R.J., 1996. Oceanic anoxia and the end-Permian mass extinction. Science, v. 272, p. 1155-1158.

Wignall, P.B. and Twitchett, R.J., 1999. Unusual intraclastic limestones in Lower Triassic carbonates and their bearing on the aftermath of the end-Permian mass extinction. Sedimentology, v. 46(2), p. 303-316.

Wignall, P.B., and Twitchett, R.J., 2002, Extent, duration and nature of the Permian-Triassic superanoxic event, in Koeberl, C., and MacLeod Kenneth, G., eds., Catastrophic events and mass extinctions; impacts and beyond., Volume 356: Geological Society of America Special Paper: Boulder, CO, USA, Geological Society of America (GSA). 2002., p. 395-413.

Woods, A.D., and Baud, A., 2008, Anachronistic facies from a drowned Lower Triassic carbonate platform: Lower member of the Alwa Formation (Ba'id Exotic), Oman Mountains: Sedimentary Geology, v. 209, p. 1-14.

Xiaochi, J., and Xianging, Y., 2004, Paleogeographic implications of the Shanita-Hemigordius fauna (Permian foraminifer) in the reconstruction of Permian Tethys: Episodes, v. 27, p. 273-278.

Yanagida, J., and Pillevuit, A., 1994, Permian Brachiopods from Oman: Memoirs of the Faculty of Science, Kyushu University, Series D, Earth and Planetary Sciences, v. XXVIII, p. 61-69.

Yin H., Feng Q., Lai X., Baud A. and Tong J., 2007. The protracted Permo-Triassic crisis and multi-episode extinction around the Permian–Triassic boundary. Global and Planetary Change, v. 55 (1-3), p. 1-20.

Zuo, J., Tong, J., Qiu, H. & Zhao, L., 2006. Carbon isotope composition of the Lower Triassic marine carbonates, Lower Yangtze Region, South China. Science in China: Serie D Earth Sciences, v. 49/3, p. 225-241.